Characterization of MbaS, an Iron Responsive Sigma Factor of *Burkholderia pseudomallei*

By

Melissa J. Hauglund

A Dissertation

Presented to the
Department of Molecular
Microbiology and Immunology
and the
Oregon Health and Science University
School of Medicine

in partial fulfillment of the
requirements for the degree of

Doctor of Philosophy

June 2011

School of Medicine

Oregon Health and Science University

CERTIFICATE OF APPROVAL

This is to certify that the PhD dissertation of

Melissa Jo Hauglund

has been approved

_____

Jorge Crosa, Mentor/Advisor

_____

Scott Landfear, Committee Chair

_____

Eric Barklis, Committee Member

_____

David Farrell, Committee Member

_____

Fred Heffron, Committee Member

_____

Georgiana Purdy, Committee Member

Table of Contents

Table of Figures

Table of Tables

Acknowledgements:

There are many people whom deserve to be acknowledged for their support of my ambition to achieve a degree, their support or contribution to the work presented in herein, or both. Foremost, I must thank my family. My parents and my sister have been my support and comfort, and for that I am deeply thankful. Thank you Mom and Dad for being my shelter in a storm. My extended family, both those related by genetics and those not, have given me pieces of normalcy when I have felt overwhelm and offered to fight my dragons, both figuratively and literally, on many occasions. I only hope I was able to give as much as I received.

I would like to express my sincerest gratitude to my mentor, Jorge H. Crosa. Although I floundered frequently, you never gave up on me.

A big thank you is necessary for my Thesis Advisory Committee (Scott Landfear, Georgiana Purdy, Fred Heffron, Eric Barklis, and David Farrell). You have pushed me to do more and be more, and I think I am better for it. I will try to keep what you have taught me, especially over the last year, in my mind during future work.

A big hug goes out to my lab mates. You have done a fabulous job of making me laugh, comforting me when I wanted to cry, and ignoring me when I occasionally went completely off the deep end.

I need to acknowledge that the characterization of MbaS was initiated by A. Alice, whom also conceived of the *mbaJ* and *mbaE* promoter truncations.

Abstract

Burkholderia pseudomallei, a Gram-negative saprophyte endemic to Southeast Asia and Northern Australia, is the causative agent of melioidosis. Although numerous studies were initiated to identify and characterize virulence mechanisms utilized by this human pathogen, characterization of the iron acquisition systems is still in its infancy. Presently, only the malleobactin siderophore system of *B. pseudomallei* has been described. The work presented herein is a genetic characterization of the iron responsive sigma factor MbaS. We generated a two-plasmid system for screening the functionality of MbaS when expressed in *E. coli* and a second single plasmid system for the identification of functional promoter elements and translation initiation. We demonstrated that an ATG codon located 90 nucleotides upstream of the annotated start codon is required for expression from the *mbaS* promoter and that this upstream promoter region, which contains a putative Fur binding site, is responsive to iron. We have identified the minimal MbaS responsive promoter element of *mbaJ* and *mbaE* and characterized the MbaS DNA binding site in the promoter of *mbaJ*. Through the use of sequence homology to the characterized sigma factor PvdS from *P. aeruginosa* and mutagenesis studies, we have preliminary confirmation on the locations of the domains within MbaS for the recognition of the RNA core polymerase and the -10 DNA binding sequence. However, we were unable to identify the -35 DNA binding region. Finally, we have demonstrated

that the results generated in *E. coli* correspond to what is seen when the same constructs are used in *B. pseudomallei.*

I. Introduction

I.A. Introduction to Burkholderia pseudomallei

Burkholderia pseudomallei, a Gram-negative motile aerobic rod-shaped bacterium, is the causative agent of melioidosis and capable of causing infections in humans, animals, and plants (23, 28, 70, 81, 150, 152). *B. pseudomallei*, K96243, was the first sequenced strain (65), and is the strain utilized in the studies described herein. *B. pseudomallei* encodes for a relatively large bacterial genetic repertoire with 5855 putative open reading frames (ORFs) identified within its 7.24 megabase (Mb) genome with an average GC percentage over 68% (65). The genome is distributed over two chromosomes (Chromosome 1: 4.07 Mb and 3,460 ORFs; Chromosome 2: 3.17 Mb and 2,395 ORFs). Chromosome 1 contains the majority of genes required for core functions such as nucleotide, protein, cofactor, and macromolecule biosynthesis, while chromosome 2 contains more accessory function-related genes that are likely necessary for adapting to stress responses such as iron availability and secondary metabolite metabolism (65). The genome of the K96243 strain contains 16 genomic islands (GIs): 12 on chromosome 1 (1-12) and 4 on chromosome 2 (13-16). Of these, three appear to encode for prophages (GIs 2, 3, and 15) with the prophage encoded in GI 2 having activity against *B. mallei* (65).

Although first identified by Alfred Whitmore and C.S. Krishnaswami in 1911 (151), the more recent establishment of *B. pseudomallei* as a Category B pathogen and select agent resulted in an exponential increase in the available published data regarding this pathogen (23, 28). These data have furthered our understanding of

the virulence mechanisms of *B. pseudomallei*. Of particular importance are the following: disease manifestations resulting from *B. pseudomallei* infection often mimic symptoms of other, more common, diseases. *B. pseudomallei* displays high intrinsic resistance to available antibiotic treatments. Additionally, this pathogen affects peoples in both hemispheres and is not restricted to Southeast Asia and Northern Australia as previously described (34, 83).

I.A.i. B. pseudomallei and Disease

B. pseudomallei, endemic to Southeast Asia and Northern Australia, is an environmental saprophyte from tropical climates with latitudes ranging from 20°N to 20°S (152). The largest amount of clinical data pertaining to melioidosis comes from Thailand, where it is estimated that approximately 20% of community-acquired septicemias are caused by *B. pseudomallei* with an approximate lethality rate of 50% (51, 152). Due to a gradually increasing awareness of this pathogen by the medical professionals world wide, it is likely that the incidence of diagnosis will continue to climb.

There are three possible routes of exposure for *B. pseudomallei*. Inhalation and inoculation are the two primary routes of infection with seasonal increases in infection during the monsoon season (70, 138). Occupational or recreational exposure to standing water and mud (36), especially in individuals working in flooded rice paddies was determined as the dominant risk factor in Southeast Asia (61, 69, 135). These two routes of infection most frequently result in either a

pneumonic or cutaneous infection, respectively. The final route of infection is ingestion with several outbreaks in Australia having been attributed to contaminated drinking water (34, 35, 42, 66).

After the initial infection, the bacterium migrates through the body and forms abscesses in a variety of locations, including but not limited to the liver, spleen, brain, prostate, salivary glands, joints, and eyes (80). Due to the multiple routes of infection and the diversity of the localization of disseminated infection, the clinical presentations are highly variable. In a recent review, Wiersinga and van der Poll identify and discuss over 30 clinical features or manifestations of melioidosis (153). A number of host factors predispose individuals to acquiring the disease. Additionally, the bacteria are capable of remaining dormant for many years before manifesting any symptomatic disease. In one case, a Vietnam veteran was diagnosed with melioidosis 29 years after the supposed exposure (27). In a more recent study, a World War II veteran and former Japanese prisoner of war was diagnosed with a cutaneous *B. pseudomallei* infection 62 years after returning to the United States (95). These long periods of inactivity by the bacterium has led to the moniker of "the Vietnamese Time Bomb (54)" as over 250,000 American Vietnam veterans may be carriers of *B. pseudomallei* (150).

I.A.ii. Intracellular Survival and Virulence Mechanisms

I.A.ii.a. Intracellular Survival

There is multiple *in vitro* infection models that demonstrate *B. pseudomallei* can survive phagocytosis and replicate within neutrophils and monocyte derived cells (81). Upon internalization (Figure I.1), *B. pseudomallei* can reside in membrane bound vesicles, specifically phagolysosomes, or escape the endocytic vesicle and reside in the cytoplasm of the host cell (55, 105, 124). *B. pseudomallei* can prevent the activation of nitric-oxide synthase (iNOS) and the subsequent production of reactive nitrogen intermediates (16, 17, 143, 144). *B. pseudomallei* can inhibit DNA and protein synthesis of the phagocytic cells (90). *B. pseudomallei* escapes endocytic vesicles in as little as 15 minutes after internalization by lysing the endosomal membranes (93, 127, 129). Once in the cytoplasm, *B. pseudomallei* replicates and is propelled through the cell by inducing polar actin polymerization (55, 117, 129). These actin tails push the bacteria until they form membrane protrusions into adjacent cells (75), thereby allowing the bacteria to spread from one host cell to the next without re-exposure to the extracellular space and the innate immune system. Large multinucleated giant cells (MNGCs), resulting from cellular fusions between infected monocytes, form both in *in vitro* tissue culture and in human tissue infected with *B. pseudomallei* (60, 75, 158), however the mechanism required for this bacterial induced cellular fusion is unknown.

I.A.ii.b. Animal Infections with Melioidosis

B. pseudomallei is pathogenic to many animals in the endemic areas, including camels, horses, sheep, cattle, goats, pigs, kangaroos, koalas, alpacas, deer, cats, dogs, and marine mammals and to a lesser extent water buffalo, crocodiles, and birds (51, 152, 154). These diverse animal hosts are potential carriers for worldwide dissemination of *B. pseudomallei* via international transport of infected animals. In the laboratory setting, mice, rats, guinea pigs, hamsters, chickens, and amoeba have been utilized to study the pathogenesis of *B. pseudomallei* (51). Presently, the preferred animal models of infection include the Syrian hamster and the BALB/c mouse, representing acute and chronic disease manifestations, respectively. Utilization of these animal model systems has led to the identification and characterization of numerous virulence factors of *B. pseudomallei*, including extracellular macromolecules, intercellular signaling molecules, and numerous secretion systems.

I.A.ii.c. Identified Virulence Factors

I.A.ii.c.1. Polysaccharide

Bacterial polysaccharides are composed of variable chain lengths of saccharide molecules. These macromolecules, often greater than 100 kiloDaltons in size, have a wide range of functions: a structural component of the cell wall, protection of the bacteria from harsh environmental conditions, and helping pathogenic bacteria

evade the immune system. Four types of O-polysaccharides (O-PS) are identified in *B. pseudomallei*.

The first characterized polysaccharide of *B. pseudomallei* is that of the capsular exopolysaccharide (EPS) (123). When EPS is absent from the bacteria, there is an increased deposition of C3b on the bacterial surface leading to increased complement sensitivities (44, 106). While an acapsular mutant of *B. pseudomallei* survives internalization by macrophage, escapes the phagosome, and replicates in the cytoplasm, mice infected with EPS mutants have repeatedly increased LD_{50}s ranging from 10^4 to $>10^5$ when compared to the wild type *B. pseudomallei* LD_{50} of $\sim 10^2$, (106).

Type II O-PS is the second O-PS identified and characterized in *B. pseudomallei* (40, 112). This O-PS is the predominant lipopolysaccharide produced by *B. pseudomallei* species. Strains without the Type II O-PS have increased LD_{50}s in multiple studies in a variety of animal models and infection routes (6, 18, 94, 112, 155). At least part of this attenuation is due to impaired survival in macrophages.

The publication of the genomic sequence of the *B. pseudomallei* K96243 strain allowed for the identification of two additional genetic loci encoding biosynthetic genes for Type III O-PS and Type IV O-PS (107). Insertion disruption these two loci revealed that, although the Type IV O-PS locus plays a role in virulence, the Type III O-PS does not (112).

I.A.ii.c.2. Quorum Sensing

Quorum sensing is the mechanism by which bacteria produce, monitor and respond to extracellular signals and is important in protease production, biofilm formation, siderophore production, protease production, phospholipase C secretion, oxidative stress response, and pathogenesis of *B. pseudomallei*. Homoserine lactone (HSL) molecules synthesized by LuxI homologues and secreted to the extracellular environment. As the extracellular concentration of HSL molecules increases, there is positive feedback for the expression of *luxI* homologues and a concomitant increase in the production of HSL molecules. The LuxR family of transcription factors monitors the concentration of HSL molecules through binding with their respective cognate HSL molecules, which in turn allows for the modulation of the LuxI homologue gene expression. In addition to these classical quorum-sensing systems, *B. pseudomallei* strains also produce a newly described class of signaling molecules known as the quinolone signaling systems (146).

I.A.ii.c.2.1. BpsIR Quorum Sensing Systems

There are three *luxI* homologues encoded within the genome of *B. pseudomallei* encoding for proteins that synthesize the signaling molecules (43, 65, 118). The number of total molecules produced is dependent upon the strain of *B. pseudomallei* studied (118). The three *luxI* and five *luxR* homologues in *B. pseudomallei* K96243 genome (65) are referred to as $bpsI_{1\text{-}3}$ and $bpsR_{1\text{-}5}$, with $bpsIR_{1\text{-}3}$ co-localizing at divergent promoters and $bpsR_{4\text{-}5}$ existing as orphan open reading frames (141).

B. pseudomallei strains K96243 produces three HSL molecules, *N*-octanoyl-homoserine lactone (C8HL), *N*-(3-hydroxy-octanoyl)homoserine lactone (OHC8HL), and *N*-3-hydroxy-decanoyl)homoserine lactone (OHC10HL) (43, 76, 118, 120). When the HSL synthase molecules of the KHW strain were independently expressed in *E. coli*, $BpsI_1$ induced the production of C8HL, OHC8HL and OHC10HL, while $BpsI_2$ produced OHC8HL, OHC10HL, and OHC12HL, and the $BpsI_3$ molecule resulted in production of OHC8HL and OHC10HL (52). The *bpsIR* expression and subsequent secretion of the HSL molecules is regulated by the growth-phase with the $bpsIR_1$ system up regulated during stationary phase and the $bpsIR_2$ and $bpsIR_3$ up-regulated during exponential growth (52, 76).

Several studies have looked at the roles of each of the HSL systems in *B. pseudomallei* pathogenicity. Mutants in the $BpsIR_1$, $BpsIR_2$, $BpsIR_3$ and $BpsR_5$ genes have significant increases in the LD_{50} from 100 to 1000 fold over wild type, and an increased time to death in the inhalation model of infection in BALB/c mice (141). Mutagenesis of $bpsI_1$ and $bpsI_3$ results in decreased biofilm formation, hyersusceptibility to oxidative stress, increased production of siderophores and decreased phospholipase C production (52, 85, 141).

I.A.ii.c.2.2. 4-Hydroxy-2 Alkylquinoline Signaling Molecules

Pseudomonas species secrete an additional class of signaling molecules, the 4-hydroxy-2 alkylquinolines (HAQs) (41, 162). These molecules are synthesized via the PqsABCDE system, act in a manner similar to HSL (15), and are partially

regulated via the HSL systems (82). HAQ molecules are also secreted by *B. pseudomallei* and negatively affect the expression of the HSL molecules (146). *B. pseudomallei* mutants without HAQs result in strains with increased antifungal production, increased proteolytic activity, and increased siderophore secretion (146).

I.A.ii.c.2.3. Quorum Sensing and Efflux Transport Systems Crosstalk

One important concern for *B. pseudomallei* infection is its intrinsic resistance to a wide variety of antibiotics (65). The BpeAB-OprB is responsible for resistance to several aminoglycosides and macrolides (25). The expression of *bpeAB-oprB* is dependent upon the presence of one of its substrates, erythromycin, and entry into stationary phase of growth (24). This growth phase dependence of expression is mediated by the presence of C8HL and C10HL (26, 89). Strains lacking the *bpeAB-oprB* quorum sensing systems failed modulate siderophore secretion, phospholipase C production, and biofilm formation (24). The *bpeAB-oprB* locus is required for the secretion of HSL molecules but not for their intracellular production (26).

The activity of the BpeAB-OprB efflux pump is strain dependent (89). In the *B. pseudomallei* 1026b strain, the *bpeAB-oprB* locus functions as a broad-spectrum drug efflux system and plays a role in biofilm formation, but has no role in quorum sensing, siderophore production, or aminoglycoside secretion (89). This strain specific function of the *bpeAB-oprB* is of importance to our research into the role of

siderophores in virulence and as yet, the role of *bpeAB-oprB* has not been elucidated in the K96243 strain of *B. pseudomallei*.

I.A.ii.c.3. Flagellin

B. pseudomallei motility is conferred by the presence of a polarly located flagellum (150). Conflicting data exists as to whether the presence of a flagellum contributes to the virulence. A transposon mutagenesis screen identified 28 non-motile mutants with the majority of the mutations occurring in genes related to flagellar and chemotaxis genes (39). There was no significant difference in the virulence of a *fliC* mutant relative to the parental 1026b wild type strain when infected intraperitoneally in infant diabetic rats or Syrian hamsters (39). A later study demonstrated that an isogenic *fliC* deletion mutant in the KHW strain of *B. pseudomallei* had an LD_{50} >13,500 CFU when intranasally and intraperitoneally infecting BALB/c mice as compared to <100 CFU for the wild type strain (29).

I.A.ii.c.4. Secretion Systems

I.A.ii.c.4.1. Type II Secretion System

A single type II secretion system (T2SS) was identified in *B. pseudomallei* (65). This T2SS is required for secretion of multiple exoproducts, including protease, lipase, and phospholipase C (38). The *B. pseudomallei* genome encodes for three phospholipase C (Plc) proteins (77) that function to process phospholipids into fatty acids and other lipophilic derivatives. To date, only Plc-3 plays a role in virulence.

Expression of *plc-3* is up regulated in the Syrian hamster model of infection, and a *plc-3* deletion mutant has an increased LD_{50} of 4.5 x 10^4 CFU (versus the wild type LD_{50} of <10 CFU) (77).

The T2SS is encoded in 14 genes (BPSL0007-BPSL0018, BPSL3009-BPSL3010) (38). A *gspD* deletion mutant that lacks a structural component of the translocon was mildly attenuated in virulence (13 fold) (38) and thereby suggesting that the T2SS has a minimal role in acute infection. The role of the T2SS in chronic infections has yet to be elucidated.

I.A.ii.c.4.2. Type III Secretion Systems

Type III secretion systems (T3SS), which encode for needle-like structures used to translocate effector proteins into the cytoplasm of the host cells, are found in the genomes of a wide variety of both animal and plant gram-negative bacterial pathogens (10, 133). T3SS proteins can be subclassifed into three groups: structural apparatus, translocation apparatus, and effector proteins. The proteins in the structural apparatus form the needle complex that transport the effector proteins from the cytoplasm of the bacterial cell, through both the bacterial cell membranes and to the translocation apparatus that forms a pore in the host membrane. *B. pseudomallei* encodes for three T3SS (65), with T3SS-3 (also known as the *Burkholderia* secretion apparatus (Bsa)) contributing virulence in animals (21, 91, 100, 128, 133).

The third T3SS (T3SS-3) has significant homology to the *Salmonella typhimurium inv/spa/prg* and the *Shigella flexneri ipa/mxi/spa* T3SSs (130). Mutants in the T3SS apparatus (*bsaZ*), translocation apparatus (*bipB, bipC, bipD*), and putative effector proteins (*bopE, bopA, cif*$_{Bp}$) display variable levels of *B. pseudomallei* attenuation in animal models of infection (133).

I.A.ii.c.4.2.1. T3SS-3 Structural Apparatus: BsaZ

BsaZ is homologous to the *Salmonella typhimurium* T3SS structural protein SpaS (130). Mutagenesis of *bsaZ* resulted in significant attenuation of *B. pseudomallei* virulence in the Syrian hamster model (126). The mechanism of attenuation is unclear. Pilatz, et al. reported a significant decrease in intracellular survival, decreased membrane protrusions and actin rearrangements, and inability to escape phagocytic vesicles in the J774.2 cell line (100), while Burtnick, et al. observed delayed intracellular replication and vacuolar escape in RAW 264.7 macrophage cells (21). Combined these two reports indicate that the *bsaZ* mutation results in decreased survival or in delayed replication in the host.

I.A.ii.c.4.2.2. T3SS-3 Translocation Apparatus: BipB, BipC, and BipD

BipB, BipC, and BipD are homologous to the *S. typhimurium* T3SS translocation proteins SipB, SipC, and SipD, respectively (130). As with the *bsaZ* mutant, mutagenesis of *bip* genes results in attenuated virulence in the Syrian hamster and BALB/c mouse models of infection (126, 128). Recently the structure of BipD was

solved and showed a protein containing two long alpha helixes that form a long helical coil-coil with two small globular domains (pal 2010, Erskine 2006). It is believed that BipD oligomerizes in the host membrane forming a translocation pore for the effector proteins (pal 2010).

I.A.ii.c.4.2.3. T3SS-3 Effectors: BopE, BopA, and Cif_{Bp}

BopE is homologous to the *S. typhimurium* proteins SopE and SopE2 (126). BopE induces membrane ruffling of the host cell and promotes actin rearrangements through its activity as a guanine nucleotide exchange factor for the host cell Rho family GTPases (142). Mutagenesis of *bopE* resulted in attenuated survival of *B. pseudomallei* in J774.2 macrophage cell culture models but no change in virulence in the BALB/c mouse model (128). Although BopE is important for intracellular survival *in vitro*, its contribution to infection is minimal.

BopA is homologous to the *S. typhimurium* protein SopA (128). A *B. pseudomallei bopA* mutant displays decreased intracellular survival and increased co-localization with autophagy marker LC3 (53). Autophagy is a mechanism by which host cells capture infectious agents in double-membrane bound vacuoles and traffic them to lysosomes for clearance. Data suggests that *B. pseudomallei's* ability to survive intracellularly is in part due to its ability to avoid autophagic clearance and this is likely mediated by BopA (32). *B. pseudomallei bopA* mutants are mildly attenuated for virulence in the BALB/c mouse model (53).

Cif_{Bp} is homologous to the *Escherichia coli* Cif protein (cycle inhibiting factor, Cif_{Ec}), which is part of a family of proteins known as cyclomodulins (73). Cyclomodulins promote or inhibit cell cycle progression. It is believed that Cif_{Bp} is delivered to the host cell through T3SS-3 and may have a role in *B. pseudomallei's* ability to form multinucleated giant cells (MNGCs) as secretion of Cif_{Bp} by *E. coli* was able to halt cell cycle progression (161).

I.A.ii.c.4.3. Type IV Pili

Eight type IV pili (TFP) loci were identified in the *B. pseudomallei* K96243 genome with five loci comprising pilus associated synthesis operons (46). Mutagenesis of *pilA* in *B. pseudomallei* resulted in reduced adhesion to human epithelial cells and log reduction in virulence upon intranasal infection of BALB/c mice (12, 46).

I.A.ii.c.4.4. Type VI Secretion System

Type VI secretion systems (T6SSs) have recently been identified and characterized in a wide range of pathogenic Gram-negative bacteria (13, 72). These loci were originally termed IcmF-associated homologous protein (IAHP) clusters due to the homology between one of the T6SS genes and *icmF* of *Legionella pneumophila*'s type IV secretion system (T4SS) (67, 115). The structural components of the T6SSs are highly homologous to the structural components of T4 bacteriophage tail (13).

The *B. pseudomallei* K96243 genome encodes for six T6SS (20). T6SS-5 contains multiple genes unregulated twelve fold or more during macrophage

infection (115). A more recent study observed that the *hcp1* gene of T6SS-5, a predicted structural protein for the tube structure, is required for virulence (LD_{50} of $>10^3$ as opposed to the wild type LD_{50} of <10 in the Syrian hamster model of infection), multinucleated giant cell formation, intracellular growth, and cytotoxicity towards RAW 264.7 macrophage (20).

I.A.ii.c.5. BimA

Intracellular trafficking and cell-to-cell spread for *B. pseudomallei* is dependent upon polar actin polymerization via BimA (*Burkholderia* intracellular motility protein A) (129). BimA localizes to one pole of the bacterium were it stimulates actin polymerization (125). *B. pseudomallei bimA* mutants are incapable of inducing actin polymerization or initiating cell-to-cell spread (129). However, this strain survives phagocytosis and replicates in the host cell cytoplasm like wild type (129). A null mutant of *bimA* is attenuated in the murine model of melioidosis (117).

I.A.ii.c.6. MviN

MviN in *E. coli* contributes to the transmembrane transport of peptidoglycan precursors across the inner membrane (71). Ling, et al. showed that *mivN* is up regulated in iron-limiting medium and is essential for the virulence of *B. pseudomallei* (84). The LD_{50} for this mutant in the Syrian hamster model was 6.8 x 10^5 CFU while the wild type showed an LD_{50} of <10 CFU (84). This study used a mutant that was prematurely truncated due to a cassette insertion in the open

reading frame and was unable to generate a deletion mutant. This suggests that *mviN* may be essential for bacterial growth (84). Further studies need to be conducted to elucidate the role of this protein in *B. pseudomallei.*

I.B. Bacterial Iron Acquisition

Iron is an essential element for most organisms. At physiological conditions, iron exists as either the soluble ferrous Fe^{2+} form or the insoluble ferric Fe^{3+} form. Environmental iron is predominately insoluble ferric iron and therefore biological systems have developed an array of mechanisms for iron acquisition. To overcome the insolubility of ferric iron, bacteria can employ three methods: decreasing environmental pH to increase solubility of ferric iron, reducing ferric iron to ferrous iron, and utilizing ferric iron chelators to solublize the iron (58, 59). The bacterial mechanisms for iron chelation and acquisition are comprehensively reviewed elsewhere (4, 88) and are summarized below.

I.B.i. Multiple Routes of Iron Acquisition and Roles in Virulence

Almost all organisms require iron for survival due to its importance a variety of cellular processes, including acting in energy generation, oxygen transport, and protection against oxidative stress. However, too much intracellular iron can result in the production of free oxygen radicals through the Fenton reaction (113). Hosts minimize free iron to not only prevent DNA damage but to also suppress the growth of pathogens. Extracellular iron sequestration is primarily provided by the serum

protein transferrin and secretory fluid protein lactoferrin while intracellular iron complexes with enzymatic proteins as a co-factor or in the ferritin iron storage protein. The resulting free extracellular iron concentration is approximately 10^{-18} M in humans (19), well below the 10^{-9} M required for bacterial growth. To circumvent this iron sequestration, pathogenic bacteria employ several methods to free the bound iron.

Transferrin and lactoferrin receptors located in the bacterial outer membrane bind host transferrin and lactoferrin molecules. While bound to the outer membrane receptors, the iron ions are stripped from the sequestering proteins and internalized while the proteins are released back into the extracellular environment. This system is dependent upon an outer membrane receptor and an inner membrane TonB-ExbB-ExbD system to transduce energy from the proton motive force to the outer membrane receptor (Figure I.2). Once ferric iron reaches the periplasmic space it is bound by a ferric-binding protein and delivered to an ABC permease system for transport across the inner membrane.

Heme is the most abundant iron binding protein in the body and pathogenic bacteria can use heme as an iron source during infection. However, heme is not freely available in the host as it predominately resides within red blood cells and complexes with hemoglobin. Extracellular pathogens liberate the heme and hemoglobin from red blood cells through the production of a variety of hemolysins and proteases. Although the heme may be rapidly bound by the host's extracellular heme binding proteins (hemopexin, albumin), freed heme molecules may be directly

taken up by bacteria through receptor/TonB/ABC permease systems similar to that seen in the acquisition of iron from transferrin and lactoferrin. The bacteria may also utilize the extracellular binding proteins as sources for heme.

A third, and the most widely utilized, mechanism for bacterial iron acquisition in both the environment and in host interactions is the production and uptake of ferric binding siderophores. Siderophores frequently have higher biding affinities to ferric iron than that of the sequestering proteins, both intracellular and extracellular, and are able to strip the ferric iron from the protein complex for bacterial utilization. The siderophore system is described in more detail below.

I.B.ii. Iron Acquisition by Siderophores

Siderophores are small molecular weight compounds, typically less than 1000 daltons (22), synthesized and secreted by bacteria and fungi in response to iron restricted growth conditions. However, some remain associated with the cell envelope (example: mycobactins of mycobacteria) (104). Although in most cases it is unknown how the polar siderophores are secreted through the membrane, work by McIntosh and colleagues showed that the *E. coli* enterobactin requires the protein EntS (49). Siderophores are usually assembled by non-ribosomal peptide synthetases and utilize core groups of hydroxamates, carboxylates, and catechols as the iron binding ligand. Siderophores have extremely high specificity and affinity to ferric iron where affinity coefficients frequently exceed 10^{30} (22). To date over 500 siderophores have been identified and classified based upon the core group utilized

for iron binding. The following information regarding ferric siderophore uptake focuses on systems described for Gram-negative bacteria.

Uptake of ferric bound siderophores requires the expression of siderophore-specific receptors. Bacteria frequently produce receptors for both endogenously and exogenously produced siderophores. The receptors are structurally related and composed of a 22 β-strand tube structure with a plug domain situated within the tube. Binding of the receptor specific ferric siderophore results in a structural change occurs allowing the ferric siderophore to pass through the outer membrane (48). The energy required for this structural shift of the receptor and subsequent transport of the ferric siderophore complex is transduced from the inner membrane to the outer membrane receptor via the TonB-ExbB-ExbD protein complex (Figure I.2) (64).

The C-terminus of the TonB systems in integrated into the inner membrane with the remaining N-terminus spanning the periplasmic space to interact with the outer membrane receptor via the "TonB Box" (101). The two inner membrane proteins ExbB and ExbD are required for the transduction of the energy generated by the inner membrane's proton motive force through the TonB protein to the outer membrane receptor (101). Several species of bacteria contain multiple TonB systems required for functional uptake by specific outer membrane ferric siderophore receptors (78). In species that possess multiple TonB systems, these systems, a fourth inner membrane localized protein, TtpC, is required for the energy transduction (132).

It most cases the ferric siderophore complex is transported through the inner membrane via ABC transport systems. Once in the cytoplasm, the ferric iron is released from the siderophore either through reduction of the ferric iron and recycling of the unmodified siderophore or degradation of the siderophore immediately followed by the reduction of the ferric iron (68, 148).

I.B.iii. Characterized Iron Acquisition Systems by B. pseudomallei

B. pseudomallei produces the hydroxamate siderophore malleobactin. Early studies demonstrated that malleobactin synthesis is regulated by growth phase, inversely dependent upon the iron concentration of the growth medium, and can overcome growth deficits induced by the addition of iron chelators (159, 160). Purified malleobactin can acquire iron bound to the human glycoproteins transferrin and lactoferrin. However, malleobactin cannot acquire cell-sequestered iron, distinct from the catechol siderophores pyochelin and azurchelin (160).

Two published microarray analyses identified a combined total of over 300 *B. pseudomallei* genes differentially regulated under iron restriction (2, 140). However only 32 were differentially regulated in both studies. Of these, one locus is of particular interest because it encodes proteins with potential roles in the synthesis and uptake of the malleobactin siderophore (BPSL1774 through BPSL1787). This locus was up regulated from 2 to 25 fold under iron limitation (Figure I.3) (2). Further analysis indicated this locus produced three small molecular weight siderophores with molecular weights ranging from 635 to 789

daltons, as determined by mass spectrophotometry, in two different fractions following phase separation. Both fractions complemented growth defects in a *B. pseudomallei* malleobactin-negative strain grown under iron limitation (2). This study also demonstrated that BPSL1787 is the sigma factor controlling the expression of the malleobactin locus, therefore it was named *mbaS*. Sequence analysis identified BPSL1775 as the putative receptor responsible for the uptake of ferric-malleobactin. This function was confirmed through the generation of a deletion mutant that had increased malleobactin production but decreased growth under iron limitation (2). The role of BSPL1776 in malleobactin synthesis was demonstrated via a deletion construct that failed to produce the siderophore and could only grow in iron limiting medium with the addition of exogenous malleobactin.

I.C. Iron Regulation of Gene Expression

Genes encoding iron acquisition, storage, oxidative stress response, and a variety of other functions are regulated in an iron-dependent manner by the ferric uptake response (Fur) protein in most bacteria. Fur is a repressor that, when bound to ferrous iron, binds to promoter elements of Fur regulated genes and prevents transcription. Homodimerization of the 17 kiloDalton Fur subunits and subsequent DNA binding requires ferrous iron (30, 131). The Fur DNA binding sequence was originally proposed as the palindromic 19 base pair sequence GATAATGAT($^{A}/_{T}$)ATCATTATC (37). However, a more comprehensive sequence

analysis of Fur responsive promoters proposed that the Fur binding site is instead composed of three repeats of a six base pair sequence:

NAT([A]/[T])AT/NAT([A]/[T])AT/N/AT([T]/[A])ATN (45).

Fur often regulates the expression of "iron starvation" sigma factors. Two well-characterized systems include FecR of *E. coli* for ferric citrate transport system (5) and PvdS of *P. aeruginosa* for ferric pyoverdine transport (147).

I.C.i. Sigma Factors and Transcription

Sigma factors are DNA binding proteins that function to recruit the RNA core polymerase complex (composed of the five subunits ααββ'ω) and allow for the initiation of transcription. Sigma factors are divided into two groups, those with homology to *E. coli* σ^{70} or σ^{54}, based upon sequence (87). Most bacteria contain multiple of σ^{70} homologues and only one or two σ^{54} homologues. Table I.1 identifies the sigma factors of *E. coli* and the functions of their characterized regulons. The following review will focus solely on the σ^{70} family members.

σ^{70} homologues are divided into four groups based upon conserved sequence and function (98). The first group contains the essential sigma factors that are closely related to σ^{70}. The second group included non-essential σ factors that are closely related to σ^{70}. The third group is those sigma factors more distantly related in sequence to σ^{70} that regulate the expression of genes associated with heat-shock, bacterial sporulation, or flagellar biosynthesis. The fourth, and most divergent, group contains the extracytoplasmic function (ECF) sigma factors. ECF sigma

factors respond to signals from the environment to activate the expression of genes whose proteins function in adapting to those environmental signals. The fourth group is further composed of two subgroups (56, 74). The first contains those sigma factors whose function is modulated though anti-sigma factors (termed ECF sigma factors) and the second subgroup is composed of the remaining sigma factors in this group (termed alternative sigma factors).

Of particular interest to the work presented herein are the ECF and alternative sigma factors of group four. Our work has focused on the characterization of MbaS, which shows significant conservation to PvdS (45% identity and 61% homology). PvdS, an ECF sigma factor of *Pseudomonas aeruginosa,* is one of the most well characterized of the ECF sigma factors (reviewed in (102, 114, 145). PvdS and its homolog FpvI activate the expression of the genes necessary for the synthesis and uptake of the *P. aeruginosa* siderophore pyoverdine. PvdS expression is regulated via Fur in an iron-responsive manner (33). Once expressed, PvdS is sequestered at the inner membrane via interactions with the anti-sigma factor FpvR. The expression of FpvR also increases under iron-limiting growth conditions and thus the active intracellular levels of PvdS are maintained at a minimum. This sequestration of PvdS results in the maintenance of a basal expression of PvdS-regulated genes and subsequent pyoverdine production (116). It has been proposed that in addition to minimizing the levels of active PvdS, the FpvR-PvdS interaction protects PvdS from proteolytic turnover (108, 109). FpvR spans the inner membrane and interacts with the periplasmic tail of the pyoverdine

receptor FpvA in the outer membrane. Binding of either apo-pyoverdine or ferric-pyoverdine to the outer membrane FpvA receptor results in a signal cascade through FpvR that results in the release of the sequestered PvdS. The release of PvdS results in an increase in the expression of PvdS-regulated genes. Such response to an extracellular signal, in this case pyoverdine, is the defining aspect of ECF sigma classification.

The functional domains of σ^{70} are well characterized (Figure I.4, and Figure I.5) (62). The first, Region 1, is the least conserved and plays a role in regulating DNA binding, transcription initiation, and formation of the open DNA complex. Region 2 is the most widely conserved and is further divided into four subregions. Region 2.1 and 2.2 are required for RNA core polymerase binding and DNA melting, while regions 2.3 and 2.4 function in the recognition of the -10 DNA binding sequence in the sigma-specific promoters. Region 3 is less well conserved and is presumed to play a role in the binding of the RNA core polymerase complex. Region 4 contains the helix-turn-helix motif required for recognition of the -35 DNA binding site in the sigma-specific promoters (See Figure V.8). All σ^{70} homologues maintain two of four characterized domains from σ^{70}, regions 2 and 4.

The crystal structure of the *E. coli* RpoF (σ^{28}) interacting with the anti-sigma factor FlgM elucidated not only the tertiary structures of each region but also how anti-sigma factors preclude sigma factor interactions with RNA polymerase and DNA (Figure I.5) (121). FlgM wraps around the sigma factor to interact with the -10 DNA and RNA polymerase binding sites of Region 2 and Region 4.1.

I.C.ii. Iron Responsive Sigma Factor of B. pseudomallei

MbaS is the iron responsive sigma factor of *B. pseudomallei*. A series of experiments were conducted to determine if MbaS is regulated in the same ECF manner as PvdS (2). While PvdS is sequestered by the FpvR anti-sigma factor, it appears unlikely that there is corresponding MbaS anti-sigma factor as the *B. pseudomallei* microarray studies identified no anti-sigma factors unregulated under iron limitation (2, 139). The FpvR anti-sigma factor interacts with a periplasmic tail of the pyoverdine receptor FpvA. The malleobactin receptor FmtA (BPSL1775) does not appear to have a periplasmic tail via topology prediction (PredictProtein (111) www.predictprotein.org)). Finally, addition of exogenous malleobactin did not increase the expression of MbaS-regulated genes, as is seen with PvdS. Therefore, these two conserved sigma factors are likely regulated in a different manner. The predicted regulatory cascade of the malleobactin loci is depicted in Figure I.6. Fur represses MbaS expression under iron sufficient growth conditions. Upon iron limitation, Fur repression is relieved and MbaS is expressed, which in turn activates the expression of genes required for malleobactin biosynthesis and uptake. Once iron homeostasis has been achieved the malleobactin loci is again suppressed through the binding of Fur to the *mbaS* promoter.

I.D. Figures

Figure I.1: Intracellular Survival of *B. pseudomallei*

After phagocytosis by monocyte-derived cells (1), *B. pseudomallei* can either reside in the phagolysosome or escape into the host cell cytoplasm (2) where it can then replicate (3). *B. pseudomallei* can move throughout the host cell, force cell protrusions and infect neighboring cells through the formation of an actin tail(4). Differences in iron availability when the bacteria are extracellular as opposed to intra-phagosomal or cytoplasmic necessitate tight regulation of iron homeostasis for pathogenic bacteria.

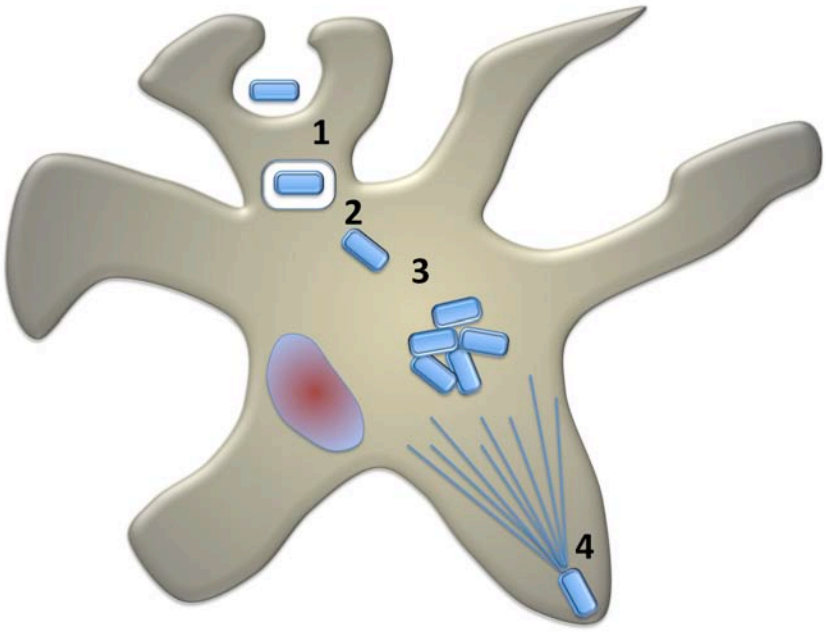
1
2
3
4

Figure I.2: Energy Dependent Iron Acquisition

Energy dependent iron acquisition in bacteria maintain a core family of proteins regardless of iron source (ex: transferrin, heme, siderophore). The iron-containing complex is recognized by a receptor in the outer membrane (OM). Iron (with or without the complexing molecule) is transported to the periplasmic space via energy derived from the inner membrane (IM) proton motive force. This energy is transduced to the receptor via the TonB-ExbB-ExbD system. The iron molecule is then transported across the inner membrane via an ABC transport system composed of a periplasmic protein, a permease, and an ATPase.

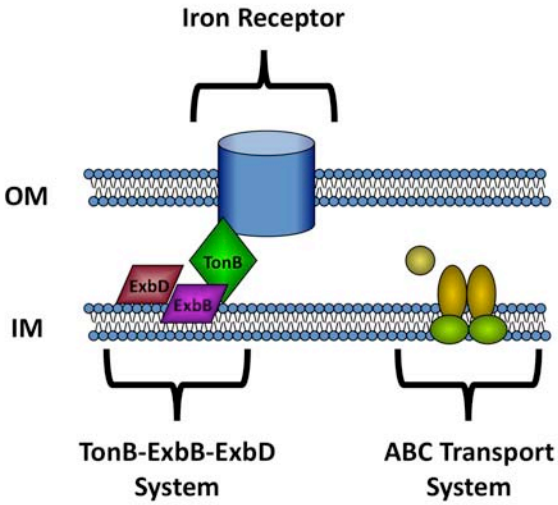
Iron Receptor
OM
TonB
ExbD
ExbB
IM
TonB-ExbB-ExbD
System
ABC Transport
System

Figure I.3: The Malleobactin Locus Response to Iron Limitation

Adapted from Alice, et al., 2006 (2). This figure indicates the relative expression of genes in the malleobactin locus under iron limitation compared to iron replete conditions. These genes include an outer membrane receptor (*fmtA*), multiple genes required for siderophore synthesis (*mbaF, mbaA, mbaI, mbaJ,* and *mbaE*), and a putative ECF sigma factor (*mbaS*).

The Malleobactin System of *B. pseudomallei*

***B. pseudomallei* ORFs**

BPSL1774-1787

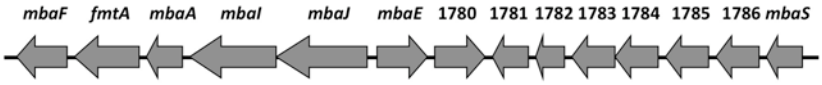

Gene Name / ORF	Proposed Function	Induction Levels (fold -Fe/+Fe)
mbaF **(BPSL1774)**	**N^5-hydroxyornithine transformase**	**7.9**
fmtA **(BPSL1775)**	**malleobactin receptor**	**5.1**
mbaA **(BPSL1776)**	**L-ornithine-N^5-oxygenase**	**7.2**
mbaI **(BPSL1777)**	**non-ribosomal peptide synthetase**	**2.4**
mbaJ **(BPSL1778)**	**non-ribosomal peptide synthetase**	**5.3**
mbaE **(BPSL1779)**	**ABC transporter**	**4.4**
BPSL1780	**hypothetical protein**	**No Change**
BPSL1781	**periplasmic iron binding protein**	**No Change**
BPSL1782	**ferric iron reductase**	**No Change**
BPSL1783	**iron transport related membrane proteins**	**No Change**
BPSL1784	**iron transport related ATP-binding protein**	**12.3**
BPSL1785	**sim to syrP (Streptomyces verticillus)**	**7.7**
BPSL1786	**sim to mbtH (Mycobacterium tuberculosis)**	**25.5**
mbaS **(BPSL1787)**	**ECF sigma factor**	**9.5**

Table I.1: Sigma Factors of *Escherichia coli*		
Sigma Factor	Regulon Function	Regulation of Sigma Factor
σ^{54} (RpoN)	Nitrogen-Limitation Adaptation	Induced Expression Under Nitrogen Limitation (110)
σ^{70} (RpoD)	General Housekeeping	Maintained (103)
σ^{38} (RpoS)	Nutrient Starvation and Stationary Phase Adaptation	Induced Expression Upon Entry to Stationary Phase, Protein Regulation via Two Component Response Regulators and Proteolysis (63)
σ^{32} (RpoH)	Heat Shock Adaptation	Induced Expression Upon Heat Shock and Proteolysis (7)
σ^{28} (RpoF)	Flagellar Biosynthesis	Induced Expression Dependent Upon Mechano-sensing and Growth Phase, Protein Expression Regulated by Anti-Sigma Factor (3, 9)
σ^{24} (RpoE)	Extracytoplasmic Signal Response	Induced Expression Upon Extracellular Signal, Protein Regulation Via Anti-Sigma Factor, Proteolysis Regulation (96)
σ^{19} (FecI)	Ferric Citrate Uptake	Induced Expression Upon Iron Limitation, Protein Regulation Via Anti-Sigma Factor (14)

Figure I.4: σ^{70} and RNA Core Polymerase Schematic Diagram

RNA core polymerase requires a sigma factor for the identification of promoter elements and transcription initiation. A: RNA core polymerase is composed of five subunits. The two α subunits are capable of interacting with upstream transcriptional elements to increase binding to the promoter. β and β' are the functional core of the complex and interact with the DNA sequence recognition σ factor. The function of the ω subunit has yet to be characterized. B: σ^{70} proteins recognize specific DNA sequences known as the -10 and -35 DNA promoter domains. The -10/-35 DNA sequence lie upstream of the transcription initiation site, the ribosome binding site (RBS), and the translation initiation site. Regions 2.3 and 2.4 of the sigma factor are specific for the -10 DNA sequence while the 4.2 region mediates interaction with the -35 DNA sequence. σ^{70} factors interact with the β subunits to recruit the RNA core complex and to initiate transcription.

A:

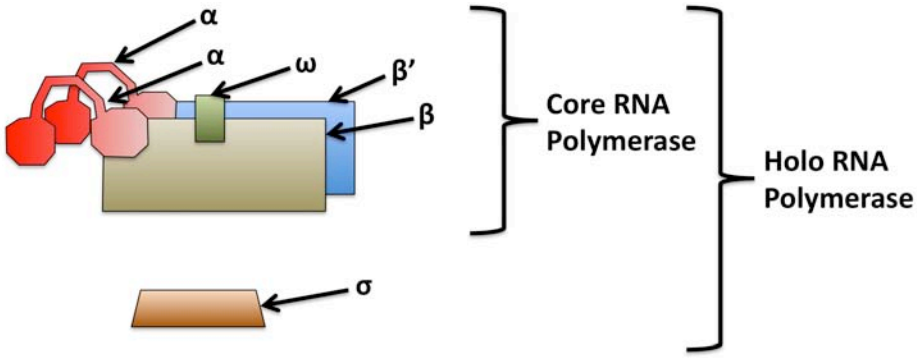
α
α
ω
β'
β
σ
Core RNA Polymerase
Holo RNA Polymerase

B:

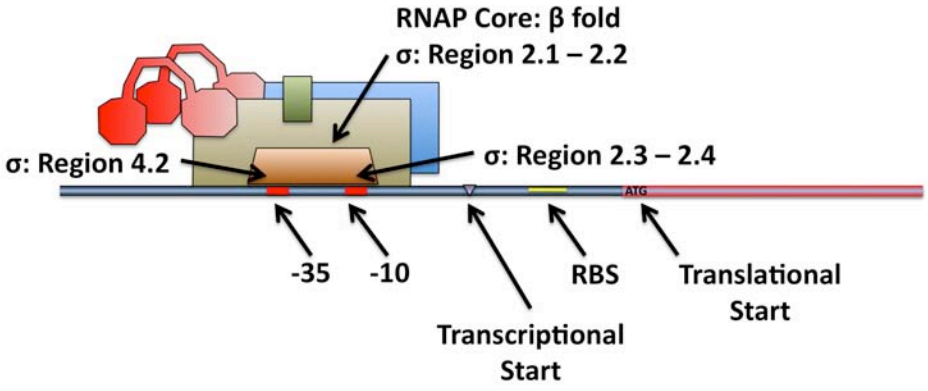
RNAP Core: β fold
σ: Region 2.1 – 2.2
σ: Region 4.2
σ: Region 2.3 – 2.4
ATG
-35
-10
RBS
Translational Start
Transcriptional Start

Figure I.5: Crystal Structure of RpoF (σ^{28})

Crystal structure of *E. coli* σ^{28}/RpoF complexed with the anti-sigma factor FlgM. The crystal structure was solved by Sorenson, et al. (121) and accessed 6/4/2011 Protein Data Bank (11), Accession ID 1RP3. Structure is depicted from three different viewpoints, rotating 120°. Blue helixes: RpoF. Purple helixes: FlgM. Region 2 is highlighted in blue. Region 3 is highlighted in pink. Region 4 is highlighted in green. Region 4.2 is highlighted in yellow. FlgM wraps around σ^{28} to interact with the -10 DNA and RNA polymerase binding sites of Region 2 and Region 4.1.

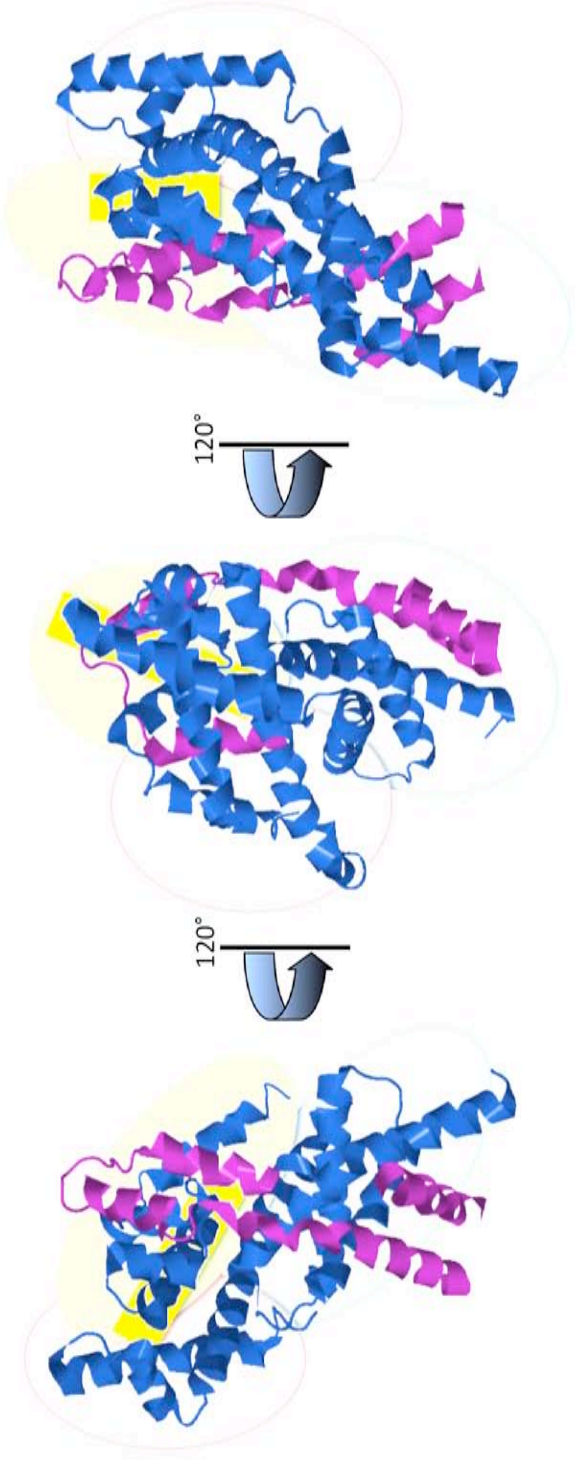
120°
120°

Figure I.6: Schematic Diagram of the Malleobactin Locus Expression Response to Iron Replete and Iron Poor Conditions

A: Under iron-replete conditions, the *mbaS* expression is repressed by Fur, which results in a repression of the malleobactin locus. B: Under iron poor conditions, Fur repression is relieved and MbaS (red arrow) activates the expression of the malleobactin biosynthesis (green arrows) and uptake (blue arrows) genes. Malleobactin is secreted through an unknown mechanism and, once secreted, it can bind to ferric iron to be taken back into the cell through the outer membrane by the FmtA protein. The iron ion is further transported through the inner membrane by unidentified ABC transport system. BPSL1774 – BPSL1787 is the malleobactin locus. C: Figure legend of icons utilized in A and B.

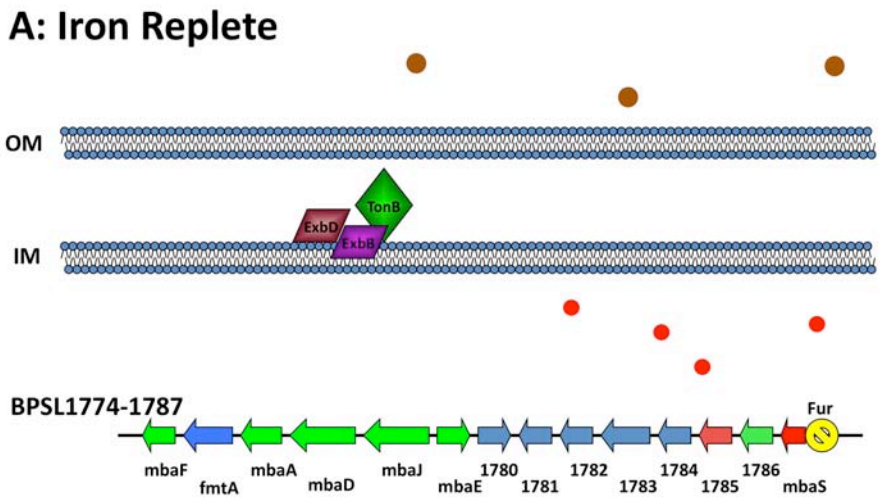
A: Iron Replete
OM
IM
TonB
ExbD
ExbB
BPSL1774-1787
Fur
mbaF
fmtA
mbaA
mbaD
mbaJ
mbaE
1780
1781
1782
1783
1784
1785
1786
mbaS

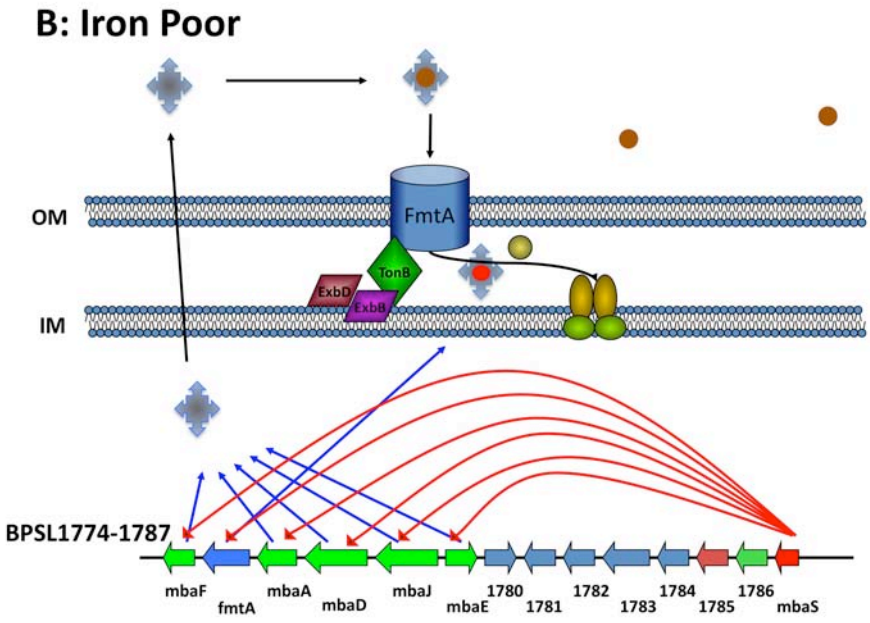
B: Iron Poor
OM
IM
FmtA
TonB
ExbD
ExbB
BPSL1774-1787
mbaF
fmtA
mbaA
mbaD
mbaJ
mbaE
1780
1781
1782
1783
1784
1785
1786
mbaS

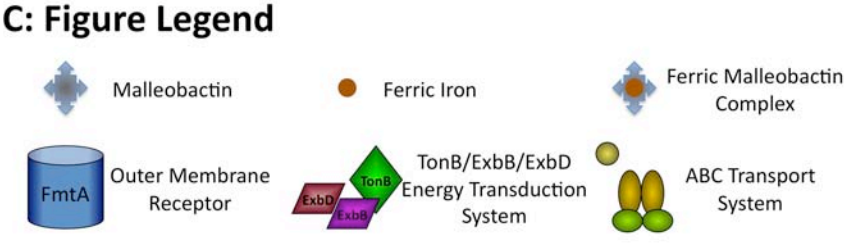
C: Figure Legend
Malleobactin
Ferric Iron
Ferric Malleobactin Complex
FmtA
Outer Membrane Receptor
TonB
ExbD
ExbB
TonB/ExbB/ExbD Energy Transduction System
ABC Transport System

II. Materials and Methods

II.A. Bacterial Growth Conditions

All *Escherichia coli* and *Burkholderia pseudomallei* strains were grown in Luria-Bertani (LB) medium at 37°C containing the following additives at the listed concentrations as necessary: ampicillin (Amp, 100 μg/ml), kanamycin (Kan, 50 μg/ml), zeocin (Zeo, 25 μg/ml), isopropyl β-D-1-thiogalactopyranoside (IPTG, 10 – 1000 μM), 2,2'-dipyridyl (DIP, 10 - 250 μM), and ferric ammonium citrate (FAC, 100 - 250 μg/ml).

II.B. Strains, Plasmids, and Primers

Strains utilized in these studies are listed in Table II.1. Plasmids utilized in Section III: Analysis of *mbaS* promoter and start codon are listed in Table II.2. Plasmids utilized in Section IV: MbaS Activation of *mbaJ* and *mbaE* Promoters are listed in Table II.3. Plasmids utilized in Section V: Mutational Analysis of MbaS are listed in Table II.4. All primers utilized in this study are listed in Table II.5.

II.C. DNA Manipulation

Plasmid DNA was prepared by using a Qiaprep miniprep kit (Qiagen). DNA digestion and ligation were performed according to the manufacturer's instruction (New England Biolab). PCR was carried out using a Mycycler™ Thermal Cycler as specified by the manufacturer (Bio-Rad Laboratories). PCR products were purified by Qiaquick PCR purification kit or Qiaquick gel extraction kit (Qiagen). The Oregon

Health and Science University MMI Research Core Facility carried out DNA sequencing reactions.

Several plasmid constructs were generated to complete the following research. The first is utilized for the direct readout of the functionality of *mbaS* promoter fragments. This plasmid encoded a *lacZ* gene lacking a functional start codon prior to the *pTac* encoded ribosomal binding site. The *mbaS* promoter region of various sizes was inserted upstream of the *lacZ* gene in such a manner to encode the putative *mbaS* start codons in frame with the *lacZ* gene. These plasmid constructs were generated by PCR amplifying the *lacZ* gene from pMLB1034 (Ref) using *lacZ-Bam*HI-F and *lacZ-Eco*RI-R primers (Table II.5). The PCR fragment was digested with *Bam*HI (NEB) and *Eco*RI (NEB) and cloned into a like digested pMMB208:Km vector (Ref). After sequence confirmation of the *lacZ* gene, *mbaS* promoter fragment was amplified using the following forward and reverse primers: S-F-290-*Hind*III and S-R-1b.T-*Bam*HI (Table II.5). The PCR amplified product was digested with *Hind*III (NEB) and *Bam*HI (NEB), gel purified and cloned into like digested pMMB208:Km-*lacZ* and the resulting plasmid p*PmbaS-2* (pMMB208:Km-*lacZ*/-290-1b.T) is listed in Table II.2. The cloning scheme is illustrated in Figure III.1. This plasmid was then transformed into the Mach1™ *E. coli* strain (Invitrogen) for the enzymatic β-galactosidase assay. It is of import to note that this construct retains the functional *pTac* promoter in the plasmid backbone that could be used to drive the expression of the *lacZ* gene as long as the encoded *mbaS* start codon was

functional. Further truncations of the *mbaS* promoter region were constructed and are identified in Table II.2.

A second two-plasmid system was necessary to assay the functionality of MbaS in *E. coli*. In this system, the same plasmid backbone of pMMB208:Km was utilized to express the MbaS protein. The MbaS expression construct was generated by PCR amplifying the *mbaS* gene and its promoter from *B. pseudomallei* genomic DNA using the 290-*mbaS*-*Hind*III forward primer and the *mbaS*-R(*Bam*HI) reverse primer listed in Table II.5, digested with the appropriate restriction enzymes, cloned into similarly digested pMMB208:Km, and then sequenced. The resulting construct is listed in Tables II.3 and II.4. The second plasmid utilized in this system was a Zeocin-resistant derivative of pQF50 (ref) that was generated by PCR amplification of the Zeocin resistance cassette utilizing the Zeo-*Stu*I-F and Zeo-*Stu*I-R primers listed in Table II.5. The PCR fragment was then digested with *Stu*I (NEB), gel purified and ligated into a like digested pQF50 plasmid. pQF50:Zeo encodes for a promoter lacking *lacZ* gene with stop codons in all three reading frames upstream of the multiple cloning site. Thus it can act as a plasmid for promoter screening. By inserting an MbaS responsive promoter upstream of the *lacZ* open reading frame we have generated a plasmid for screening the functionality of MbaS. The initial promoter chosen is that of the *mbaJ* gene, previously observed as expressed in an MbaS dependent manner (Alice 2006). To do this, the *mbaJ* promoter in its entirety through approximately 50 nucleotides of the *mbaJ* open reading frame was amplified utilizing the J.F.1.*Bam*HI and J.R.*Hind*III primer set (Table II.5). After

digestion with the appropriate restriction enzymes, the promoter fragment of 700 nucleotides was cloned into like digested pQF50:Zeo. This construct and further derivatives are listed in Tables II.3 and II.4. The cloning scheme for this two plasmid system is depicted in Figure IV.1. The two plasmids were co-transformed into the Mach1™ *E. coli* strain (Invitrogen).

Mutagenesis of promoter fragments and the open reading frame of *mbaS* were generated through splicing by overlap extension. Primers are listed in Table II.5.

II.D. RNA Purification

After growth for expression, 2 OD_{600} equivalents of *E. coli* cells were harvested by centrifugation and resuspended in 0.5 mls of Purezol reagent (Invitrogen). RNA was purified following the manufacturer's protocol. DNA digestion and further RNA decontamination was conducted utilizing the mini RNeasy Kit (Qiagen) following the manufacturer's recommended protocol. In the case of *B. pseudomallei*, the following modifications to the protocol were made to observe proper procedures and confirmation that samples were not contaminated in the BioSafety Level 3 facility prior to removing samples to the BioSafety Level 2 laboratory. All centrifugations were conducted in the biosafety cabinet and 10% of each resuspended sample volume was plated onto LB medium and incubated at 37°C for a minimum of 48 hours to demonstrate the absence of viable cell contamination.

II.E. qRT-PCR Analysis

RNA concentration was measured using a Nanodrop Spectrophotometer (Thermo Scientific). cDNA was generated utilizing random hexamer primers (Invitrogen) using SuperScript II (Invitrogen) using the manufacturers protocol with 100 ng of RNA in a 20 µl volume. 1 µl of cDNA reaction was used for qRT-PCR with Power SybrGreen (ABI) in a 25 µl volume. The reaction was carried out on a StepOnePlus real-time PCR instrument (Applied Biosystems) using the following protocol: 95°C for 10 minutes followed by 50 cycles of 95°C for 15 seconds and 60°C for 1 minute. Normalized C_T (ΔC_T) values were obtained by comparing against the *E. coli* glyceraldehyde-3-phosphate dehydrogenase (*gapA*) gene for samples isolate from *E. coli* and against the *B. pseudomallei gapA* gene for those samples isolated from *B. pseudomallei*.

II.F. Western Blot Analysis

After growth for expression, 2 OD_{600} equivalents of *E coli* cells were harvested by centrifugation and resuspended in 500 µl of 2x Laemmli SDS Sample Buffer. Total cell lysates were then boiled for 10 minutes before being loaded into the sample well of a 10% or a 12% Criterion XT Bis-Tris gel (Bio-Rad) and electrophoresed in MOPS buffer (Bio-Rad) at 70 mV for 2 hours followed by 120 mV until the dye front had run off the gel. Gels were transferred to nitrocellulose using 10 mM CAPS pH 11.0 buffer with 10% methanol at 400 mA overnight at 4°C. After slicing the membrane horizontally, each half was probed with either a custom chicken

polyclonal MbaS antibody (generated and purified by Aves Labs (Tigard, Oregon, USA) against the MbaS epitope CRRQTLENTYHADEDDGLD) at a 1:2500 dilution in TBS-Tween with 5% milk or with an anti-DnaK (Assay Design) at a dilution of 1:10,000 in TBS-Tween with 5% milk. In the case of *B. pseudomallei* western blots samples were boiled for a minimum of 20 minutes, followed by plating 10% of the sample volume on LB agar and incubated at 37°C for a minimum of 48 hours to demonstrate the absence of viable cells prior to removing samples from the BSL3 for further processing in the BSL2 laboratory.

II.G. β-galactosidase Assay

Cells were grown under gene induction conditions as described. Induced liquid cultures were mixed at a 2:1:1 ratio with 2 volumes of cell culture, 1 volume YPER Reagent (Pierce, Thermo Scientific), and 1 volume BPER Reagent (Pierce, Thermo Scientific) and incubated at 37°C for 30 minutes to permeabilize the cells. 100 µl of permeabilized cells was mixed with 100 µl of 2x Z Buffer (120 mM Na_2HPO_4, 80 mM NaH_2PO_4, 20 mM KCl, 2 mM $MgSO_4$, 100 mM β-mercaptoethanol, 0.8 mg/ml *o*-nitrophenyl-β-D-galactopyranoside, pH 7.0) in 96 well optically transparent tissue culture plates. Plates were incubated at 37°C for desired time points, until a measurable yellow color appeared, and OD_{420} and OD_{550} were measured utilizing a microplate reader (Dynatech Laboratories). Miller units were calculated as described by Miller., 1972 (57).

II.H. Tables

Table II.1: Strains Used in this Study			
	Name	**Purpose**	**Reference**
E. coli Strains			
	Mach1™	Cloning and *lacZ* Expression, F– Φ80*lacZ*ΔM15 Δ*lacX*74 *hsdR*(rK–, mK+) Δ*recA*1398 *endA*1 *tonA*	Invitrogen
	S17 λpir	Conjugation, λ-*pir* lysogen; *thi pro hsdR hsdM+ recA* RP4 2-Tc::Mu-Km::Tn7(Tp^R $Sm^{R)}$	Simon (1983)
B. pseudomallei Strains			
	K96243	Wild type Strain, Gm^R Ap^R	S. Songsivilai, Siriraj Hospital
	K96243 Δ*amrAB*	Deletion of AmrAB Efflux System, Gm^R Ap^R Km^S Zeo^S	(A. Alice & H. Naka)
	K96243 Δ*amrAB*Δ*mbaS*	Deletion of MbaS in Δ*amrAB* Background, Gm^R Ap^R Km^S Zeo^S	(A. Alice)

Table II.2: Plasmids Utilized in Section III: Analysis of *mbaS* promoter and start codon		
Name	**Description**	**Reference**
pCR2.1	General TA Cloning Vector, Ap^R, Km^R	Invitrogen
pMMB208:Km	Expression Vector, Km^R *Ptac*	Liu, et al., (2009)
pRK2013	Helper Plasmid for Conjugation, Km^R	Figurski, et al., (1971)
p*Pempty*	Promoter and Start Codon Screening *lacZ*: pMMB208:Km-*lacZ*	This Study
pCR-*mbaS*Large	Large Genomic Fragment Encompassing *mbaS* for Further Cloning	This Study
p*PmbaS-1*	MbaS Promoter/Start Codon Screen Construct (Stops at Upstream Start Codon):pMMB208:Km-*lacZ*/(-290-1a)	This Study
p*PmbaS-2*	MbaS Promoter/Start Codon Screen Construct (Stops at Annotated Start Codon TTG): pMMB208:Km-*lacZ*/(-290-1b.T)	This Study
p*PmbaS-2+C*	MbaS Promoter/Start Codon Screen Construct (Stops at Annotated Start Codon TTG): pMMB208:Km-*lacZ*/(-290-1b.T), Cytosine Insertion Upstream of 1b TTG	This Study
p*PmbaS-3*	MbaS Promoter/Start Codon Screen Construct (Stops at Annotated Start Codon TTG Mutagenized to ATG): pMMB208:Km-*lacZ*/(-290-1b.A)	This Study
p*PmbaS-3+C*	MbaS Promoter/Start Codon Screen Construct (Stops at Annotated Start Codon TTG Mutagenized to ATG): pMMB208:Km-*lacZ*/(-290-1b.A), Cytosine Insertion Upstream of 1b ATG	This Study
p*PmbaS-4*	MbaS Promoter/Start Codon Screen Construct (Stops at Upstream Start Codon): pMMB208:Km-*lacZ*/(-41-1a)	This Study
p*PmbaS-5*	MbaS Promoter/Start Codon Screen Construct (Stops at Annotated Start Codon TTG): pMMB208:Km-*lacZ*/(-41-1b.T)	This Study
p*PmbaS-5+C*	MbaS Promoter/Start Codon Screen Construct (Stops at Annotated Start Codon TTG): pMMB208:Km-*lacZ*/(-41-1b.T), Cytosine Insertion Upstream of 1b TTG	This Study
p*PmbaS-6*	MbaS Promoter/Start Codon Screen Construct (Stops at Annotated Start Codon TTG Mutagenized to ATG): pMMB208:Km-*lacZ*/(-41-1b.A)	This Study
p*PmbaS-6*	MbaS Promoter/Start Codon Screen Construct (Stops at Annotated Start Codon TTG Mutagenized to ATG): pMMB208:Km-*lacZ*/(-41-1b.A), Cytosine Insertion Upstream of 1b ATG	This Study
p*PmbaS-7*	MbaS Promoter/Start Codon Screen Construct (Stops at Annotated Start Codon TTG): pMMB208:Km-lacZ/(-71-1b.T)	This Study
p*PmbaS-7+C*	MbaS Promoter/Start Codon Screen Construct (Stops at Annotated Start Codon TTG): pMMB208:Km-lacZ/(-71-1b.T), Cytosine Insertion Upstream of 1b TTG	This Study
p*PmbaS-8*	MbaS Promoter/Start Codon Screen Construct (Stops at Annotated Start Codon TTG Mutagenized to ATG): pMMB208:Km-*lacZ*/(-71-1b.A)	This Study
p*PmbaS-8+C*	MbaS Promoter/Start Codon Screen Construct (Stops at Annotated Start Codon TTG Mutagenized to ATG): pMMB208:Km-*lacZ*/(-71-1b.A), Cytosine Insertion Upstream of 1b ATG	This Study

Table II.3: Plasmids Utilized in Section IV: MbaS Activation of *mbaJ* and *mbaE* Promoters		
Name	**Description**	**Reference**
pCR2.1	General TA Cloning Vector, Ap^R, Km^R	Invitrogen
pMMB208:Km	Expression Vector, Km^R *Ptac*	Liu, et al., (2009)
pRK2013	Helper Plasmid for Conjugation, Km^R	Figurski, et al., (1971)
pQF50	Promoter Screening *lacZ*, Ap^R	Farinha, et al., (1990), Gift from P. Greenburg
pFZE1	Zeocin Resistance Cassette Flanked by Inverted Repeats and Inverted MCSs	Gift from H. Schweizer
pQF50:Zeo	Zeo^R Cassette Replacing Ap^R Cassette	This Study
pCR-*mbaS*Large	Large Genomic Fragment Encompassing *mbaS* for Further Cloning	This Study
pMMB:*290mbaS*	*mbaS* Expression Construct Containing 290 Nucleotide Endogenous Promoter from Upstream Start Codon Through 50 Nucleotides Past Stop Codon	This Study
pMMB:*41mbaS*	*mbaS* Expression Construct Containing 41 Nucleotide Endogenous Promoter from Upstream Start Codon Through 50 Nucleotides Past Stop Codon	This Study
p*J(700)*	MbaJ Promoter Screen: pQF50:Zeo/pMbaJ(700)	This Study
p*J(300)*	MbaJ Promoter Screen: pQF50:Zeo/pMbaJ(300)	This Study
p*J(200)*	MbaJ Promoter Screen: pQF50:Zeo/pMbaJ(200)	This Study
p*J(150)*	MbaJ Promoter Screen: pQF50:Zeo/pMbaJ(150)	This Study
p*E(700)*	MbaE Promoter Screen: pQF50:Zeo/pMbaE(700)	This Study
p*E(250)*	MbaE Promoter Screen: pQF50:Zeo/pMbaE(250)	This Study
p*E(180)*	MbaE Promoter Screen: pQF50:Zeo/pMbaE(180)	This Study
p*J(200-10)*	SDM Promoter Mutant of MbaJ to the -10 DNA Binding Sequence for MbaS: pQF50:Zeo/pMbaJ(200 -10mut)	This Study
p*J(200-35)*	SDM Promoter Mutant of MbaJ to the -35 DNA Binding Sequence for MbaS: pQF50:Zeo/pMbaJ(200 -35mut)	This Study
p*J(200-10/-35)*	SDM Promoter Mutant of MbaJ to the -10/-35 DNA Binding Sequence for MbaS: pQF50:Zeo/pMbaJ(200 -10/-35mut)	This Study

Table II.4: Plasmids Utilized in Section V: Mutagenesis of MbaS		
Name	**Description**	**Reference**
pCR2.1	General TA Cloning Vector, Ap^R, Km^R	Invitrogen
pMMB208:Km	Expression Vector, Km^R *Ptac*	Liu, et al., (2009)
pRK2013	Helper Plasmid for Conjugation, Km^R	Figurski, et al., (1971)
pQF50	Promoter Screening *lacZ*, Ap^R	Farinha, et al., (1990), Gift from P. Greenburg
pFZE1	Zeocin Resistance Cassette Flanked by Inverted Repeats and Inverted MCSs	Gift from H. Schweizer
pQF50:Zeo	Zeo^R Cassette Replacing Ap^R Cassette	This Study
pMMB208:Km-*lacZ*	Promoter and Start Codon Screening *lacZ*	This Study
pCR-*mbaS*Large	Large Genomic Fragment Encompassing *mbaS* for Further Cloning	This Study
pMMB208:Km/ (-290)*mbaS*	*mbaS* Expression Construct Containing 290 Nucleotide Endogenous Promoter from Upstream Start Codon Through 50 Nucleotides Past Stop Codon	This Study
pMMB208:Km/ (-41)*mbaS*	*mbaS* Expression Construct Containing 41 Nucleotide Endogenous Promoter from Upstream Start Codon Through 50 Nucleotides Past Stop Codon	This Study
p*J(200)*	MbaJ Promoter Screen: pQF50:Zeo/pMbaJ(200)	This Study
p*E(250)*	MbaE Promoter Screen: pQF50:Zeo/pMbaE(250)	This Study
pMMB208:Km/ (-290)*mbaS*(D77A)	*mbaS* Mutant Expression Construct Containing 290 Nucleotide Endogenous Promoter from Upstream Start Codon Through 50 Nucleotides Past Stop Codon	This Study
pMMB208:Km/ (-290)*mbaS*(D81A)	*mbaS* Mutant Expression Construct Containing 290 Nucleotide Endogenous Promoter from Upstream Start Codon Through 50 Nucleotides Past Stop Codon	This Study
pMMB208:Km/ (-290)*mbaS*(D112A)	*mbaS* Mutant Expression Construct Containing 290 Nucleotide Endogenous Promoter from Upstream Start Codon Through 50 Nucleotides Past Stop Codon	This Study
pMMB208:Km/ (-290)*mbaS*(R115A)	*mbaS* Mutant Expression Construct Containing 290 Nucleotide Endogenous Promoter from Upstream Start Codon Through 50 Nucleotides Past Stop Codon	This Study
pMMB208:Km/ (-290)*mbaS*(E127A)	*mbaS* Mutant Expression Construct Containing 290 Nucleotide Endogenous Promoter from Upstream Start Codon Through 50 Nucleotides Past Stop Codon	This Study
pMMB208:Km/ (-290)*mbaS*(S139A)	*mbaS* Mutant Expression Construct Containing 290 Nucleotide Endogenous Promoter from Upstream Start Codon Through 50 Nucleotides Past Stop Codon	This Study
pMMB208:Km/ (-290)*mbaS*(E141A)	*mbaS* Mutant Expression Construct Containing 290 Nucleotide Endogenous Promoter from Upstream Start Codon Through 50 Nucleotides Past Stop Codon	This Study

pMMB208:Km/ (-290)*mbaS*(R165A)	*mbaS* Mutant Expression Construct Containing 290 Nucleotide Endogenous Promoter from Upstream Start Codon Through 50 Nucleotides Past Stop Codon	This Study
pMMB208:Km/ (-290)*mbaS*(R172A)	*mbaS* Mutant Expression Construct Containing 290 Nucleotide Endogenous Promoter from Upstream Start Codon Through 50 Nucleotides Past Stop Codon	This Study
pMMB208:Km/ (-290)*mbaS*(R174A)	*mbaS* Mutant Expression Construct Containing 290 Nucleotide Endogenous Promoter from Upstream Start Codon Through 50 Nucleotides Past Stop Codon	This Study
pMMB208:Km/ *(-290)mbaS*(E176A)	*mbaS* Mutant Expression Construct Containing 290 Nucleotide Endogenous Promoter from Upstream Start Codon Through 50 Nucleotides Past Stop Codon	This Study
pMMB208:Km/ (-290)*mbaS*(R197A)	*mbaS* Mutant Expression Construct Containing 290 Nucleotide Endogenous Promoter from Upstream Start Codon Through 50 Nucleotides Past Stop Codon	This Study
pMMB208:Km/ (-290)*mbaS*(D198A)	*mbaS* Mutant Expression Construct Containing 290 Nucleotide Endogenous Promoter from Upstream Start Codon Through 50 Nucleotides Past Stop Codon	This Study
pMMB208:Km/ (-290)*mbaS*(ΔC13)	*mbaS* Mutant Expression Construct Containing 290 Nucleotide Endogenous Promoter from Upstream Start Codon Through 50 Nucleotides Past Stop Codon	This Study
pMMB208:Km/ (-290)*mbaS* (115RRQT:AAAA)	*mbaS* Mutant Expression Construct Containing 290 Nucleotide Endogenous Promoter from Upstream Start Codon Through 50 Nucleotides Past Stop Codon	This Study
pMMB208:Km/ (-290)*mbaS* (120ENTY:AAAA)	*mbaS* Mutant Expression Construct Containing 290 Nucleotide Endogenous Promoter from Upstream Start Codon Through 50 Nucleotides Past Stop Codon	This Study
pMMB208:Km/ (-290)*mbaS* (126DEDD:AAAA)	*mbaS* Mutant Expression Construct Containing 290 Nucleotide Endogenous Promoter from Upstream Start Codon Through 50 Nucleotides Past Stop Codon	This Study
pMMB208:Km/ (-290)*mbaS* (174REET:AAAA)	*mbaS* Mutant Expression Construct Containing 290 Nucleotide Endogenous Promoter from Upstream Start Codon Through 50 Nucleotides Past Stop Codon	This Study
pMMB208:Km/ (-290)*mbaS*(C114A)	*mbaS* Mutant Expression Construct Containing 290 Nucleotide Endogenous Promoter from Upstream Start Codon Through 50 Nucleotides Past Stop Codon	This Study
pMMB208:Km/ (-290)*mbaS*(C206A)	*mbaS* Mutant Expression Construct Containing 290 Nucleotide Endogenous Promoter from Upstream Start Codon Through 50 Nucleotides Past Stop Codon	This Study
pMMB208:Km/ (-290)*mbaS*(C216A)	*mbaS* Mutant Expression Construct Containing 290 Nucleotide Endogenous Promoter from Upstream Start Codon Through 50 Nucleotides Past Stop Codon	This Study
pMMB208:Km/ (-290)*mbaS*(C220A)	*mbaS* Mutant Expression Construct Containing 290 Nucleotide Endogenous Promoter from Upstream Start Codon Through 50 Nucleotides Past Stop Codon	This Study
pMMB208:Km/ (-290)*mbaS*(C230A)	*mbaS* Mutant Expression Construct Containing 290 Nucleotide Endogenous Promoter from Upstream Start Codon Through 50 Nucleotides Past Stop Codon	This Study
pMMB208:Km/ (-290)*mbaS* (C216A/C220A)	*mbaS* Mutant Expression Construct Containing 290 Nucleotide Endogenous Promoter from Upstream Start Codon Through 50 Nucleotides Past Stop Codon	This Study

Table II.5: Primers Utilized in This Study		
Name	**Sequence**	**Purpose**
MbaS-C1	ATTGCTTGGCCATTGAGCAAACAT	Chromosomal Amplification
MbaS-C2	ACCGCGTAGACGACGTCGTCG	Chromosomal Amplification
ZEO-S-3	AGGCCTCGGCTTATCTCTGATGTTAC	Blunt End Cloning
ZEO-S-4	AGGCCTGTCAACAGCAATGGATTTCGG	Blunt End Cloning
lacZ-BamHI-F	GGATCCCGTCGTTTTACAACGTCGTGACTG	Amplification of *lacZ* from pMLB1034
lacZ-EcoRI-R	GAATTCCTCAGGGTCAATGCCAGAGCGCTTCG	Amplification of *lacZ* from pMLB1034
S-F-290-HindIII	TTAAGCTTGAAGAGCGGCACGTTGCCGGCGGC	MbaS Promoter Fragment -290 Nucleotides From Upstream Start ATG
S-F-41-HindIII	TTAAGCTTACGTTAGATTGCTTGCCATTGAGC	MbaS Promoter Fragment -41 Nucleotides From Upstream Start ATG
S-F-71-HindIII	TTAAGCTTGGCCGGCGCCGGCAAAACCGTTAC	MbaS Promoter Fragment -71 Nucleotides From Annotated Start TTG
S-R-1a-BamHI	TTGGATCCATGGATTCTCCAGATGTTTGCTC	MbaS Promoter Fragment Upstream Start ATG
S-R-1b.A-BamHI	TTGGATCCATGGACGGGCGCGGCGGCGGGTGC	MbaS Promoter Fragment Annotated TTG Mutated to ATG
S-R-1b.T-BamHI	TTGGATCCAAGGACGGGCGCGGCGGCGGGTGC	MbaS Promoter Fragment Annotated TTG
lacZ-SacI-R	GAGCTCTTATTTTTGACACCAGAC	*lacZ* Sequencing Primer
LacZseq2	CTGTATCGCTGGATCAAATC	*lacZ* Sequencing Primer
LacZseq3	CTGGATGTCGCTCCACAAGG	*lacZ* Sequencing Primer
LacZseq1	CATAAACCGACTACACAAATC	*lacZ* Sequencing Primer
SR	GGATCCGTTGACGACGACCGCGTAGACGAC	BamHI Encoding, Full MbaS Amplification
J-CGT-F	CTTCAACAATGAGCATAATCACGGGCGAAATTTTTTACCGAGCCGTTTAT	SOE Mutagenesis of MbaJ Promoter
JCGT-R	ATAAACGGCTCGGTAAAAAATTCGCCCGTGATTATGCTCATTGTTGAAG	SOE Mutagenesis of MbaJ Promoter
JTAAAA-F	CTTCAACAATGAGACGAATCACGGGCGAAATTGGGGCCCGAGCCGTTTAT	SOE Mutagenesis of MbaJ Promoter
JTAAAA-R	ATAAACGGCTCGGGCCCCAATTTCGCCCGTGATTCGTCTCATTGTTGAAG	SOE Mutagenesis of MbaJ Promoter
JTAAAA-CGT-F	CTTCAACAATGAGCATAATCACGGGCGAAATTGG	SOE Mutagenesis of MbaJ

	GGCCCGAGCCGTTTAT	Promoter
JTAAAA-CGT-R	ATAACGGCTCGGGCCCCAATTTCGCCCGTGATTAT GCTCATTGTTGAAG	SOE Mutagenesis of MbaJ Promoter
J.R.HindIII	AAAAGCTTGAGTCGCGCAAGCGCGTGGATTCG	MbaJ Promoter Amplification
J.F.1.BamHI	AAGGATCCCATTGTTGAAGCGGCCCCTCTTGC	MbaJ Promoter Amplification
J.F.2.BamHI	AAGGATCCGACATCGGCAACCCGATGAGCATA	MbaJ Promoter Amplification
J.F.3.BamHI	AAGGATCCACGCCCCTCGGCCGAGCCGCCGCG	MbaJ Promoter Amplification
J.F.4.BamHI	AAGGATCCCACGGGTCAATAAGGGAATCGGAT	MbaJ Promoter Amplification
E.R.HindIII	AAAAGCTTGAGCAGCGCGACTATCAGGCGCCG	MbaE Promoter Amplification
E.F.1.BamHI	AAGGATCCGAAGGACGCACCCGCGCCTTGCCG	MbaE Promoter Amplification
E.F.2.BamHI	AAGGATCCTCGAGGATCGAACACGGGCAAAGC	MbaE Promoter Amplification
E.F.3.BamHI	AAGGATCCAGGGCGTGAAGTCCGTTGGATCCG	MbaE Promoter Amplification
MbaS-D77A-1	CCGCGCGGAGGCGGTGGTGCACG	SOE Mutagenesis of MbaS
MbaS-D77A-2	CGTGCACCACCGCCTCCGCGCGG	SOE Mutagenesis of MbaS
MbaS-D81A-1	GACGTGGTGCACGCGGTGTTCGTGAA	SOE Mutagenesis of MbaS
MbaS-D81A-2	TTCACGAACACCGCGTGCACCACGTC	SOE Mutagenesis of MbaS
MbaS-D112A-1	CGCGTCGATCGCGGCGTGCCGCC	SOE Mutagenesis of MbaS
MbaS-D112A-2	GGCGGCACGCCGCGATCGACGCG	SOE Mutagenesis of MbaS
MbaS-R115A-1	CGACGCGTGCGCGCGCCAGACGC	SOE Mutagenesis of MbaS
MbaS-R115A-2	GCGTCTGGCGCGCGCACGCGTCG	SOE Mutagenesis of MbaS
MbaS-E127A-1	CCACGCGGACGCGGACGACGGCC	SOE Mutagenesis of MbaS
MbaS-E127A-2	GGCCGTCGTCCGCGTCCGCGTGG	SOE Mutagenesis of MbaS
MbaS-S139A-1	GCCCGAGCTGGCGCCGGAGGCCG	SOE Mutagenesis of MbaS
MbaS-S139A-2	CGGCCTCCGGCGCCAGCTCGGGC	SOE Mutagenesis of MbaS
MbaS-E141A-1	GCTGTCGCCGGCGGCCGCGCTCG	SOE Mutagenesis of MbaS
MbaS-E141A-2	CGAGCGCGGCCGCCGGCGACAGC	SOE Mutagenesis of MbaS
MbaS-R165A-1	CGCGCGCAGCGCGGCCGCGTTCG	SOE Mutagenesis of MbaS
MbaS-R165A-2	CGAACGCGGCCGCGCTGCGCGCG	SOE Mutagenesis of MbaS
MbaS-R172A-1	CGAGATGGTGGCGCTGCGCGAGG	SOE Mutagenesis of MbaS
MbaS-R172A-2	CCTCGCGCAGCGCCACCATCTCG	SOE Mutagenesis of MbaS
MbaS-R174A-1	GGTGCGGCTGGCGGAGGAGACGC	SOE Mutagenesis of MbaS
MbaS-R174A-2	GCGTCTCCTCCGCCAGCCGCACC	SOE Mutagenesis of MbaS
MbaS-E176A-1	GCTGCGCGAGGCGACGCTGCAGAG	SOE Mutagenesis of MbaS
MbaS-E176A-2	CTCTGCAGCGTCGCCTCGCGCAGC	SOE Mutagenesis of MbaS
MbaS-R197A-1	ACTTCATGGTCGCGGACGCCGAGCG	SOE Mutagenesis of MbaS
MbaS-R197A-2	CGCTCGGCGTCCGCGACCATGAAGT	SOE Mutagenesis of MbaS
MbaS-D198A-1	CATGGTCCGCGCGGCCGAGCGGC	SOE Mutagenesis of MbaS

MbaS-D198A-2	GCCGCTCGGCCGCGCGGACCATG	SOE Mutagenesis of MbaS
MbaS-ΔC13-1	GGCGTTTTGCGGCGCCCGCGCGTAGACGCGGCGCACGCGGTGCG	SOE Mutagenesis of MbaS
MbaS-ΔC13-2	CGCACCGCGTGCGCCGCGTCTACGCGCGGGCGCCGCAAAACGCC	SOE Mutagenesis of MbaS
MbaS-115RRQT-1	CGCAACGCGTCGATCGACGCGTGCGCCGCCGCGGCGCTCGAGAACACCTACCACGCGGAC	SOE Mutagenesis of MbaS
MbaS-115RRQT-2	GTCCGCGTGGTAGGTGTTCTCGAGCGCCGCGGCGGCGCACGCGTCGATCGACGCGTTGCG	SOE Mutagenesis of MbaS
MbaS-120ENTY-1	GACGCGTGCCGCCGCCAGACGCTCGCGGCCGCCGCCCACCGCGACGAGGACGACGGCCTC	SOE Mutagenesis of MbaS
MbaS-120ENTY-2	GAGGCCGTCGTCCTCGTCCGCGTGGGCGGCGGCCGCGAGCGTCTGGCGGCGGCACGCGTC	SOE Mutagenesis of MbaS
MbaS-126DEDD-1	ACGCTCGAGAACACCTACCACGCGGCCGCGGCCGCCGGCCTCGACGTGCCGTCGCCCGAG	SOE Mutagenesis of MbaS
MbaS-126DEDD-2	CTCGGGCGACGGCACGTCGAGGCCGGCGGCCGCGGCCGCGTGGTAGGTGTTCTCGAGCGT	SOE Mutagenesis of MbaS
MbaS-174REET-1	GCCGCGTTCGAGATGGTGCGGCTGGCCGCGGCGGCGCTGCAGAGCGCCGCGCGCGCGCTG	SOE Mutagenesis of MbaS
MbaS-174REET-2	CAGCGCGCGCGCGGCGCTCTGCAGCGCCGCCGCGGCCAGCCGCACCATCTCGAACGCGGC	SOE Mutagenesis of MbaS
MbaS-C114A-1	GCAACGCGTCGATCGACGCGGCCCGCCGCCAGACGCTCGAGAA	SOE Mutagenesis of MbaS
MbaS-C114A-2	TTCTCGAGCGTCTGGCGGCGGGCCGCGTCGATCGACGCGTTGC	SOE Mutagenesis of MbaS
MbaS-C206A-1	CCGAGCGGCACTGCGTCGCGGCCGTCGACGCGTCCGAGCGCGG	SOE Mutagenesis of MbaS
MbaS-C206A-2	CCGCGCTCGGACGCGTCGACGGCCGCGACGCAGTGCCGCTCGG	SOE Mutagenesis of MbaS
MbaS-C216A-1	CGTCCGAGCGCGGGCTCGCGGCCCCGGCGTTTTGCGGCGCCCG	SOE Mutagenesis of MbaS
MbaS-C216A-2	CGGGCGCCGCAAAACGCCGGGGCCGCGAGCCCGCGCTCGGACG	SOE Mutagenesis of MbaS
MbaS-C220A-1	GGCTCGCGTGCCCGGCGTTTGCCGGCGCCCGCGCGCGGACGGT	SOE Mutagenesis of MbaS
MbaS-C220A-2	ACCGTCCGCGCGCGGGCGCCGGCAAACGCCGGGCACGCGAGCC	SOE Mutagenesis of MbaS
MbaS-C230A-1	GCGCGCGGACGGTAAAAAAAGCCGTGCGCGATTCGTCTATCGA	SOE Mutagenesis of MbaS
MbaS-C230A-2	TCGATAGACGAATCGCGCACGGCTTTTTTTACCGTCCGCGCGC	SOE Mutagenesis of MbaS
MbaS-C216/220A-1	GAGCGCGGGCTCGCGGCCCCGGCGTTTGCCGGCGCCCGCG	SOE Mutagenesis of MbaS
MbaS-C216/220A-2	CGCGGGCGCCGGCAAACGCCGGGGCCGCGAGCCCGCGCTC	SOE Mutagenesis of MbaS
EcGapA_rtF	CGGTTTTGGCCGTATCGGTCGC	qRT-PCR Primer
EcGapA_rtR	GTCGAAACGGCCGTGAGTGGAG	qRT-PCR Primer
BPSL1787rtF	GCTCGTCGATGTGCTGGTCGC	qRT-PCR Primer
BPSL1787rtR	GTGTTCTCGAGCGTCTGGCGG	qRT-PCR Primer
BPSL2952rtF	CATCACGACGTCGACGCCCAG	qRT-PCR Primer

BPSL2953rtR	GCGAAGACCAACGCGCACCTG	qRT-PCR Primer
M13F	GTAAAACGACGGCCAG	Sequencing from pCR2.1
M13R	CAGGAAACAGCTATGAC	Sequencing from pCR2.1
208SEQ-R	GACCACCGCGCTACTGCCGCCAGG	Sequencing and SOE Amplification from pMMB208
208SEQ-F#3LONG	CGGCTCGTATAATGTGTGGAATTGTGAGCGGATAACAATTTCACAC	Sequencing and SOE Amplification from pMMB208
pQF-seq-F-SphI	CGCCGCCGCAAGGAATGGTGCATG	Sequencing
pQF-seq-R-lac	CCATTCAGGCTGCGCAACTGTTCC	Sequencing

III. Characterization of *mbaS* Promoter and Start Codon

III.A. Introduction

Several studies have identified and initially characterized the *B. pseudomallei* malleobactin siderophore synthesis and uptake locus (2, 159, 160). Malleobactin is a hydroxamate type siderophore produced by *B. pseudomallei*. This entire locus is unregulated under iron-limiting growth conditions and is regulated by the malleobactin sigma factor (MbaS, BPSL1787) (Figures I.3 and 1.6) (2). Sigma factors are a class of proteins that function in the recognition of DNA promoter elements and in the recruitment of the RNA core polymerase complex of proteins for the initiation of transcription. Thus the regulation of sigma factors is critical for the regulation of gene expression. MbaS falls into a subset of σ^{70} sigma factors classified as extracytoplasmic function (ECF) sigma factors (102) based on their responsiveness to extracellular signals. However, MbaS does not respond to the extracellular signals in a manner similar to its *P. aeruginosa* ECF homolog PvdS (further discussed in Section I.C).

The annotated sequence of *mbaS* of *B. pseudomallei* indicates translation starts at a TTG codon. Located upstream of this TTG is an in frame ATG codon. The purpose of the research presented in this section is to identify which of these two codons acts as the functional start codon of *mbaS*. Additionally, the promoter of *mbaS* contains a putative Fur binding sequence (2).

Overall, these studies have: 1) identified the correct open reading frame for *mbaS* and revealed that the annotated translational initiation site is incorrect, and 2)

confirmed that transcription of the *mbaS* gene is induced under iron-limiting conditions.

III.B. Results

III.B.i. Proof of function

The core construct utilized in this section is an *mbaS* promoter including the annotated start fused to a *lacZ* gene lacking a start codon (Figure III.1). To assay the activity of the full *mbaS* promoter fragment spanning from 290 nucleotides upstream of the upstream start ATG codon through the annotated start TTG codon (NCBI Gene ID: 3093703) (p*PmbaS-2*, Table II.2), an overnight culture of Mach1 *E. coli* containing *pPmbaS*-2 was grown with antibiotic selection in LB medium then subcultured at a 1:50 dilution into LB medium with or without 1 mM IPTG to induce gene expression. After 3.5 hours growth, samples were taken and β-galactosidase activity was assayed. This assay demonstrated a five-fold up-regulation of LacZ activity when the full *mbaS* promoter and annotated start codon is fused to *lacZ* upon IPTG induction (Figure III.2) when compared to the non-induced control.

III.B.ii. Analysis of Promoter Elements of mbaS

The NCBI annotated sequence for the *mbaS* gene reports a 621 nucleotide open reading frame that starts with a TTG codon (NCBI Gene ID: 3093703, +1b in Figure III.3). However, located 90 nucleotides upstream of this annotated start codon is an in-frame ATG codon (+1a in Figure III.3). Sequence analysis of the immediate

upstream nucleotide promoter sequence of the upstream ATG identifies a putative ribosomal binding site (GGAGA) (Figure III.4), whereas there are no obvious promoter elements are identifiable between the upstream ATG and the annotated TTG, suggesting misannotation of the *mbaS* open reading frame in *B. pseudomallei* K96243. Further *in silico* analysis utilizing the Softberry bprom (119) and Fruitfly.org (86) promoter analysis software reveal a potential transcriptional start site at 26 nucleotides upstream of the first upstream ATG start codon (Triangle in Figure III.4). Additionally, a putative Fur binding site was identified 46 nucleotides upstream of the first ATG start codon overlapping a putative sigma 70 DNA binding sequence (Black box in Figure III.3, underlined in Figure III.4) (2). This *mbaS* promoter region is exceptionally low in GC% content when compared to the rest of the genome (36 in 135 nucleotides vs. 69% genomic average) indicating the potential for additional transcriptional element binding sites. These identified promoter elements of *mbaS* are depicted in Figure III.3 and Figure III.4.

III.B.iii. mbaS Promoter Activity and Start Codon in E. coli

A series of promoter fragments including either the first upstream start codon (+1a), both start codons (+1a and +1b), or the annotated start codon (+1b) from *mbaS* were cloned into a *lacZ* fusion vector lacking the start codon (plasmids are listed in Table II.2 and Figure III.5). These constructs included a set of promoters that contained a mutation from TTG to ATG at the annotated start site (red A in Figure III.5). *E. coli* strains containing these plasmids were grown as previously

described and induced by IPTG induction for 3.5 hours before samples were taken for β-galactosidase activity assay (Figure III.6). Promoters that spanned the upstream start codon had significant β-galactosidase levels (Figure III.6, constructs p*PmbaS*-1 through p*PmbaS*-6). However, when the upstream start codon was not included (as in the case of the constructs containing only 71 nucleotides of the 90 nucleotide gap between the two start codons), no β-galactosidase activity was detected (Figure III.6, constructs p*PmbaS*-7 and p*PmbaS*-8). Strains carrying constructs that terminated with the first upstream start codon (p*PmbaS*-1 and p*PmbaS*-4) have significantly higher β-galactosidase activity than those that encoded both start codons (p*PmbaS*-2, 3, 4, and 6). Additionally, insertion of a cytosine residue immediately upstream of the annotated start codon abolished all β-galactosidase activity (p*PmbaS*-2+C, 3+C, 5+C, 6+C, 7+C, and 8+C in Figure III.6). The strains were also induced by iron restriction (Figure III.7). Only constructs that encoded for the Fur binding site upstream of the showed iron responsive β-galactosidase activity (plasmids p*PmbaS-1*, p*PmbaS-2*, and p*PmbaS-3)*. In all cases, results were normalized against empty vector control (p*Pempty*).

III.B.iv. mbaS Promoter Activity and Start Codon in B. pseudomallei

The plasmids described in Section III.B.iii were conjugated into the *B. pseudomallei* Δ*amrABΔmbaS* strain. Enzymatic activity was assayed as previously described for *E. coli*. The results seen in *B. pseudomallei* were consistent with those seen in *E. coli* (Figure III.8) with the exception that those promoters starting at 41 nucleotides

upstream of the upstream ATG start codon had significantly reduced levels when compared to *E. coli*.

III.C. Discussion

Previous attempts to study the function of MbaS were hampered by reliance upon the published annotation data. Thus, the identification of the *mbaS* start codon was necessary. Our genetic experiments show that the ATG located 90 nucleotides upstream of the annotated start of TTG is the most-likely start codon. In order to irrefutably claim that the upstream ATG encodes the start methionine, it would be necessary to generate a C-terminal tagged MbaS protein, purify it, and then conduct N-terminal sequencing. However, we have strong evidence to support our model that the up-stream ATG is the functional start codon.

In silico analysis of the *mbaS* promoter reveals several identifiable motifs. There is a potential ribosomal binding site (GGAGA) located five nucleotides upstream of what we believe is the functional ATG codon, and preceding that by 18 nucleotides is a putative transcriptional initiation site. These two promoter regions were identified based solely upon *in silico* analysis and have yet demonstrated. This demonstration would likely require the use of 5' sequencing through the procedure known as 5' rapid amplification of cDNA ends (5'-RACE).

mbaS expression is likely regulated by the repressor Fur and potentially autoregulated through positive feedback. A putative Fur-binding site is located site 46 nucleotides upstream of the functional start codon. The annotation of this site is supported by the evidence that those *mbaS* promoter constructs wherein the promoter starts 41 nucleotides upstream of the start codon are non-responsive to iron limitation (data not shown). Sequence analysis predict of the *mbaS* promoter

identified a possible MbaS binding site that overlaps the Fur binding site. Further analysis of the MbaS binding sequence can be found in Section IV. This MbaS binding site identification could be due to the fact that both MbaS and Fur bind to AT rich DNA promoter elements and thus leading to a misidentification of the binding site in the *mbaS* promoter. Further characterization of these binding sites should be demonstrated both genetically, through site directed mutagenesis of the longer *mbaS* promoter to confirm an abolishment of this regulation, and biochemically, through the purification of *B. pseudomallei* Fur and MbaS proteins and electromobility shift assays against the *mbaS* promoter.

The possibility exists that *mbaS* regulation may also depend upon additional regulatory elements not yet identified. As discussed in the Introduction (Section I.A.ii.c.1.3), quorum sensing has been demonstrated to affect the production of siderophores in *B. pseudomallei*. Thus, the quorum sensing regulator $BpsR_1$ may directly affect the expression of MbaS. However, as the DNA binding sequence of this regulator has not yet been elucidated, there remains a wide array of experiments necessary to demonstrate the possibility of this direct regulation. Experiments that could demonstrate BpsR1 interaction with the *mbaS* promoter would necessitate the purification of $BpsR_1$, followed by electromobility shift assays and DNase footprinting.

The variation in the activity of the MbaS promoter/start codon *lacZ* fusions when expressed in *E. coli* (Figure III.6) versus when expressed in *B. pseudomallei* (Figure III.8), specifically the almost complete abolishment of expression from the

constructs containing the -41 nucleotide promoter fragment, is most likely due to the inability of *B. pseudomallei* to drive the expression of the plasmid encoded *pTac* promoter.

III.D. Figures

Figure III.1: *mbaS* Promoter Analysis Construct

Schematic diagram for the generation of an *mbaS* promoter and start codon fused to a *lacZ* gene lacking a start codon. The *lacZ* gene lacking its endogenous start codon was cloned into the pMMB208:Km vector backbone. This vector encodes for a *pTac* promoter that is induced upon the addition of IPTG. The *mbaS* promoter/start codon fragment was cloned upstream of *lacZ* gene. The promoter of *mbaS* contains an *in silico* identified translational start (yellow bar), ribosomal binding site (purple triangle), and -10 and -35 DNA binding sequences (red bars) which overlap a putative Fur binding site.

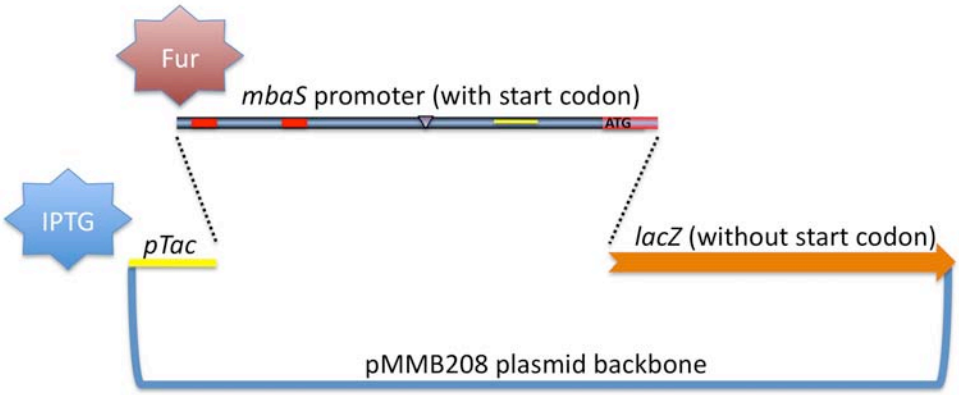
Fur
mbaS promoter (with start codon)
ATG
IPTG
pTac
lacZ (without start codon)
pMMB208 plasmid backbone

Figure III.2: *mbaS* Promoter and Start Codon Activation of Expression of *lacZ*: Proof of Function

The long (290 nucleotides from the upstream start codon) *mbaS* promoter through the annotated start codon (TTG located 90 nucleotides downstream from the first start codon) was cloned in frame with the start codon-less *lacZ* gene in the pMMB208:Km background plasmid (p*PmbaS*-2, Figure III.1). Expression was induced in LB medium with 1 mM IPTG. Miller Units for β-galactosidase reporter activities are an average of triplicate biological replicates, each measured in triplicate. Error bars indicate standard deviation around the mean. Samples were normalized to an empty vector control (p*Pempty*) by subtracting Miller Units generated in p*Pempty* from p*PmbaS-2* cultures.

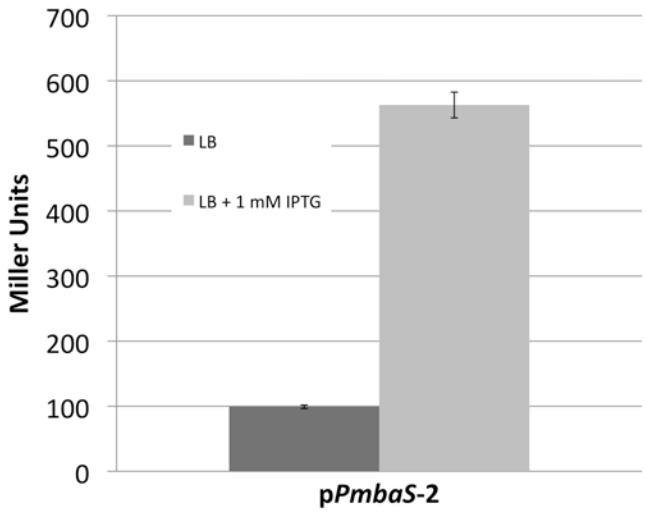
700
600
500
400
300
200
100
0
Miller Units
LB
LB + 1 mM IPTG
pPmbaS-2

Figure III.3: *mbaS* Promoter Schematic Diagram

Characterization of *mbaS* Promoter and Transcriptional Start Site. +1b indicates the annotated start site for *mbaS*. +1a indicates a putative start site located 90 nucleotides upstream of the annotated +1b site. The yellow region is 135 nucleotides of approximately 36% GC, relative to the 68 % GC average of B*. pseudomallei*. The black region is the putative Fur binding site located 46 and 136 nucleotides upstream of the +1a and +1b translational start sites, respectively.

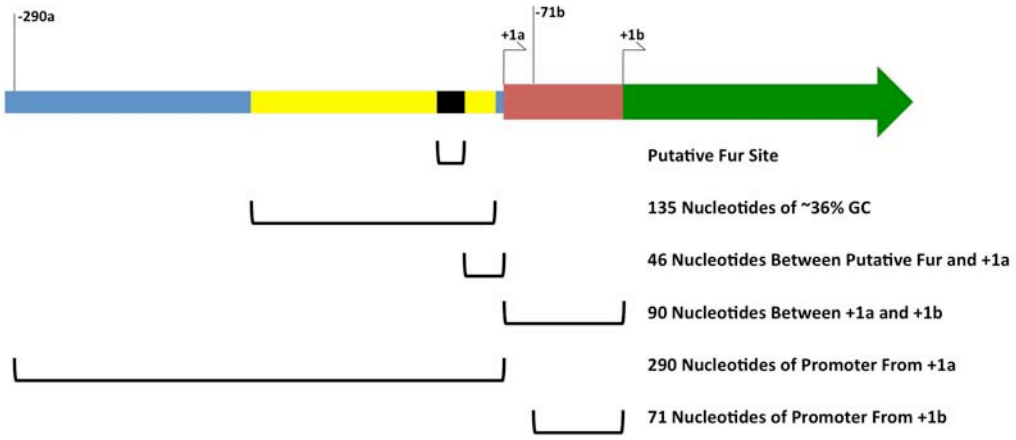
-290a
-71b
+1a
+1b
Putative Fur Site
135 Nucleotides of ~36% GC
46 Nucleotides Between Putative Fur and +1a
90 Nucleotides Between +1a and +1b
290 Nucleotides of Promoter From +1a
71 Nucleotides of Promoter From +1b

Figure III.4: *mbaS* Promoter Sequence

In silico analysis of *mbaS* Promoter Sequence. -35/-10 sigma 70 recognition sequence is located 5 nucleotides upstream of a putative transcriptional start site (identified with a bold C and blue triangle). A ribosomal binding site is located 4 nucleotides upstream of the upstream start codon (identified as Start a) and is identified in italics. The red I symbols indicate locations where cloning resulted in truncated promoter fragments in constructs shown in Figure III.5. The putative Fur binding site is highlighted in green text. Upstream start codon is identified as a green ATG and labeled Start a. The annotated start codon is identified as a green TTG and is labeled as Start b. Mutants of promoter fragments resulting in either a cytosine insertion just prior to the annotated start codon or a T to A mutation to encode for an ATG to replace the annotated TTG are identified with green.

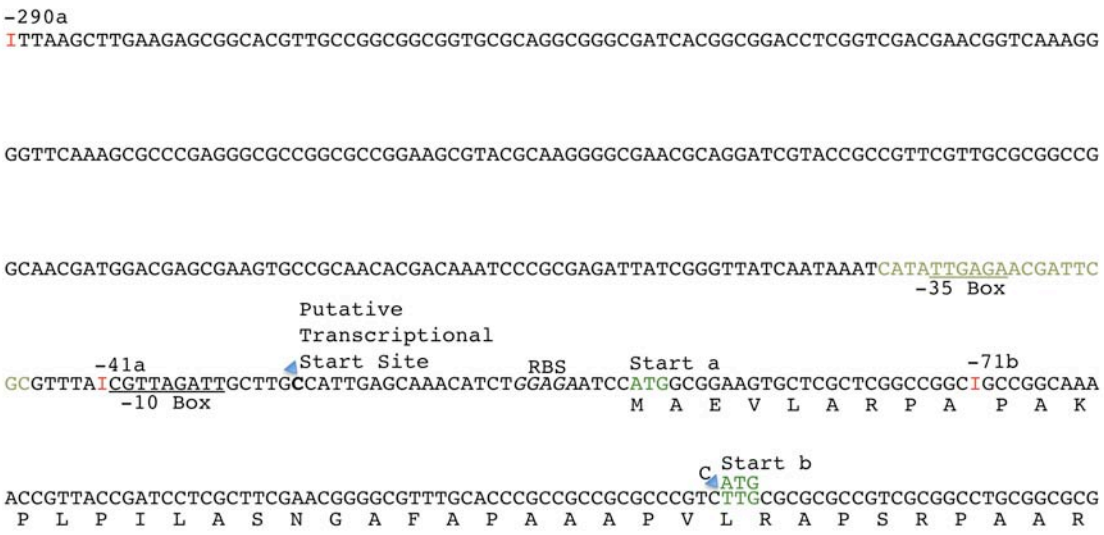
-290a
ITTAAGCTTGAAGAGCGGCACGTTGCCGGCGGCGGTGCGCAGGCGGGCGATCACGGCGGACCTCGGTCGACGAACGGTCAAAGG
GGTTCAAAGCGCCCGAGGGCGCCGGCGCCGGAAGCGTACGCAAGGGGCGAACGCAGGATCGTACCGCCGTTCGTTGCGCGGCCG
GCAACGATGGACGAGCGAAGTGCCGCAACACGACAAATCCCGCGAGATTATCGGGTTATCAATAAATCATATTGAGAACGATTC
-35 Box
Putative
Transcriptional
Start Site
-41a
RBS
Start a
-71b
GCGTTTAICGTTAGATTGCTTGCCATTGAGCAAACATCTGGAGAATCCATGGCGGAAGTGCTCGCTCGGCCGGCIGCCGGCAAA
-10 Box
M A E V L A R P A P A K
Start b
C ATG
ACCGTTACCGATCCTCGCTTCGAACGGGGCGTTTGCACCCGCCGCCGCGCCCGTCTTGCGCGCGCCGTCGCGGCCTGCGGCGCG
P L P I L A S N G A F A P A A A P V L R A P S R P A A R

Figure III.5: Schematic Diagram of *mbaS* Promoter Fusions to *lacZ*

Assorted *mbaS* promoter fusions spanning either the upstream start codon or the down stream start codon. Promoters start at 290 or 41 nucleotides upstream of the upstream start codon or 71 nucleotides upstream of the annotated start codon. *mbaS* promoter description is in Figure III.3. Black bars indicate the included *mbaS* promoter component included in each construct. Black ATG indicates the upstream start codon. Black TTG indicates the annotated start codon. ATG with a red A at the site of the annotated start codon indicates a point mutation from TTG to ATG. Orange arrows indicate the presence of a start codon lacking *lacZ* gene. Plasmid names are listed on the right. Additional mutations were generated in those constructs spanning the annotated start codon by insertion of a cytosine immediately upstream of the start codon to generate a frame shift in translation from the upstream start codon and are identified in further figures as (p*PmbaS-#+C).*

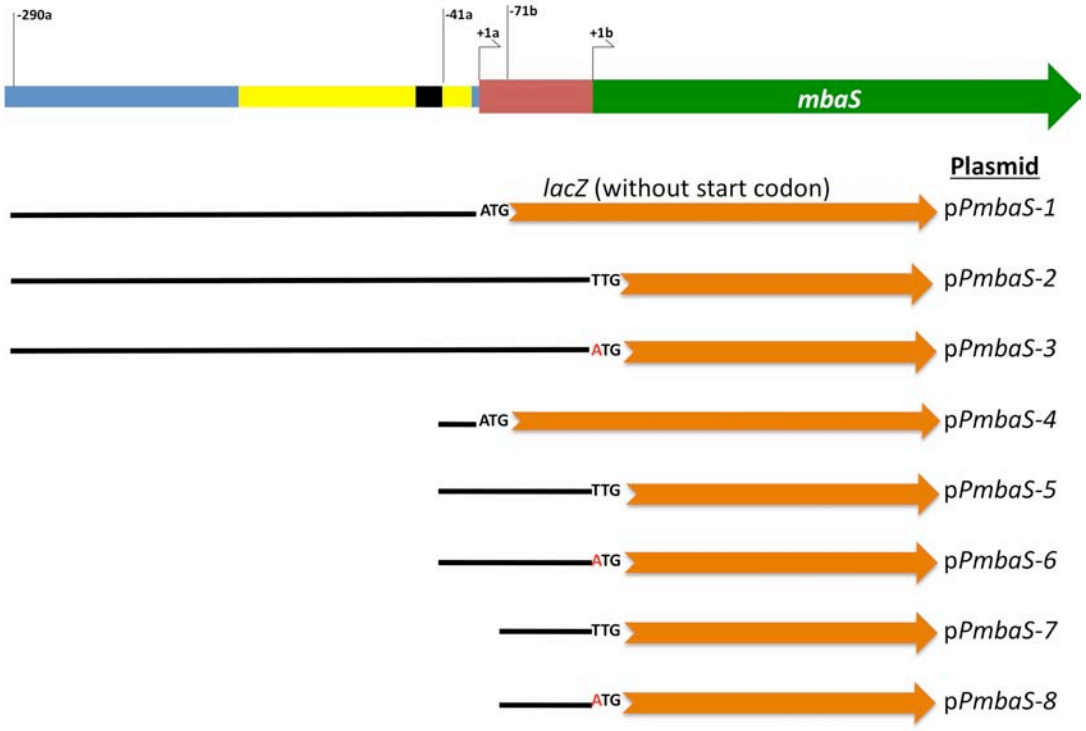
-290a
-41a
-71b
+1a
+1b
mbaS
Plasmid
lacZ (without start codon)
ATG
pPmbaS-1
TTG
pPmbaS-2
ATG
pPmbaS-3
ATG
pPmbaS-4
TTG
pPmbaS-5
ATG
pPmbaS-6
TTG
pPmbaS-7
ATG
pPmbaS-8

Figure III.6 *mbaS* Promoter and Start Codon Activity in *E. coli*: IPTG Induction

Plasmid constructs with promoter truncations and included start codons are depicted in Figure III.5. A: β-galactosidase activity measured for each construct under inducing (LB with 1 mM IPTG) and non-inducing (LB) growth conditions. Averages of biological triplicate and experimental triplicate are graphed. Error bars indicate standard deviations about the mean. B: Modified from Figure III.5 for reference.

A:

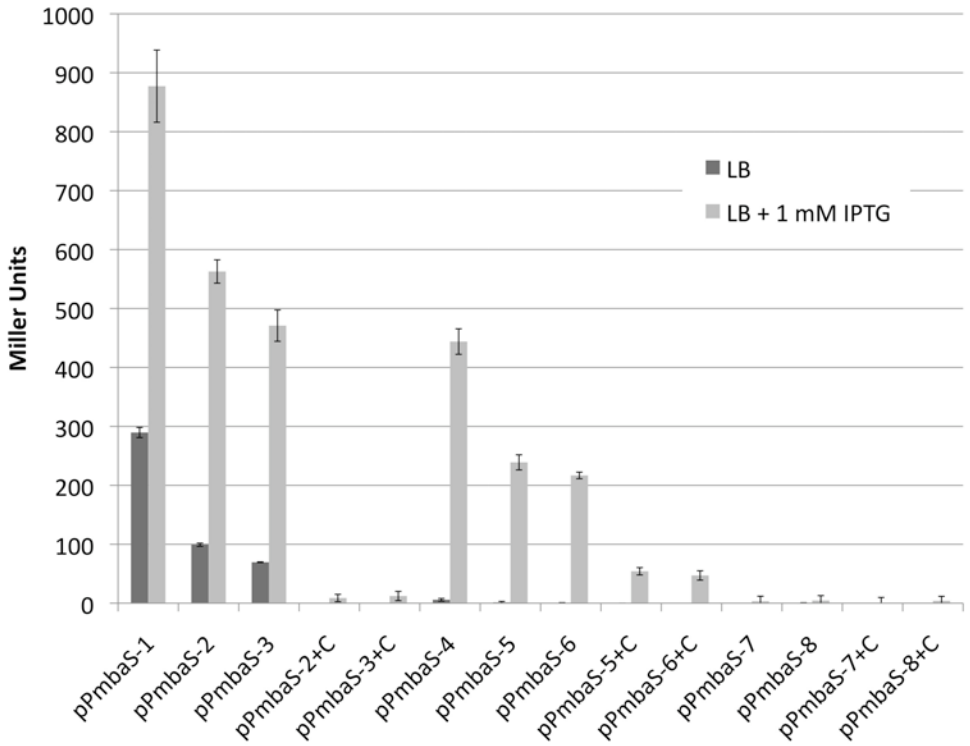
Miller Units
1000
900
800
700
600
500
400
300
200
100
0
LB
LB + 1 mM IPTG
pPmbaS-1
pPmbaS-2
pPmbaS-3
pPmbaS-2+C
pPmbaS-3+C
pPmbaS-4
pPmbaS-5
pPmbaS-6
pPmbaS-5+C
pPmbaS-6+C
pPmbaS-7
pPmbaS-8
pPmbaS-7+C
pPmbaS-8+C

B:

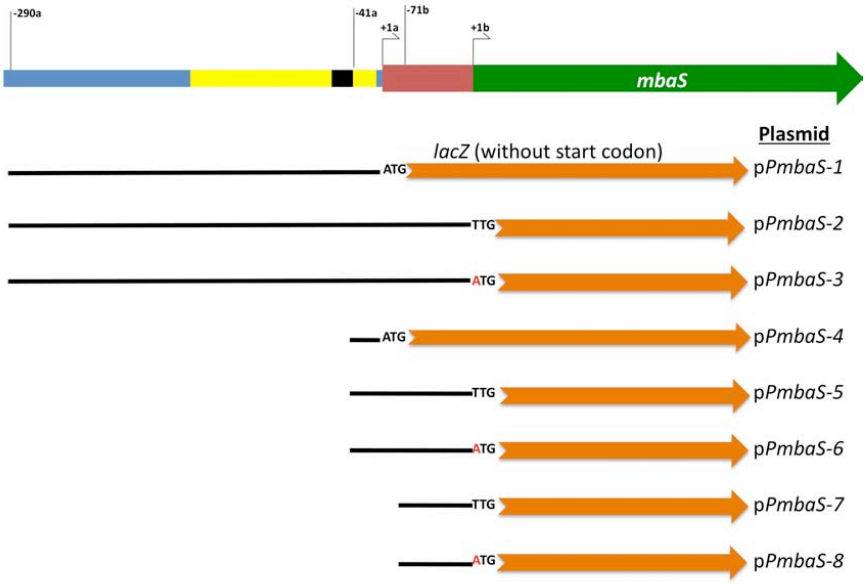
-290a
-41a
-71b
+1a
+1b
mbaS
Plasmid
lacZ (without start codon)
ATG
pPmbaS-1
TTG
pPmbaS-2
ATG
pPmbaS-3
ATG
pPmbaS-4
TTG
pPmbaS-5
ATG
pPmbaS-6
TTG
pPmbaS-7
ATG
pPmbaS-8

Figure III.7: *mbaS* Promoter and Start Codon Activity in *E. coli*: Iron Regulation

Expression was induced by growth of cultures in LB medium containing Constructs utilized in this assay are described in Figure III.5. A: β-galactosidase activity measured for each construct variable iron concentrations (addition of ferric ammonium chloride (FAC)) and iron limitation was achieved with increasing concentrations of the iron chelator dipyridyl (DIP). B: Modified from Figure III.5 for reference.

A:

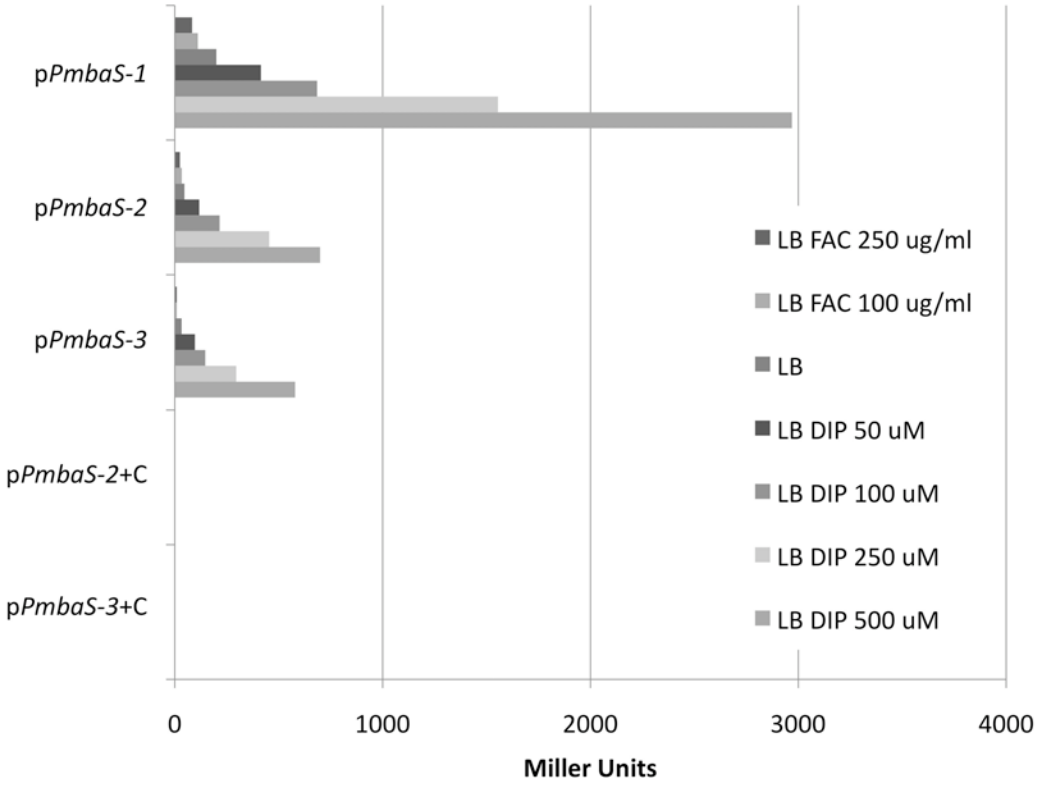
pPmbaS-1
pPmbaS-2
pPmbaS-3
pPmbaS-2+C
pPmbaS-3+C
LB FAC 250 ug/ml
LB FAC 100 ug/ml
LB
LB DIP 50 uM
LB DIP 100 uM
LB DIP 250 uM
LB DIP 500 uM
0
1000
2000
3000
4000
Miller Units

B:

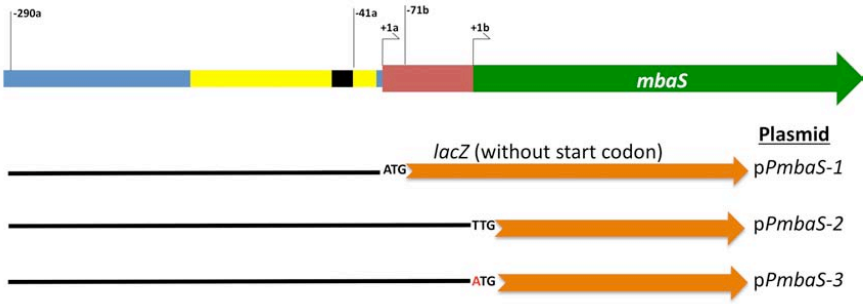
-290a
-41a
+1a
-71b
+1b
mbaS
Plasmid
lacZ (without start codon)
ATG
pPmbaS-1
TTG
pPmbaS-2
ATG
pPmbaS-3

Figure III.8: *mbaS* Promoter and Start Codon Activity in *B. pseudomallei*

Plasmid constructs (described in Figure III.5) were conjugated into the *B. pseudomallei* K96243 *ΔamrABΔmbaS* strain. A: *mbaS* promoter driven expression of *lacZ* was induced by growth in iron limitation (100 μM dipyridyl (DIP)) and IPTG induction (1 mM). Expression was suppressed by addition of ferric ammonium chloride (250 μg/mL FAC). Averages of experimental triplicate are graphed. Error bars indicate standard deviations about the mean. B: Modified from Figure III.5 for reference.

A:

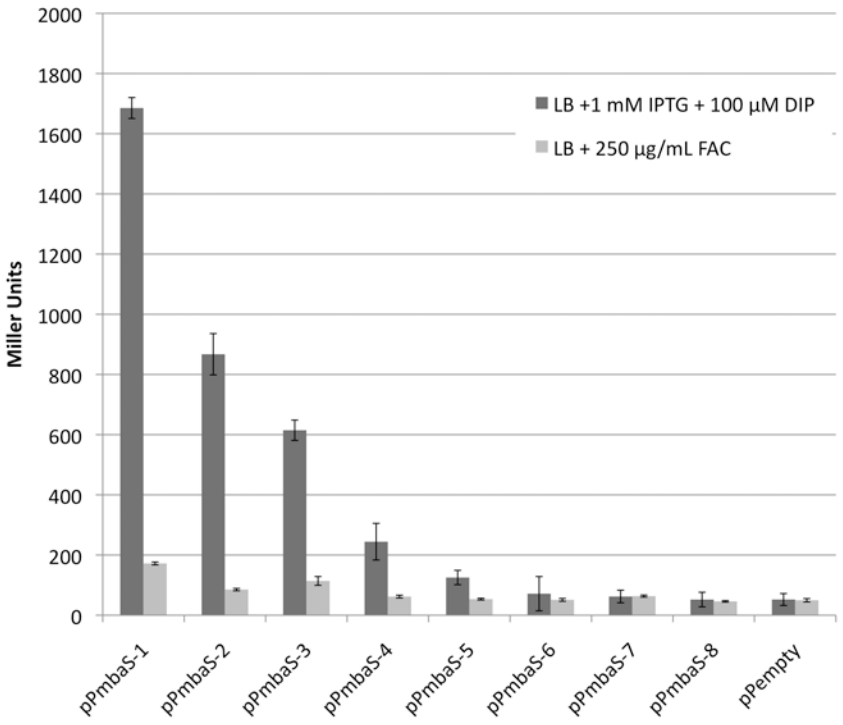
2000
1800
1600
1400
1200
1000
800
600
400
200
0
Miller Units
LB +1 mM IPTG + 100 µM DIP
LB + 250 µg/mL FAC
pPmbaS-1
pPmbaS-2
pPmbaS-3
pPmbaS-4
pPmbaS-5
pPmbaS-6
pPmbaS-7
pPmbaS-8
pPempty

B:

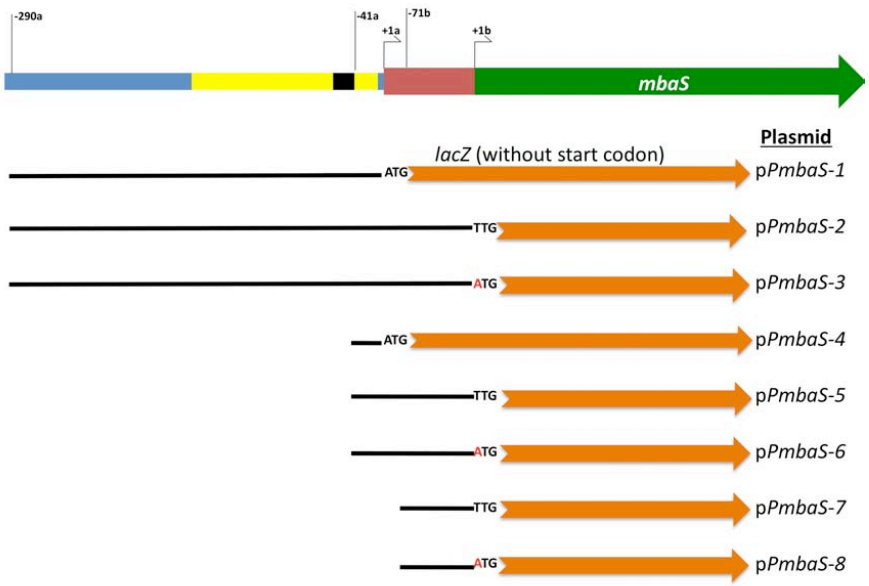
-290a
-41a
+1a
-71b
+1b
mbaS
Plasmid
lacZ (without start codon)
ATG
pPmbaS-1
TTG
pPmbaS-2
ATG
pPmbaS-3
ATG
pPmbaS-4
TTG
pPmbaS-5
ATG
pPmbaS-6
TTG
pPmbaS-7
ATG
pPmbaS-8

IV. Characterization of MbaS Binding Site

IV.A. Introduction

The purpose of this section is two fold. The first is to determine if MbaS protein expression or function is affected by the size of the promoter region of *mbaS*. Two *mbaS* expression constructs were generated with either 290 or 41 nucleotides of the endogenous *mbaS* promoter. Expression profiles, both RNA and protein, and functionality of MbaS were characterized. The second purpose of this section is to confirm MbaS activation of the *mbaJ* and *mbaE* promoters. Previous studies have observed that *mbaJ* and *mbaE* are only expressed when *mbaS* is expressed in *B. pseudomallei* (2).

IV.B. Results

IV.B.i. Description of Two Plasmid System Employed in this Section

The two plasmid systems utilized in this section is illustrated in Figure IV.1. The first plasmid is for the expression of MbaS. *mbaS* including the 290 endogenous promoter described in Section III through the entire open reading frame of *mbaS* was cloned into the multiple cloning site of pMMB208:Km and named pMMB:*290mbaS*. The second plasmid utilized acts as a functional target of the expressed MbaS protein. In this second construct, the MbaS responsive promoter of *mbaJ* is cloned into the multiple cloning site of pQF50:Zeo to generate a promoter fusion to *lacZ* and is named pJ(700) (Figure IV.1).

IV.B.i.a. Proof of Function of Two Plasmid System

The ability of MbaS to drive expression from the *mbaJ* promoter was assayed. The two plasmids (MbaS expression plasmid: pMMB:*290mbaS* and *mbaJ* promoter plasmid: pJ(700)) were co-transformed into the Mach1 *E. coli* strain. Overnight cultures grown in LB medium with appropriate antibiotic selection were subcultured at a dilution of 1:50 into LB medium with or without 1 mM IPTG and 100 ug/ml dipyridyl (DIP) to fully activate both promoters present in the MbaS expression vector. The cultures were allowed to grow for 3.5 hours at 37°C with shaking. At this time samples were taken for RNA purification and qRT-PCR analysis, western blot analysis, and β-galactosidase activity.

MbaS expression was measured at both the RNA and protein level (Figure IV.2). The *mbaS* RNA confirmed transcription from this plasmid system (Figure IV.2A). The MbaS antibody recognized a protein band of an approximate molecule weight in the culture sample containing the induced expression of MbaS that was absent in the empty vector control (Figure IV. 2B). The ability of MbaS to activate the *mbaJ* promoter was also confirmed through the β-galactosidase assay (Figure IV.3). Induction of expression of MbaS resulted in a five-fold increase in the β-galactosidase activity produced from the *mbaJ* promoter when compared with the non-induced control. All samples in this study were normalized to the background exhibited by the two empty vectors (pMMB208:Km and pQF50:Zeo) co-transformed and treated like the experimental samples.

IV.B.ii. Comparison of -290 and -41 mbaS Promoter Fragments in the Expression and Functionality of MbaS

Two constructs were utilized to determine the role of the endogenous *mbaS* in the expression and activity of MbaS (Figure IV.4). The first construct spanned from 290 nucleotides upstream of the functional start codon through the entire *mbaS* open reading frame (pMMB:*290mbaS*) including the putative Fur binding site, and reflects the promoter start codon fragment utilized in Section III that resulted in the highest levels of β-galactosidase activity (p*PmbaS*-1, Figures III.6). The second construct utilized the shorter 41 nucleotide *mbaS* promoter fragment lacking the putative Fur binding site through the entire *mbaS* open reading frame (Figure IV.4) and reflects those constructs studied in Section III that resulted in a more moderate β-galactosidase activity (pMMB:*41mbaS*) (p*PmbaS-4*, Figure III.6). Upstream of each of the inserted *mbaS* promoters in this expression vector is the plasmid encoded *pTac* promoter. These two plasmids were co-transformed independently with the *mbaJ* promoter – *lacZ* fusion plasmid (pJ(200) Figure IV.8). Cultures were grown in varying amounts of iron (from iron replete 250 ug/ml FAC to iron restricted of 250 μM DIP) with varying amounts of IPTG added and harvested as previously described and processed for RNA purification, western blot analysis, and β-galactosidase activity.

Figures IV.5 and IV.6 show that both the *mbaS* RNA level and the MbaS protein level, and the activity driven from the *mbaJ* promoter fragment by the expression of functional MbaS (Figure IV.7) in the 41 nucleotide background were

only responsive to the addition of IPTG. However, the -290 nucleotide promoter construct was responsive to both IPTG and the level of iron restriction in the growth medium. The western blot in Figure IV.6 band A corresponds to MbaS. Band B is a cross reacting band that is occasionally seen in all samples, including the empty vector control (data not shown). In the case of the pMMB:*41mbaS* construct in Figure IV.6B, there is a decrease in the amount of MbaS under the combined expression induction of high iron and high IPTG concentrations. This decrease in MbaS protein is not seen in the pMMB:*290mbaS* expression construct under the same conditions.

IV.B.iii. Characterization of DNA Binding Sequence of MbaS

IV.B.iii.a. In Silico Analysis of MbaS Target Promoters

To genetically confirm the ability of MbaS to activate expression of *mbaJ* and *mbaE*, a series of promoter truncations were generated for the promoter regions of *mbaJ* and *mbaE*, two genes previously demonstrated as regulated by MbaS and proposed to function in the synthesis of malleobactin (2). The *mbaJ* and *mbaE* promoters are divergent from the same non-coding region and the promoter analyzed was determined by the directionality of the cloning of the intergenic region between *mbaJ* and *mbaE* (Figure IV.8). The truncations depicted in Figure IV.8 were cloned upstream of the *lacZ* gene in pQF50:Zeo (Figure IV.1) and include either 60 or 90 nucleotides of the *mbaJ* or *mbaE* open reading frame, respectively. Conserved putative MbaS DNA binding sites were identified in the promoter regions of both

mbaJ (83 nucleotides upstream of the annotated start codon, sequence identified as p*mbaJ* in Figure IV.8) and *mbaE* (90 nucleotides upstream of the annotated start codon, sequence identified as p*mbaE* Figure IV.8) based on homology to the binding sites of PvdS of *P. aeruginosa* (157) and OrbS of *B. cenocepacia* (1) (Figure IV.8). A set of tranversion mutations was made in the 700 and 200 nucleotide promoter fragments of *mbaJ* to the putative MbaS -10 and/or the putative MbaS -35 DNA binding site (sequence identified as m*mbaJ* in Figure IV.8). Mutant promoters were generated using SOE (splicing by overlap extension) mutagenesis on their corresponding wild type promoter background. The plasmids and primers used to generate these constructs are listed in Tables II.4 and II.2, respectively.

IV.B.iii.b. Identification of the MbaS DNA Binding Region in Target Promoters

The assorted *mbaJ* and *mbaE* promoter truncations were co-transformed with the pMMB:*290mbaS* expression vector previously described. MbaS protein expression was induced by the addition of 1 mM IPTG and 100 μM DIP and β-galactosidase activity was determined as previously described. MbaS activated the expression of the pJ(700), pJ(300), pJ(200), pE(700), and pE(250) constructs but not the pJ(150) or the pE(180) constructs (Figure IV.9). This indicates that the MbaS binding sequence resides in the nucleotide sequences between the pJ(200) and pJ(150) and between the pE(250) and pE(180) regions.

IV.B.iii.c. Functional Analysis of Mutagenized MbaS Target Promoters

The previous data (Section III) indicate that the MbaS DNA binding site lies between 85 and 161 nucleotides upstream of the MbaE start codon and between 87 and 145 nucleotides upstream of the MbaJ start codon. Sequence alignment of these two regions, along with previously published observations (2) comparing the DNA binding sequences of PvdS (*P. aeruginosa*) (157) with OrbS (*B. cenocepacia*) (1) reveal a putative MbaS binding sequence of TAAA(N16)CGT located 83 and 90 nucleotides upstream of the annotated start codons of *mbaJ* and *mbaE*, respectively (Figure IV.8 and Figure IV.9). Tranversion mutagenesis of the putative MbaS binding site (either the -10 binding region, -35 binding region, or both -10/-35 binding regions) was utilized to confirm the MbaS recognition sequence (labeled as mMbaJ in Figure IV.8). In this case adenines were exchanged for cytosines and thymines were exchanged for guanines. Mutant promoter fragments were generated utilizing the SOE PCR method (149) with the relevant primers listed in Table II.4 for both the 200 and the 700 nucleotide *mbaJ* promoter fragments. The plasmid constructs were co-transformed with the pMMB:*290mbaS* plasmid and β-galactosidase activity was monitored as previously described. Figure IV.10 displays the results of this mutagenesis study as pertains to the 200 nucleotide *mbaJ* promoter fragments. The results seen with the 700 nucleotide mutant *mbaJ* promoter fragments are consistent with those seen in the mutant 200 nucleotide *mbaJ* promoter fragments (data not shown). Mutagenesis of either the putative

MbaS -10 or -35 DNA binding sequence, or mutagenesis of both sites, resulted in β-galactosidase activity comparable to the background levels.

IV.C. Discussion

Previously described *in silico* analysis of the *mbaS* promoter (Section III) identified a putative Fur binding site 46 nucleotides upstream of the functional start codon. The data illustrated in Figures IV.5, IV.6 and IV.7 confirms that the upstream promoter region of *mbaS*, upstream of 41 nucleotides prior to the functional start codon, is required for iron responsive expression of MbaS. However, further validation of this binding site should be demonstrated both genetically, through site directed mutagenesis of the longer *mbaS* promoter to confirm an abolishment of this regulation, and biochemically, through the purification of *B. pseudomallei* Fur protein and electromobility shift assays against the *mbaS* promoter.

Additional, sequence analysis predicts a possible MbaS binding site that overlaps the Fur binding site in the *mbaS* promoter. This MbaS binding site identification could be due to the fact that both MbaS and Fur bind to AT rich DNA promoter elements and thus leading to a misidentification of the binding site in the *mbaS* promoter. However, it is not uncommon to find a positive feedback loop of some sort in the regulation of sigma factors (8, 31, 47, 136). Thus, it could be possible that there are actually three "levels" of MbaS protein expression regulation. The first level would be the full repression under iron replete conditions. The second level would result from relieving of the Fur repression at mild iron limiting growth conditions. And finally, once some level of the MbaS protein is accumulated in the bacterial cells, there is further up-regulation of MbaS expression.

Now that we have demonstrated that it is possible to achieve functional and soluble MbaS expression, in order to validate the presence of the putative MbaS binding site(s) within its own promoter, we would need to conduct further biochemical studies using electromobility shift assays and DNase footprinting.

Incorporating the upstream start codon results in an *mbaS* open reading frame of 711 nucleotides encoding for a protein with the predicted size of 25.6 kiloDaltons. It is interesting to note that in all of the western blot data presented in this work, the MbaS antibody recognizes a band of approximately 28 kiloDaltons.

We have demonstrated through genetic analysis that MbaS activates *mbaJ* and *mbaE* expression through binding to the TAAA(N16)CGT consensus sequence located 83 and 90 nucleotides upstream of the annotated start codons of each of these genes, respectively. However, we were unable to identify any additional promoter elements for *mbaJ* or *mbaE* through *in silico* analysis.

IV.D. Figures

Figure IV.1: Plasmid Constructs for This Research

Plasmids utilized to screen for the functional expression of the iron responsive sigma factor MbaS. The first plasmid in this system would express MbaS, utilizing either the *pTac* promoter (expressed with the addition of IPTG) or the endogenous *mbaS* promoter (relieved of Fur repression through iron limitation). MbaS would then activate the expression of *lacZ* through recruitment of the RNA core polymerase to activate transcription from the *mbaJ* promoter and resulting in a functional readout of β-galactosidase activity. The blue and purple lines are the *mbaS* and *mbaJ* promoters, respectively. The red boxes are the predicted -35 and -10 DNA sequences in each promoter. The purple triangle indicates the predicted transcriptional start site. The yellow box is the predicted ribosomal binding site.

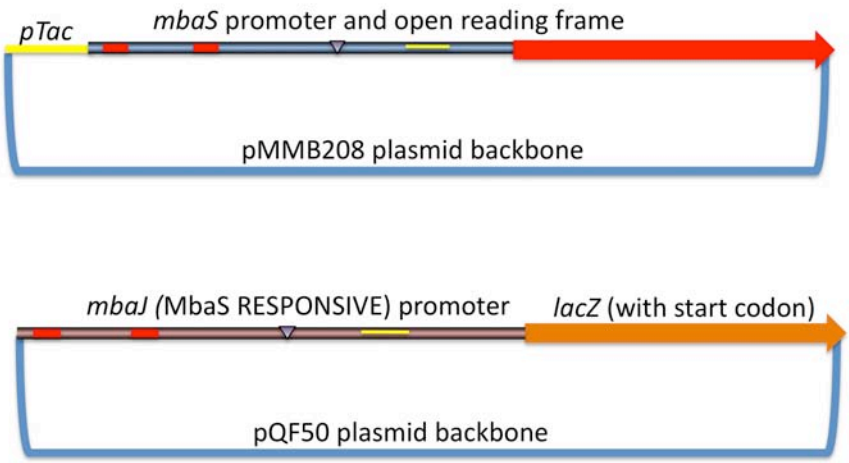
pTac
mbaS promoter and open reading frame
pMMB208 plasmid backbone
mbaJ (MbaS RESPONSIVE) promoter
lacZ (with start codon)
pQF50 plasmid backbone

Figure IV.2: Expression of MbaS

mRNA levels and western blot analysis of MbaS expression in the-two plasmid system. A: cDNA was generated from total purified RNA. C_t values were first normalized to the *E. coli gapA* gene expression and second normalization occurred to an empty vector control (pMMB208:Km). The ΔΔCt value of 14 represents the relative expression compared to the empty vector control. B: Western blot membranes were probed for both the *E. coli* DnaK protein and for MbaS. Arrow indicates the MbaS specific band.

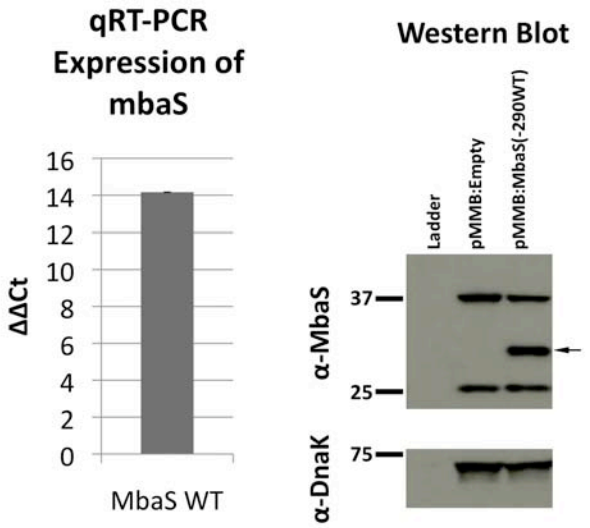
qRT-PCR
Expression of
mbaS
16
14
12
10
8
6
4
2
0
ΔΔCt
MbaS WT
Western Blot
Ladder
pMMB:Empty
pMMB:MbaS(-290WT)
α-MbaS
37
25
α-DnaK
75

Figure IV.3: MbaS Activation of *mbaJ* Promoter Fused to *lacZ*

The ability of MbaS to activate the *mbaJ* promoter fused to *lacZ* was assayed. Samples were grown in induction medium containing both 1 mM IPTG and 100 ug/ml dipyridyl (DIP) for full induction from both encoded promoters in the pMMB:*290mbaS* construct. β-galactosidase activity was normalized to like treated samples containing the pMMB208:Km and pQF50:Zeo empty vectors.

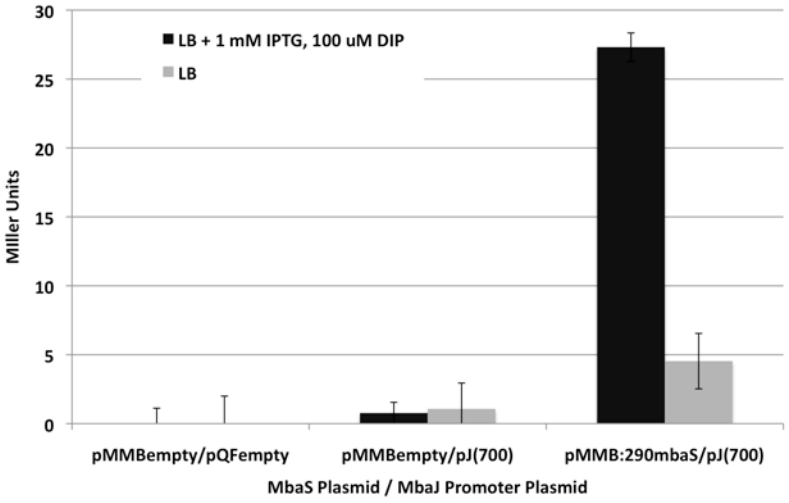
30
25
20
15
10
5
0
Miller Units
LB + 1 mM IPTG, 100 uM DIP
LB
pMMBempty/pQFempty
pMMBempty/pJ(700)
pMMB:290mbaS/pJ(700)
MbaS Plasmid / MbaJ Promoter Plasmid

Figure IV.4: Schematic Diagram of *mbaS* Expression Constructs

Two constructs were generated to express *mbaS*. The first construct includes 290 nucleotides of the promoter of *mbaS* and the entire open reading frame (top). The second construct includes 41 nucleotides of the *mbaS* promoter (starting after the putative Fur binding site, black box) and the entire *mbaS* open reading frame (bottom). Both of these constructs include the upstream functional start codon (+1a).


-290a
-41a
-71b
+1a
+1b
mbaS
-41a
-71b
+1a
+1b
mbaS

Figure IV.5: qRT-PCR Analysis of Combinational Iron-Limitation and IPTG Induction of Expression of *mbaS*

MbaS expression was induced from the pMMB:*290mbaS* construct (A) and the pMMB:*41mbaS* construct (B) under variable iron and IPTG concentrations. RNA was purified and *mbaS* expression quantified. First normalization (ΔC_T) was determined against the *E. coli gapA* gene and second normalization ($\Delta\Delta C_T$) was against *mbaS* expression without IPTG and at the highest iron concentration (250 ug/ml FAC, left most column in each graph). C: Modified from Figure IV.4 for reference.

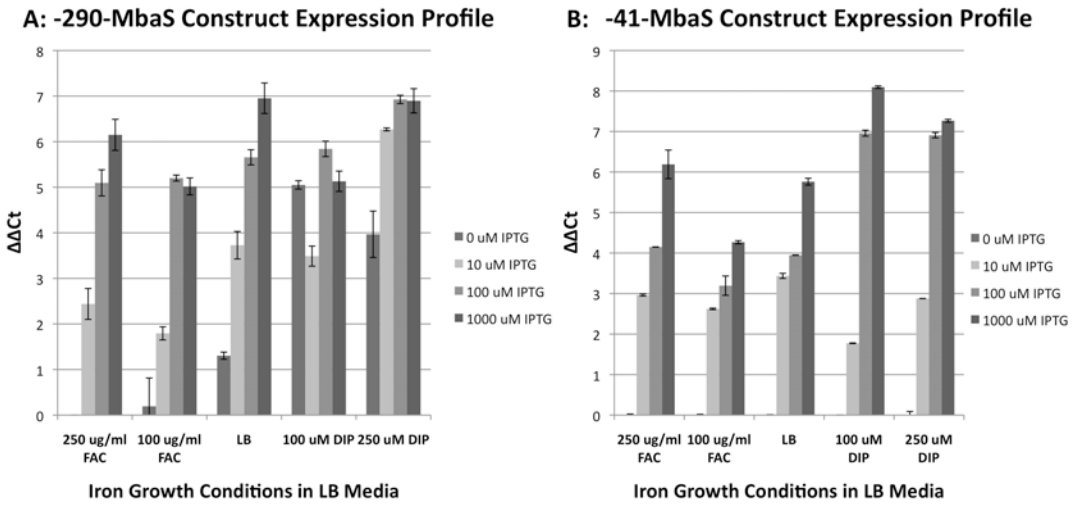
A: -290-MbaS Construct Expression Profile
ΔΔCt
0 uM IPTG
10 uM IPTG
100 uM IPTG
1000 uM IPTG
250 ug/ml FAC
100 ug/ml FAC
LB
100 uM DIP
250 uM DIP
Iron Growth Conditions in LB Media
B: -41-MbaS Construct Expression Profile
ΔΔCt
0 uM IPTG
10 uM IPTG
100 uM IPTG
1000 uM IPTG
250 ug/ml FAC
100 ug/ml FAC
LB
100 uM DIP
250 uM DIP
Iron Growth Conditions in LB Media

C:


-290a
-41a
-71b
+1a
+1b
mbaS
-41a
-71b
+1a
+1b
mbaS

Figure IV.6: Figure II.11: Western Blot Analysis of Combinatorial Iron-Limitation and IPTG Induction of Expression of MbaS

MbaS expression was induced from the pMMB:*290mbaS* construct (A) and the pMMB:*40mbaS* construct (B) under variable iron and IPTG concentrations. Whole cell lysates were processed as described. Band A corresponds to MbaS. Band B is a cross-reacting band that appears in many samples under high IPTG concentration, including empty vector (pMMB208:Km). DnaK from *E. coli* was used as a loading control for all samples. C: Modified from Figure IV.4 for reference.

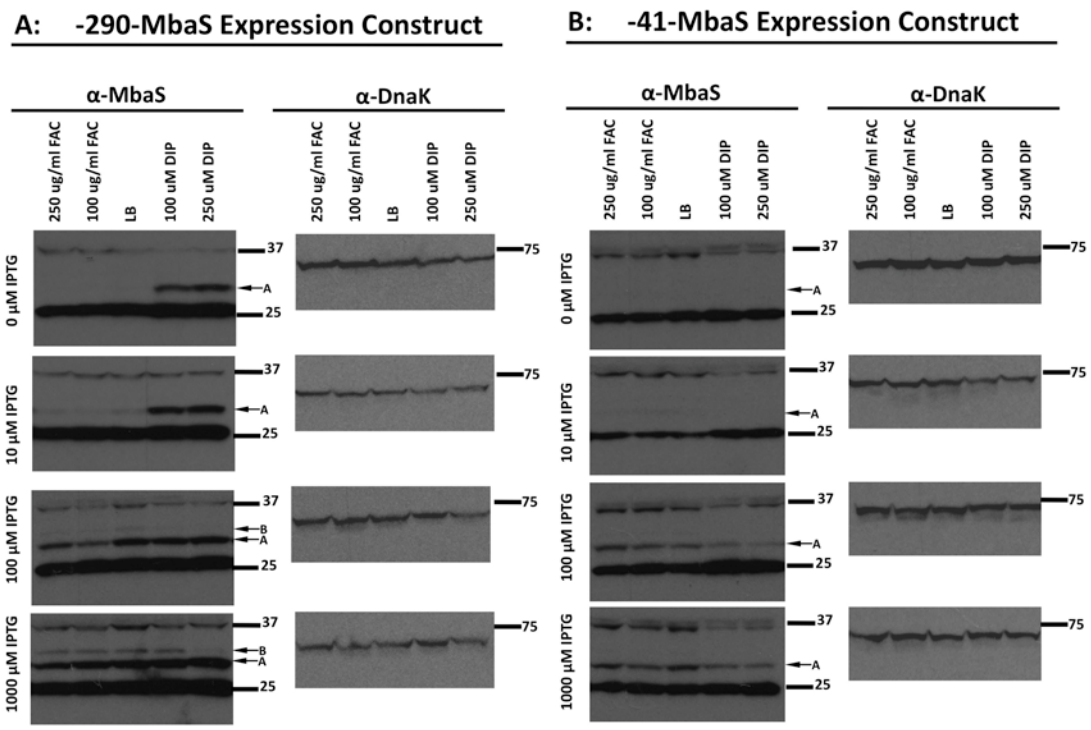
A: -290-MbaS Expression Construct
B: -41-MbaS Expression Construct
α-MbaS
α-DnaK
250 ug/ml FAC
100 ug/ml FAC
LB
100 uM DIP
250 uM DIP
0 µM IPTG
10 µM IPTG
100 µM IPTG
1000 µM IPTG
37
25
75
A
B

C:


-290a
-41a
-71b
+1a
+1b
mbaS

Figure IV.7: β-galactosidase Analysis of Combinatorial Iron-Limitation and IPTG Induction of Expression of MbaS on the Activity of *mbaJ* Promoter

MbaS protein expression was induced from the pMMB:*290mbaS* construct (A) and the pMMB:*41mbaS* construct (B) under variable iron and IPTG concentrations with the pJ(200) (plasmid containing 200 nucleotides of the *mbaJ* promoter fused to *lacZ*) as a functional readout. β-galactosidase assays were carried out as previously described. C: Modified from Figure IV.4 for reference.

A:

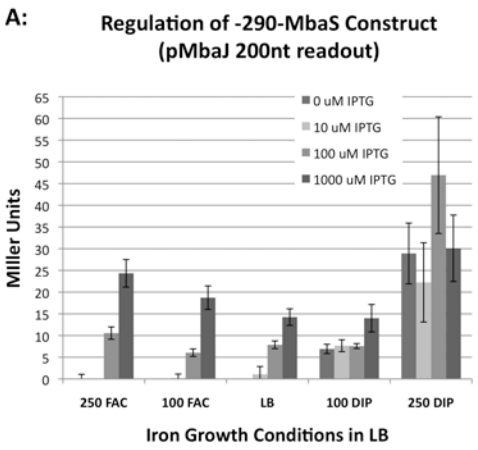
Regulation of -290-MbaS Construct
(pMbaJ 200nt readout)
Milller Units
0 uM IPTG
10 uM IPTG
100 uM IPTG
1000 uM IPTG
250 FAC
100 FAC
LB
100 DIP
250 DIP
Iron Growth Conditions in LB

B:

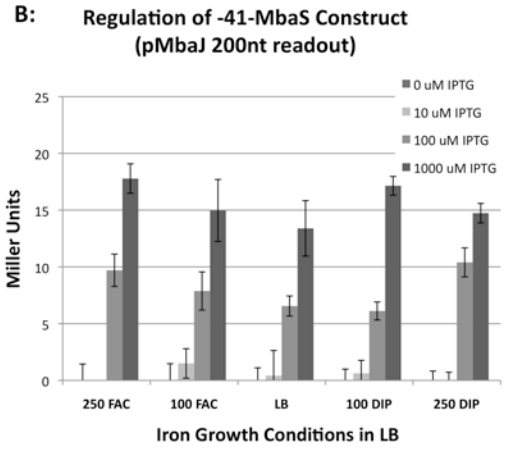
Regulation of -41-MbaS Construct
(pMbaJ 200nt readout)
Miller Units
0 uM IPTG
10 uM IPTG
100 uM IPTG
1000 uM IPTG
250 FAC
100 FAC
LB
100 DIP
250 DIP
Iron Growth Conditions in LB

C:


-290a
-41a
-71b
+1a
+1b
mbaS
-41a
-71b
+1a
+1b
mbaS

Figure IV.8: *In silico* Analysis of *mbaJ* and *mbaE* Promoters and Plasmid Constructs

mbaJ and *mbaE* are expressed from a divergent promoter and have previously been observed to require MbaS for expression (ref). The intergenic region between the two MbaS responsive genes *mbaJ* and *mbaE* were sequentially truncated to identify the MbaS binding domain (labeled as truncations). Due to sequence homology, we identified a putative -10 and -35 binding site in front of both of the MbaS responsive genes (red blocks) likely to encode for the MbaS DNA binding sequence. These sequences were mutated both individually and in parallel (depicted as green blocks and letters under the "mutants" heading) in both the 200 and 700 nucleotide promoter fragments of *mbaJ*. The lower panel in the figure shows the -10 and -35 binding sites for OrbS (iron responsive sigma factor of *B. cenocepacia*) and PvdS (iron responsive sigma factor of *P. aeruginosa*), sequence alignment of *mbaJ* and *mbaE* promoter regions with predicted -10 and -35 sites (pMbaJ and pMbaE, respectively), and the putative MbaS binding sequence. mMbaJ indicates the mutations that were introduced into the -10 and -35 boxes of pMbaJ.

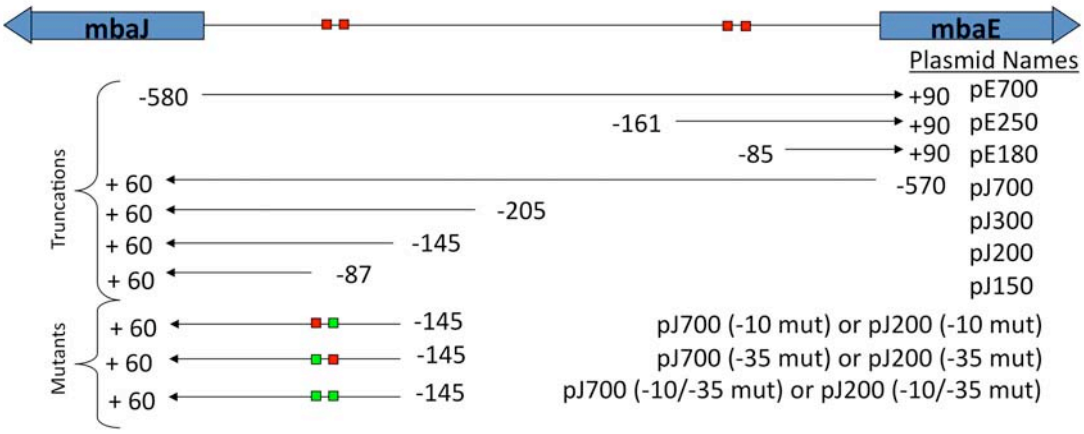

	-35		-10	
mMbaJ	GCCCC	(N16)	ATG	
pMbaJ	CGG**TAAAA**AATTTCGCCCGTGATT**CGT**CTC	(N80)	ATG	
pMbaE	GGG**TAAAG**ATTCGGCGCGCCCATT**CGT**CTA	(N87)	ATG	
MbaS	TAAAA	(N16)	CGT	
OrbS	TAAAA	(N16)	CGT	
PvdS	TAAAT	(N16)	CGT	

Figure IV.9: MbaS Activation of *mbaJ* and *mbaE* Promoter Truncations

A: MbaS protein expression for the activation of *mbaJ* and *mbaE* promoter truncations was induced by growth in LB medium containing 1 mM IPTG and 100 μM dipyridyl (DIP). β-galactosidase activity was determined as previously described. Samples were normalized to the dual empty vectors (pMMB208:Km and pQF50:Zeo) treated the same as the experimental samples. Error bars are indicative of the standard deviation about the mean. Asterisks indicate samples with significantly decreased levels of β-galactosidase activity compared to their respective full-length 700 nucleotide constructs. B: Modified Figure IV.8 for reference.

A:

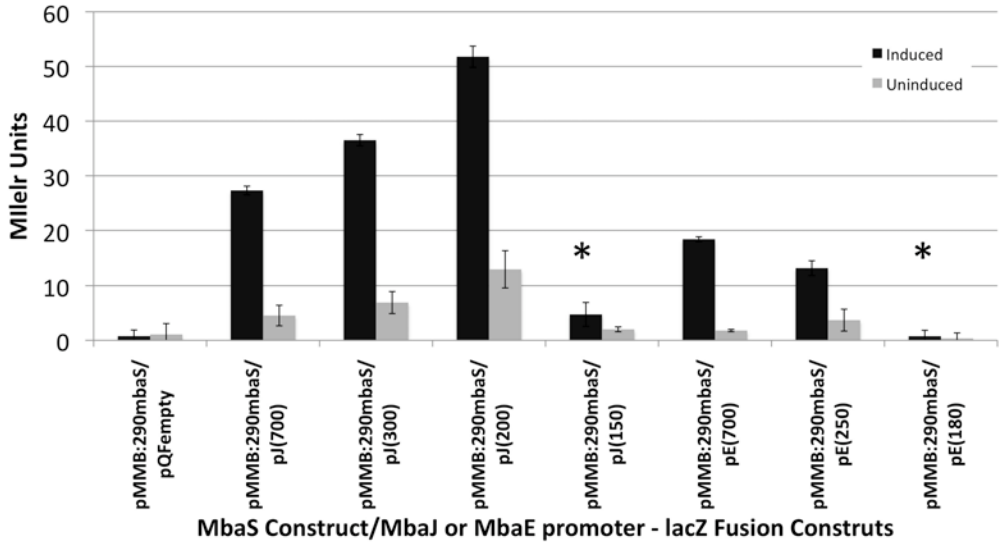
60
50
40
30
20
10
0
MIlelr Units
Induced
Uninduced
*
*
pMMB:290mbaS/ pQFempty
pMMB:290mbaS/ pJ(700)
pMMB:290mbaS/ pJ(300)
pMMB:290mbaS/ pJ(200)
pMMB:290mbaS/ pJ(150)
pMMB:290mbaS/ pE(700)
pMMB:290mbaS/ pE(250)
pMMB:290mbaS/ pE(180)
MbaS Construct/MbaJ or MbaE promoter - lacZ Fusion Construts

B:

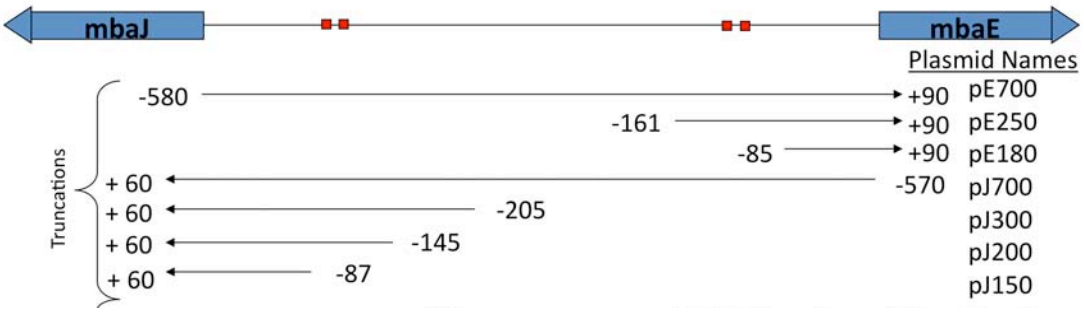
mbaJ
mbaE
Plasmid Names
-580
+90 pE700
-161
+90 pE250
-85
+90 pE180
-570 pJ700
pJ300
pJ200
pJ150
Truncations
+ 60
+ 60
+ 60
+ 60
-205
-145
-87

Figure IV.10: MbaS Activation of Mutant *mbaJ* Promoters

A: MbaS protein expression for the activation of *mbaJ* promoter mutations was induced by growth in LB medium containing 1 mM IPTG and 100 μM dipyridyl (DIP). β-galactosidase activity was determined as previously described. Samples were normalized to the dual empty vectors (pMMB208:Km and pQF50:Zeo) treated the same as the experimental samples. Asterisks indicate samples with significantly decreased levels of β-galactosidase activity when compared to the non-mutated control J(200). B: Modified Figure IV.8 for reference.

A:

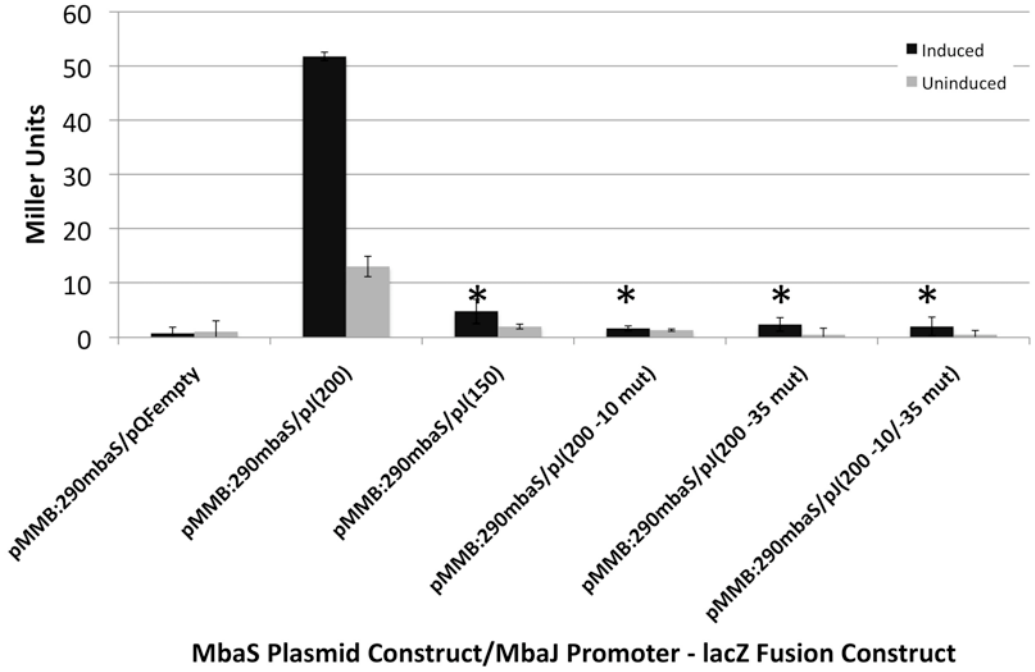

B:

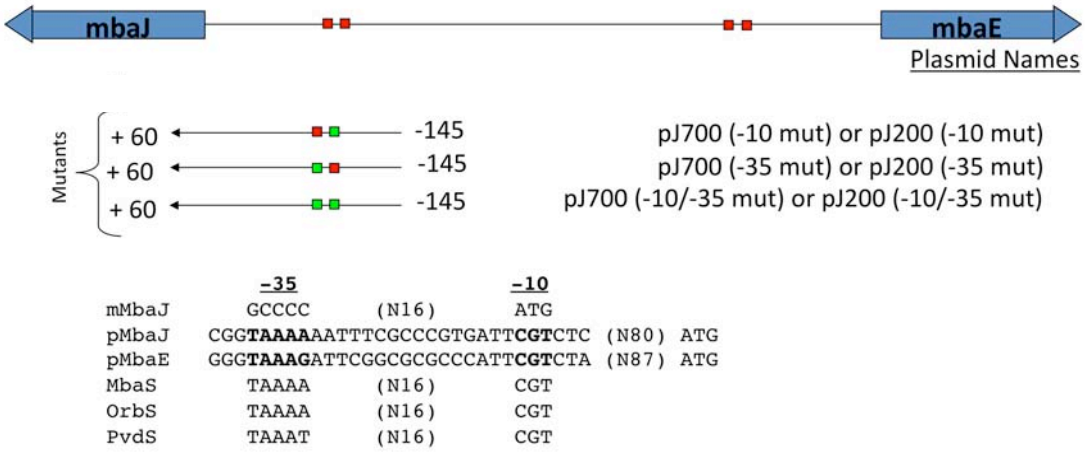

	-35		-10	
mMbaJ	GCCCC	(N16)	ATG	
pMbaJ	CGG**TAAAA**AATTTCGCCCGTGATT**CGT**CTC	(N80)	ATG	
pMbaE	GGG**TAAAG**ATTCGGCGCGCCCATT**CGT**CTA	(N87)	ATG	
MbaS	TAAAA	(N16)	CGT	
OrbS	TAAAA	(N16)	CGT	
PvdS	TAAAT	(N16)	CGT	

V. Mutagenesis of MbaS

V.A. Introduction

Expression of the genes required for malleobactin synthesis and uptake is regulated by the alternative sigma factor MbaS. MbaS, part of the sigma 70 class of sigma factors, shares significant homology with the *Pseudomonas aeruginosa* extracytoplasmic function (ECF) sigma factor PvdS.

Sigma 70 homologues contain several, if not all, of the functional domains identified in sigma 70. The three functionally conserved domains are 1) regions 2.1 and 2.2 which bind to the RNA core polymerase for the activation of transcription, 2) regions 2.3 and 2.4 that recognize the -10 DNA binding sequence and is responsible for the initial DNA melting and 3) region 4 which recognizes the -35 DNA binding sequence and encodes for a conserved helix-turn-helix structural motif (Figure I.5) (102). Previous work by Wilson and Lamont (156) identified 26 amino acids with specific roles in mediating these interactions in PvdS of *P. aeruginosa* (identified in Figure V.1). The additional two regions are not highly conserved and have been implicated in inhibition of non-specific binding of the sigma factor (region 1) and maintaining the structure of the sigma factor (region 3) (102).

Due to the similarities and differences seen in the regulation of MbaS and PvdS (discussed in Section I), it is of interest to compare the primary amino acid sequence of these two sigma factors to identify if those conserved residues in the three conserved domains are also functionally relevant. The mutant data presented

in this section demonstrate the functional conservation of the amino acids in Region 2.1 and 2.3, but not in Region 4.

V.B. Results

V.B.i. Sequence Analysis of MbaS

To identify MbaS residues that function in RNA core polymerase recruitment, -10 DNA sequence recognition, or -35 DNA sequence recognition (Figure V.1A), sequence alignments were performed comparing MbaS to PvdS of *P. aeruginosa*, and OrbS of *B. cencocepacia* (Figure V.1B). Sequences were conserved between MbaS and PvdS for Regions 2 and Regions 4 (identified in Figure V.1A). Wilson and Lamont (2006) have previously identified 26 amino acids between these two regions that resulted in either attenuated or abolished function in PvdS (highlighted as Red in Figure V.1B) (156). Of those characterized residues in PvdS, six were selected to be repeated in MbaS to generate two point mutations in each of the three identified functional regions (RNA core interaction: D77A and D81A, -10 DNA recognition: D112A and R115A, -35 DNA recognition: R197A and D198A). A second class of mutants were generated in residues that are conserved between MbaS and PvdS and reside within region 3 but were not previously characterized in PvdS (C127A, S139A, E141A, and R165A) or in quadruple (115REET:AAAA, 120ENTY:AAAA, and 126DEDD:AAAA). These quadruple mutants span the antigenic epitope used to generate the polyclonal MbaS antibody that is used in this study. The final class of mutants generated were selected based upon conservation

between MbaS, OrbS, and other annotated sigma factors of *B. pseudomallei* but not with PvdS (C114A, R172A, E176A, C206A, C220A, quadruple 174REET:AAAA, and C-terminal 13 amino acid deletion). All of these mutants are identified in Figure V.1B by highlighting the residues in red for those previously characterized in PvdS or green for the remaining mutated residues. Mutations were generated utilizing SOE PCR mutagenesis in the pMMB:*290mbaS* plasmid backbone with mutation specific primers (Table II.4).

V.B.ii. Expression Analysis of MbaS Constructs in E. coli

Since mutagenesis of MbaS may result in non-expression of the MbaS RNA or the protein, it is of primary importance to determine the expression profiles at both levels prior to examining the functionality of each of the mutations generated. In all cases these expression profiles were determined in the same *E. coli* samples utilized for the functional analysis. The MbaS expression constructs were co-transformed with the appropriate *mbaJ* or *mbaE* promoter fusions to *lacZ* (for system description see Section IV). Overnight cultures containing the appropriate plasmids were subcultured into liquid medium containing antibiotic selection at a 50-fold dilution. Expression was induced with the addition of 1 mM IPTG and 100 μM/ml DIP and repressed with the addition of 100 μg/ml FAC. Cultures were incubated for 3.5 hours at 37°C and samples were taken for qRT-PCR analysis, protein analysis, and β-galactosidase production.

V.B.ii.a. qRT-PCR Analysis of MbaS Expression

Samples were first normalized to the expression of the *E. coli gapA* gene and second normalization was against the empty vector control. qRT-PCR analysis revealed an average $\Delta\Delta C_T$ of 14, which corresponds to a 16,384 (2^{14}) fold gene expression (Figure V.2). Due to the high GC nature of the *mbaS* open reading frame, we were unable to construct PCR primers that did not overlap with at least a couple of the point mutations. These overlapping sites are indicated in Figures V.1 and V.2 with an asterisks and likely the reason for the reduced expression profile for the R115A, 115RRQT:AAAA, and 120ENTY:AAAA mutations.

V.B.ii.b. Western Blot of Protein Expression

Protein levels were determined for each of the mutant MbaS constructs. 2 OD_{600} equivalents of each sample were harvested and resuspended in 500 µl of 2x SDS sample buffer and processed as described. The same volume of each sample was loaded in each gel. After transfer to nitrocellulose membranes each gel was probed with both the α-MbaS antibody and α-DnaK to confirm consistent loading (Figure V.3). In order to visual MbaS in all samples, the total protein loaded was such that the DnaK levels consistently overwhelmed the gels. Thus, we were never able to see the MbaS protein levels when samples were loaded to quantities that did not result in DnaK overloading (data not shown). We have relied on the fact that we have used identical culture concentrations for each of the samples to confirm MbaS expression. Figure V.3A depicts a moderate exposure time of 10 minutes while Figure V.3B

shows the same membrane with a long exposure time of 20 minutes. In all samples there was some level of MbaS protein expressed in the cells and is identified as Band A in each frame. The 120ENTY:AAAA quadruple mutant consistently results in two bands, one at the expected size for MbaS as previously determined and one slightly smaller (identified as Band C in Figure V.3). The quadruple 126DEDD:AAAA consistently resulted in a smaller band with the approximate size equivalent to that of the smaller band in the 120ENTY:AAAA mutation. Mutations 174REET:AAAA and ΔC13 had such low protein expression that they were only visible after extended exposure times. Additionally, due to the size shifts seen in the aforementioned mutants, the pMMB:*41mbaS* expression construct was also utilized in this series of western blots to confirm that any size variation was not due to possible mutations that may have occurred to the *mbaS* promoter. There was no difference in the size of the wild type MbaS protein comparing the two promoter constructs. The reduction of protein expressed between the two promoter constructs is consistent with what is seen in Section IV. Band B corresponds to a cross-reacting band frequently seen in all samples after extended exposures.

V.B.iii. Activity of Mutant MbaS Constructs in E. coli

The activity of each of the generated mutants was assayed as previously described for the two-plasmid system in Section IV. Each mutant was co-transformed with either the pJ200 construct or the pE250 construct, expression of MbaS was induced, and β-galactosidase activity measured. The mutants were subdivided into two

groups, those six that corresponded with previously studied residues in PvdS and the remaining fourteen. Of the previously characterized PvdS residues, the homologous D77A, D81A, D112A, and R115A mutations in MbaS generated proteins that were unable to activate the promoters of either *mbaJ* or *mbaE* (identified with asterisks in Figure V.4). This confirms the belief that the D77 and D81 residues likely mediate the interaction with the RNA core polymerase and that the D112 and R115 residues mediate the -10 DNA sequence recognition. However, the R197A and D198A, which should correspond to the -35 DNA recognition site, showed no reduction in β-galactosidase production for either promoter tested (Figure V.4). As for the remaining mutations, only the quadruple mutants (115RRQT:AAAA, 120ENTY:AAAA, and 174REET:AAAA) yielded reduced β-galactosidase activity (Figure V.5). The 115RRQT:AAAA mutation overlaps the R115A mutation previously mentioned to have reduced function and the 120ENTY:AAAA flanks this region, confirming that this area, at least from amino acids 115 through 124 play a role in the function of MbaS. Although the 174REET:AAAA mutation did have decreased function, the E176A mutation did not have a significant decrease in function (Figure V.5). Thus, considering the decreased protein levels of 1774REET:AAAA, it is likely that the quadruple mutation destabilizes the protein. The other protein with a significant expression decrease in Figure III.3, ΔC13, appeared to have relatively normal functional levels of β-galactosidase (Figure V.5).

V.B.iv. Expression and Functional Analysis of MbaS Constructs in B. pseudomallei

Work presented in this section so far has been conducted in *E. coli*. Although we have demonstrated that the 290 nucleotide promoter of *mbaS* is functional in *B. pseudomallei* (Section III), we have not yet demonstrated that we can express functional MbaS protein or that there is a direct relationship between what is seen in the two-plasmid β-galactosidase assay in *E. coli* and restoration of function in *B. pseudomallei* for the mutant constructs. For the purposes of this study, four plasmids were chosen to confirm the relationship between what is seen in *E. coli* and *B. pseudomallei*. These plasmids include an empty vector control (pMMB208:Km), the MbaS wild type expressing construct (pMMB:*290mbaS)*, a non-functional point mutation (pMMB:*290mbaS*(D77A)), and a functional point mutation (pMMB:*290mbaS*(S139A)). These expression constructs were conjugated into the *B. pseudomallei ΔamrABΔmbaS* strain background. Deletion of the *amrAB* efflux pump resulted in increased sensitivity of this strain to kanamycin.

V.B.iv.a. Expression Analysis of Mutant MbaS Constructs in B. pseudomallei

MbaS expression was confirmed at both the RNA and the protein levels. Overnight liquid samples were subcultured at a 1 to 50 dilution into LB medium containing either 100 μg/ml FAC for repression of expression or 250 μM DIP for induction of expression. After 6 or 24 hours of growth, samples were taken for RNA analysis (6 hour and 24 hour time points) or western blot analysis (24 hour time point). All samples were normalized to the culture density prior to processing

RNA samples were processed as described. qRT-PCR normalization was first conducted against the *B. pseudomallei gapA* gene (BPSL2952) and second normalization was against the empty vector control (pMMB208:Km). Both time points, which correspond to early log phase (6 hours) and stationary phase (24 hours) revealed significant expression of MbaS (Figure V.6A).

Due to low cell density and volume limitations imposed for working in the BSL3, we were unable to recover enough cells from the 6 hour time point to conduct a reliable western analysis of the MbaS protein levels. The 24 hour samples did demonstrate significant MbaS protein levels. However, instead of the expected single band at approximately 28 kDa as seen in *E. coli* (Figure V.6B, band A) there was a second larger band in all samples that contained an MbaS expression construct (Figure V.6b, band B). At this time we are unable to say which of these two bands correspond to the functional MbaS or if both are functional MbaS with possible post-translational modifications generating this doublet.

V.B.iv.b. Activity of Mutant MbaS Constructs in B. pseudomallei

The four previously described MbaS complementation vectors were tested for their ability to eliminate growth defects seen in the *B. pseudomallei ΔamrABΔmbaS* strain background. Overnight cultures were subcultured into iron restrictive (LB medium containing 250 μM DIP) or iron replete (LB medium containing 100 μg/ml FAC) medium at a 1 to 50 dilution and incubated for 24 hours at which time the OD_{600} was measured. Figure III.7A demonstrates that the *mbaS* deletion reduced the final

OD_{600} to approximately 0.2 as compared to the wild type strain value 2 under iron limitation. The wild type and the S139A mutation were able to significantly restore this growth defect while the D77A mutation was not (Figure III.7A). The second assay utilized to determine the functionality of MbaS is that of the Chrome azurol S (CAS) plate assay. Secreted siderophores are able to chelate the iron bound to chrome azurol S and induce a color change from blue to orange/yellow. Two µl of overnight liquid culture of each of the complementation strains was spotted onto CAS plates and incubated at 37°C for 36 to 48 hours. Representative images of the resulting CAS halos are depicted in Figure III.7B. The empty vector-complemented *mbaS* deletion construct and the D77A mutant complementation strains had negligible halo development, while the wild type and S139A complemented strains had halos comparable to the parent strain of *B. pseudomallei* (Figure III.7B).

V.C. Discussion

The purpose of this section was two fold. First to demonstrate the functional conservation between the residues of MbaS and the previously characterized PvdS of *P. aeruginosa*. Secondly, we needed to demonstrate that the results of the functional assays developed for *E. coli* could be translated to the production of a functional MbaS construct in *B. pseudomallei*. Toward these ends we generated six point mutants in residues of MbaS corresponding to characterized residues of PvdS its three functional domains. The MbaS point mutants D77A and D81A correspond to mutations demonstrated as functional in the RNA core polymerase binding of PvdS (Figure V.1). In this study, we have observed that these two mutations abolish the ability of MbaS to activate transcription from the *mbaJ* and *mbaE* promoters. The D112A and R115A point mutations in MbaS correspond with mutations made in PvdS that function in the recognition of the -10 DNA recognition by PvdS. These two mutations in MbaS also resulted in an inhibition of β-galactosidase activity driven from either of the *mbaJ* or *mbaE* promoters. The fifth and sixth mutations corresponding to those in PvdS with reduced activity, R197A and D198A, which were predicted to function in the -35 DNA promoter sequence, showed no functional defects in the assay used.

Further analysis of the functional location of the R197A and D198A point mutations demonstrated that these two mutations likely lie too the far toward the N-terminus to mediate strong interactions with the -35 DNA sequence. Figure V.8 shows the sequence alignment of region 4.2 of MbaS and RpoE of *E. coli*. The crystal

structure of region 4 of RpoE complexed with the -35 DNA sequence (conducted by Lane and Darst, 2006 (79), accessed from the Protein Data Bank (11)) show that mutations generated in region 4.2 of MbaS do not align with the four residues observed to mediate the sigma factor – DNA interaction. Additional mutations will need to be generated to confirm the role of this region if MbaS and should be conducted in the amino acid residues Q189, T190, F194, and M195. These four residues align with those seen in both PvdS (Figure V.1) and RpoE (Figure V.8) to mediate the -35 DNA interaction.

Additional mutations were generated, primarily in Region 3 of the protein. We are unable to make any conclusive statements regarding the function of these residues due to a) overlap with the -10 DNA binding site or b) apparent protein truncations/modifications resulting in variable protein expression profiles. Further studies are necessary to 1) identify residues mediating the -35 DNA sequence recognition and 2) confirm that the domains function are as predicted. Additional studies to confirm domain function could include the use of whole cell lysate immunoprecipitation against the RNA core polymerase to confirm MbaS interaction and MbaS purification followed by electromobility shift assays to confirm DNA binding. Although previous attempts to purify MbaS have failed, due to the use of the annotated sequence for construct design, there is now substantial data to support the belief that MbaS purification is possible.

A factor limiting the amount of research conducted on *B. pseudomallei* is the fact that it is classified as a Biosafety Level 3 (BSL3) Select Agent. By conducting the

vast majority of the presented research in *E. coli*, we have circumvented the myriad of limitations involved in working with *B. pseudomallei* in the BSL3 facility. However, it is necessary to support all conclusions gained when working in a different system with findings in the original bacteria. In this case, we demonstrated the conserved functionality of two MbaS mutants between *E. coli* and *B. pseudomallei*. It is critical to point out that none of the liquid assays for *B. pseudomallei* were allowed to grow past 24 hours and the CAS plate assays past 48 hours. Extending the growth times past this point results in a partial restoration of iron limiting growth and CAS halo production, likely due to the pyochelin siderophore whose biosynthetic genes are encoded within the *B. pseudomallei* genome (65).

However, we did see one unexpected anomaly between the two systems and that is the apparent size of the MbaS protein when expressed in *E. coli* as opposed to when expressed in *B. pseudomallei*. The dual protein bands observed when expressing MbaS in *B. pseudomallei* are most likely due to proteolysis of this protein, with the higher molecular weight band corresponding to the full length protein (Figure V.6). This is not an unsupported supposition as PvdS is truncated when the bacteria are grown under oxygen limiting conditions (50, 122). Another possibility is that MbaS is post-translationally modified. The most likely form of post-translational modification for DNA binding proteins is phosphorylation. Further work is necessary to elucidate the presence of these two bands. One method to address this would be the purification of a tagged MbaS protein from *B.*

pseudomallei, followed by western blot analysis with anti-phosphorylation specific antibodies, or mass specrophotometry.

V.D. Figures

Figure V.1: Sequence Comparison and Mutation Identification

A: Sequence alignments of MbaS with PvdS (*P. aeruginosa*) and OrbS (*B. cenocepacia*) using ClustalW (134). A: Sigma 70 domain identification in the MbaS protein. RNA core polymerase, -10 DNA recognition, and -35 DNA recognition sites are underlined. Predicted secondary structure is indicated. Mutations generated in this study are identified. Approximate location of PCR primers used for the qRT-PCR analysis are indicated. B: OM: sequence conservation of MbaS compared to OrbS. OMP: sequence conservation between OrbS, MbaS, and PvdS. The red letters in the PvdS sequence indicate residues mutated by Wilson and Lamont, 2006 (156). The red letters in the MbaS sequence correspond to point mutations generated in this study that have corresponding residues studied by Wilson and Lamont, 2006 (156). The green residues in the MbaS sequence indicate additional point mutations generated in this study.

A:

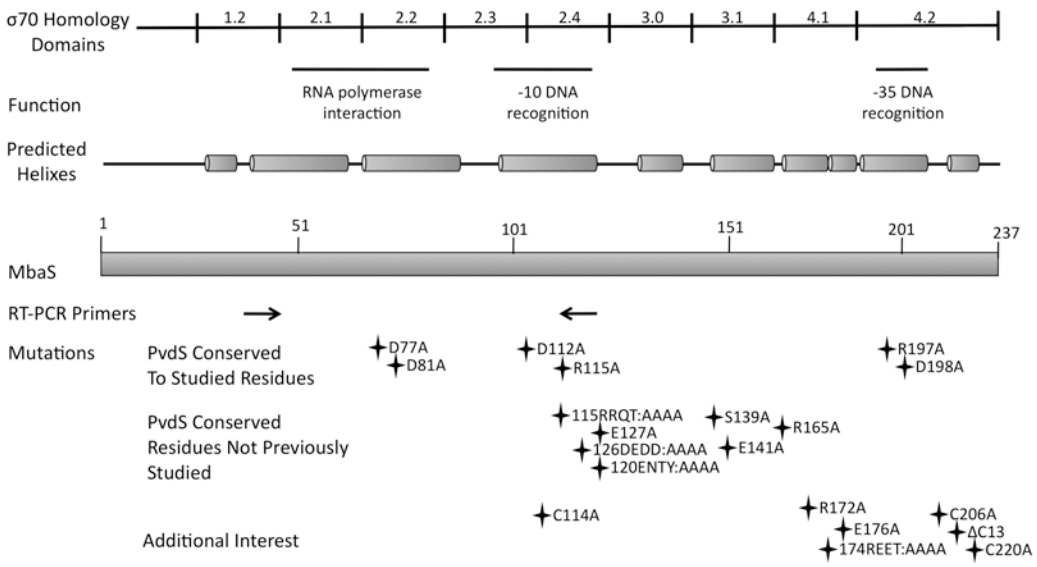

B:

```
OM       ***** ***.* . *:*.*   :.* ***  * .*.* *:        **:***:::*
OrbS   MAMAEVLDRPAAAAANPFLGSYPDLPPRAAPRARRASEPRAQG-------ALLDVLISHR
MbaS   --MAEVLARPAPAKPLPILASNGAFAPAAAPVLRAPSRPAARTPGAREHGALVDVLVANR
PvdS   --MSEQLS-----------------------TRRCDTP-----------LLQAFVDNR
OMP      *:* *                          *  . *            *::.:: :*

OM     .***::*************************:***** *:**********************
OrbS   AMLVNVARGFVGCASRAEDVVHDVFVKLVEFPNQD-AVRQPVAYVTRMVRNASIDACRRQ
MbaS   PMLVKLARGFVGCASRAEDVVHDVFVKLVDFPNQD-AIRQPVAYVTRMVRNASIDACRRQ
PvdS   TILVKIAARITGCRSRAEDVVQDAFFRLQSAPQITSSFKAQLSYLFQIVRNLAIDHYRKQ
OMP    .:**::*  :.** *******:*.*.:* . *:   :.:  ::*: ::*** :**  *:*

OM     .***.**::****:****** :*****:.*****:*: ** :******************
OrbS   NLENVYHTEEDDGFDVPSPEPTPEAALMTRDTLRRVWAALDDLPARSRAAFEMVRLREET
MbaS   TLENTYHADEDDGLDVPSPELSPEAALVVRDTLRHVYDALAQLPARSRAAFEMVRLREET
PvdS   ALEQKYSGPEEEGLNVVIQGASPETSHINYATLEHIADALTELPKRTRYAFEMYRLHGVP
OMP     **: *   *::*::*     :**:: :   **.::  ** :** *:* **** **:  .

OM     **:***********************. *:**..**:***.* *.***
OrbS   LQTAARALNVSQTLVHFMVRDAERHCAECLDACHRGVACPVFLGGRARRR----------
MbaS   LQSAARALNVSQTLVHFMVRDAERHCVACVDASERGLACPAFCGARARTVKKCVRDSSIE
PvdS   QKDIAKELGVSPTLVNFMIRDALVHCRKVTAE-RQGDNVTHLSARR-------------
OMP     :  *: *.** ***:**:***  **       .:*   . : . *
```

Figure V.2: qRT-PCR Expression Profile of *mbaS* RNA Expression for Mutant MbaS Constructs

MbaS expression was induced by the addition of 1 mM IPTG and 100 μM dipyridyl (DIP) to growth medium. Samples were grown, harvested, and processed as described elsewhere. The samples were normalized against the *E. coli gapA* gene and against the empty vector control. Asterisks indicate those mutations that overlap with the gene specific primers utilized in the PCR. Error bars indicated the standard deviation about the mean.

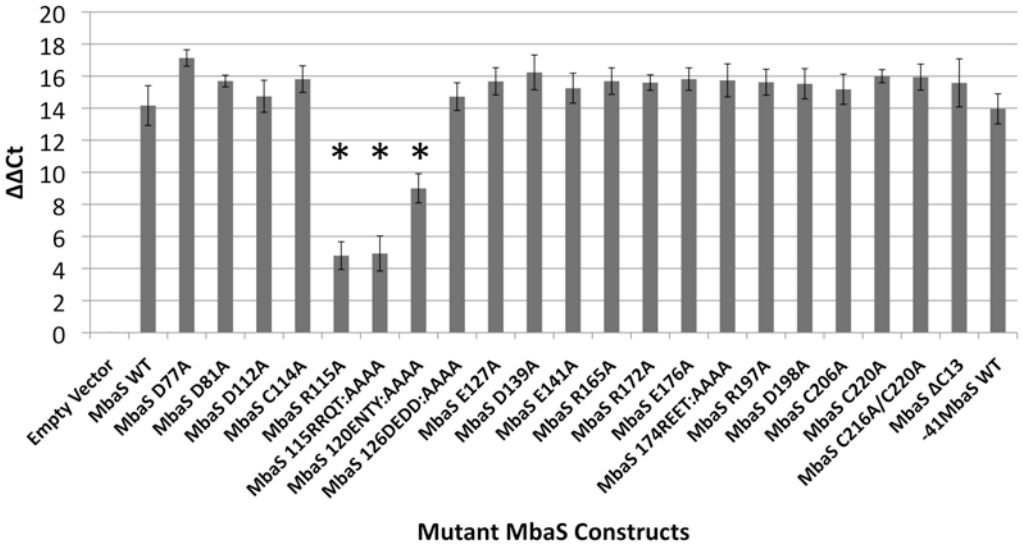
20
18
16
14
12
10
8
6
4
2
0
ΔΔCt
*
*
*
Empty Vector
MbaS WT
MbaS D77A
MbaS D81A
MbaS D112A
MbaS C114A
MbaS R115A
MbaS 115RRQT:AAAA
MbaS 120ENTY:AAAA
MbaS 126DEDD:AAAA
MbaS E127A
MbaS D139A
MbaS E141A
MbaS R165A
MbaS R172A
MbaS E176A
MbaS 174REET:AAAA
MbaS R197A
MbaS D198A
MbaS C206A
MbaS C220A
MbaS C216A/C220A
MbaS ΔC13
-41MbaS WT
Mutant MbaS Constructs

Figure V.3: Western Blot Confirmation of Mutant MbaS Expression in *E. coli*

The presence of MbaS protein was confirmed by western blot. A: A 10 minute exposure. B: A 20 minute exposure. Band A: MbaS protein as seen in wild type expression samples. Band B: a cross-reacting band. Band C: Mutation specific band. Whole cell samples were processed as previously described. Numbers to the left of each panel indicate the positions of the 37 kDa and 25 kDa molecular weight markers.

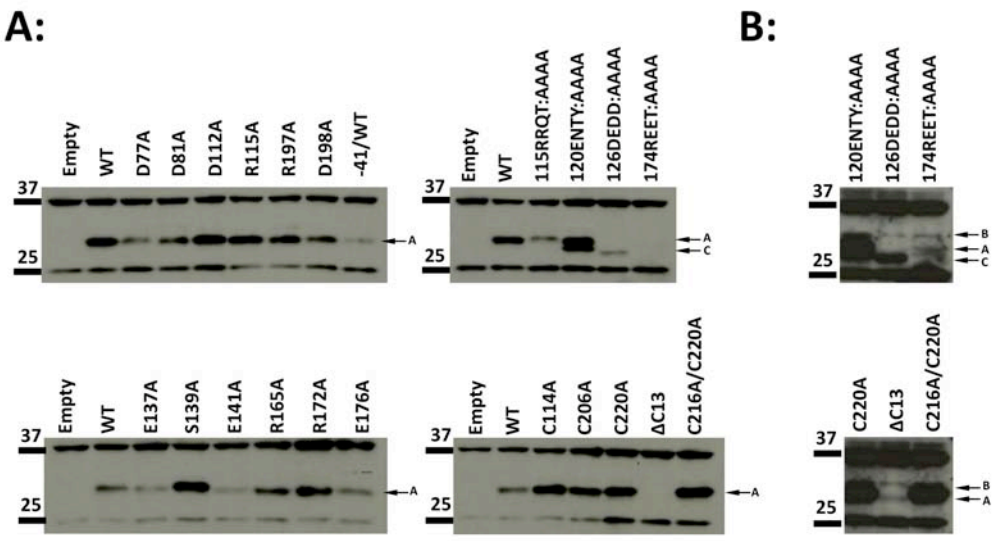
A:
B:
Empty
WT
D77A
D81A
D112A
R115A
R197A
D198A
-41/WT
115RRQT:AAAA
120ENTY:AAAA
126EDD:AAAA
174REET:AAAA
E137A
S139A
E141A
R165A
R172A
E176A
C114A
C206A
C220A
ΔC13
C216A/C220A
37
25
A
B
C

Figure V.4: Mutant MbaS Activation of *mbaJ* and *mbaE* Promoters in *E. coli*.

The β-galactosidase activity profiles for the mutant MbaS constructs that correspond to the characterized PvdS residues. Expression was induced by growth in LB medium with 1 mM IPTG and 100 μM dipyridyl (DIP). Samples were normalized to an empty vector controls (pMMB208:Km versus pQF50:Zeo). A: MbaS activation of the 250 nucleotide promoter fragment of *mbaE*. B: MbaS activation of the 200 nucleotide promoter fragment of *mbaJ*. Asterisks indicate those mutants with reduced β-galactosidase activity. Error bars indicate the standard deviation about the mean.

A: Mutant MbaS Activation of *mbaE* Promoter Fragment

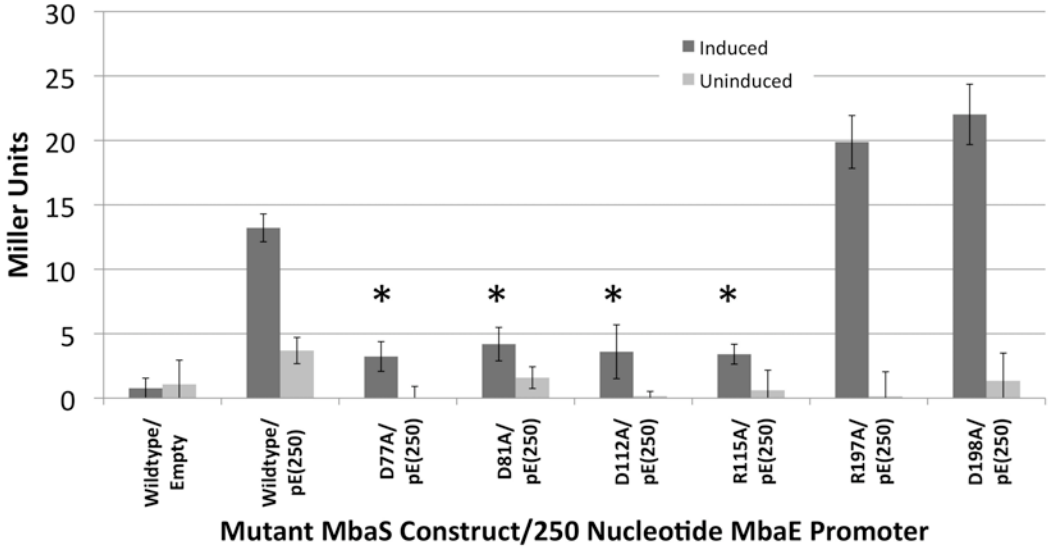

B: Mutant MbaS Activation of *mbaJ* Promoter Fragment

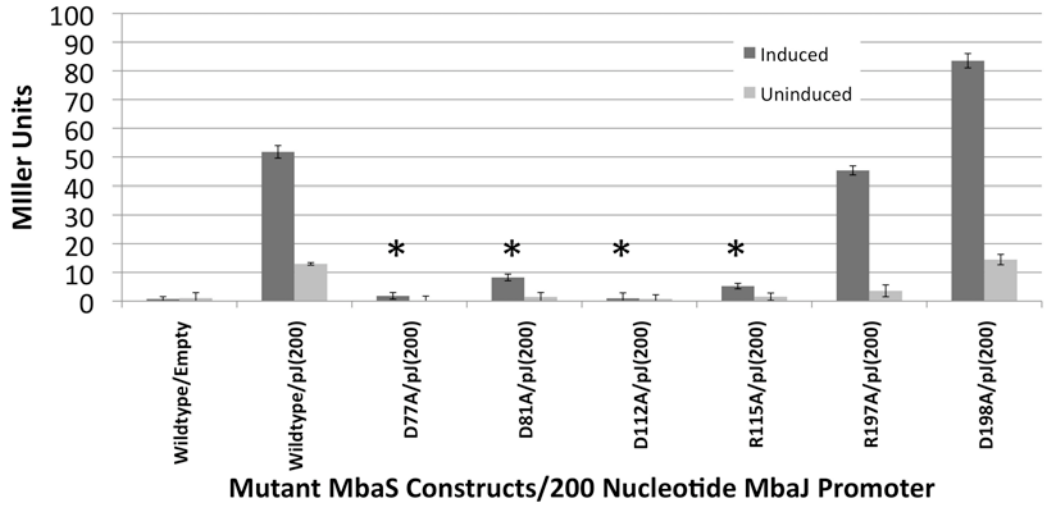

Figure V.5: Mutant MbaS Activation of *mbaJ* Promoter in *E. coli*.

The β-galactosidase activity profiles for the mutant MbaS constructs that correspond to the characterized PvdS residues. Expression was induced through growth in LB medium with 1 mM IPTG and 100 μM dipyridyl (DIP). Samples were normalized to an empty vector controls (pMMB208:Km versus pQF50:Zeo). A: MbaS activation of the 250 nucleotide promoter fragment of *mbaE*. B: MbaS activation of the 200 nucleotide promoter fragment of *mbaJ*. Asterisks indicate those mutants with reduced β-galactosidase activity. Error bars indicate the standard deviation about the mean.

A: Mutant MbaS Activation of *mbaE* Promoter

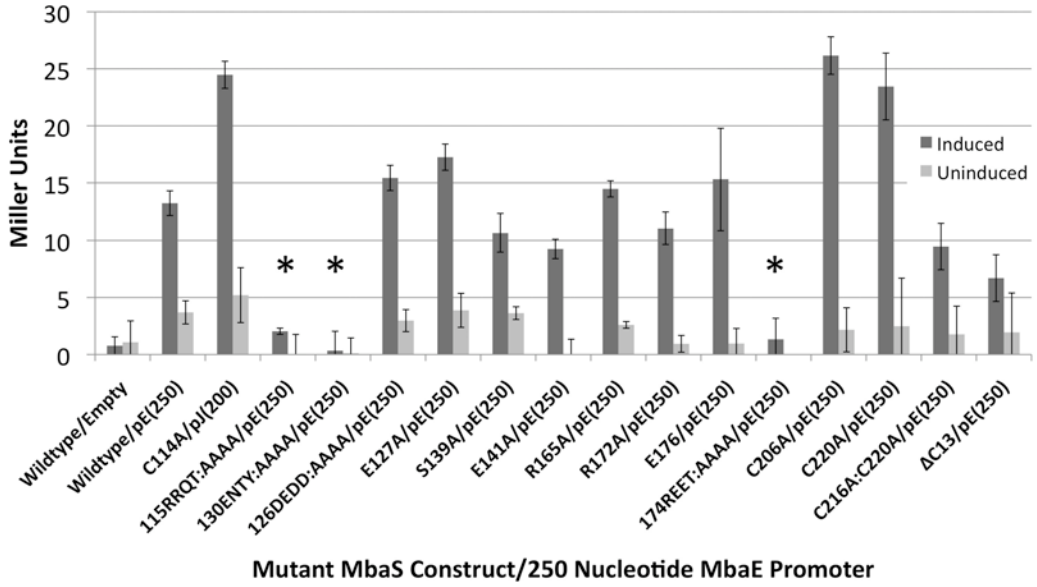

B: Mutant MbaS Activation of *mbaJ* Promoter

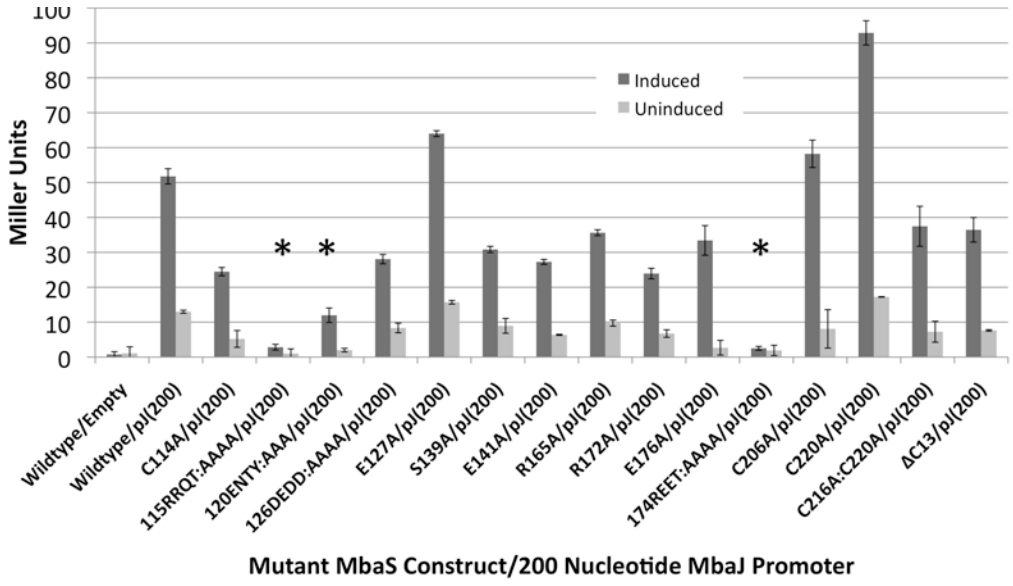

Figure V.6: RNA and Western Blot Analysis of MbaS Expression in *B. pseudomallei.*

Plasmids were conjugated into the *B. pseudomallei ΔamrABΔmbaS* strain (identified as ΔΔ in figure). A: qRT-RNA expression profile for MbaS complementation vectors. RNA was purified from samples in early log phase (6 hour time point) and stationary phase (24 hour time point). Samples were first normalized against the *B. pseudomallei gapA* gene and second normalization was against the empty vector control. B: Western blot of MbaS expression constructs. Samples were taken from stationary phase (24 hour) cultures and normalized to OD_{600}. Two potential MbaS bands were identified (bands A and B). No loading control was used. Cultures were normalized to the same density prior to processing. Error bars indicate the standard deviation about the mean.

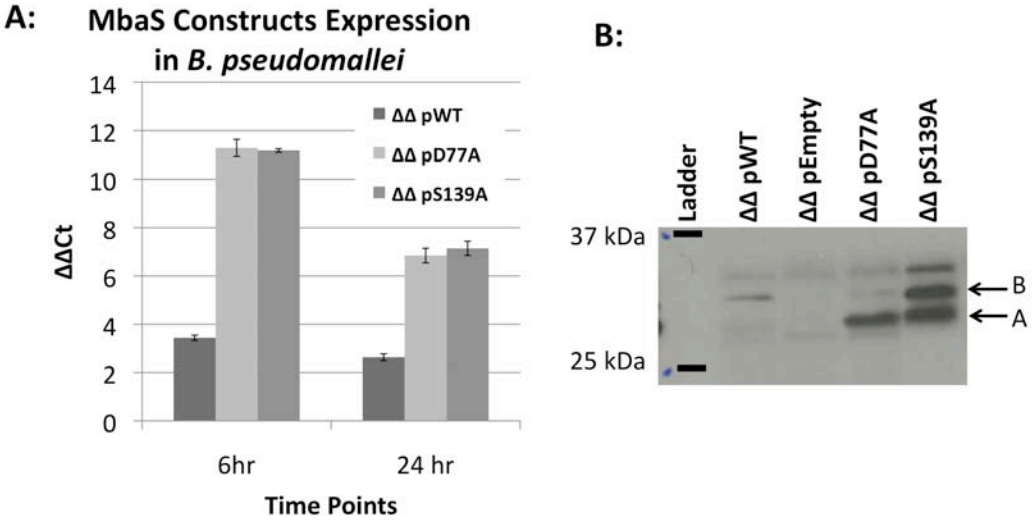
A:
MbaS Constructs Expression in B. pseudomallei
ΔΔCt
14
12
10
8
6
4
2
0
ΔΔ pWT
ΔΔ pD77A
ΔΔ pS139A
6hr
24 hr
Time Points
B:
Ladder
ΔΔ pWT
ΔΔ pEmpty
ΔΔ pD77A
ΔΔ pS139A
37 kDa
25 kDa
B
A

Figure V.7: MbaS Functional Complementation

A: Growth of MbaS complemented strains under iron limitation. Cultures were grown in either iron limiting medium (250 μM dipyridyl (DIP)) or iron replete medium (100 μg/ml ferric ammonium citrate (FAC)). Final culture density was measured at 24 hours post inoculation at OD_{600}. B: Chrome Azurol S (CAS) assay determination of siderophore production. Two μl of overnight liquid cultures were spotted onto CAS plates and incubated for 36 to 48 hours.

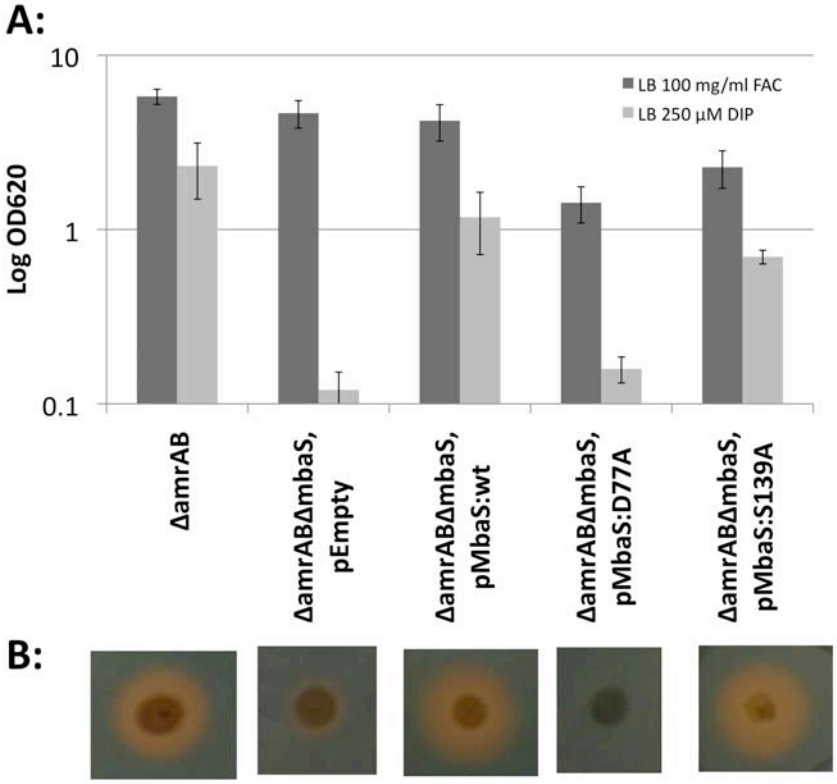
A:
10
1
0.1
Log OD620
LB 100 mg/ml FAC
LB 250 µM DIP
ΔamrAB
ΔamrABΔmbaS, pEmpty
ΔamrABΔmbaS, pMbaS:wt
ΔamrABΔmbaS, pMbaS:D77A
ΔamrABΔmbaS, pMbaS:S139A
B:

Figure V.8: Region 4.2 of MbaS (*B. pseudomallei*) Aligned to RpoE (*E. coli*)

Sequence alignment of region 4.2 from MbaS of *B. pseudomallei* against RpoE of *E. coli*. The crystal structure for region 4 (amino acid 122 through 191) of RpoE (pink structure) interacting with the -35 DNA binding region (purple DNA sequence). The crystal structure was solved by Lane and Darst, 2006 (79) and accessed 6/4/2011 Protein Data Bank, Accession ID 2H27 (11). Amino acid G168 of RpoE is the first residue of the major alpha helix of region 4.2 that sits within the major grove of the DNA helix. Residues of RpoE highlighted in green were observed to be of primary importance in the -35 DNA interaction (79). Amino acid residues of MbaS highlighted in red are those mutated in this study.

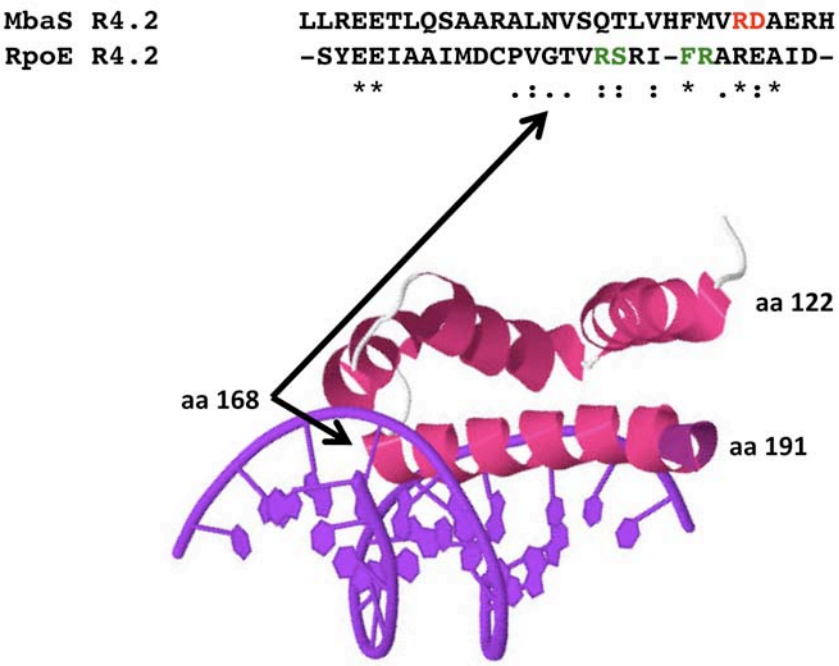
MbaS R4.2 LLREETLQSAARALNVSQTLVHFMVRDAERH
RpoE R4.2 -SYEEIAAIMDCPVGTVRSRI-FRAREAID-
** .:.. :: : * .*:*
aa 122
aa 168
aa 191

VI. Summary and Conclusions

Burkholderia pseudomallei is endemic to Southeast Asia and Northern Australia and more recently has been isolated from tropical regions in the Americas. In order to develop functional vaccines or treatment protocols it is of critical importance to understand the mechanisms of virulence. In order to manifest disease, bacteria have adapted an array of mechanisms for overcoming iron sequestration by the host. One common virulence mechanism for bacteria is the acquisition of iron from the host utilizing siderophores, small molecular weight iron binding compounds. The synthesis and uptake of malleobactin, the *B. pseudomallei* siderophore, is regulated by the expression of the MbaS sigma factor (Alice 2006). The purpose of this study was to 1) identify the functional start codon of MbaS, 2) generate a functional assay for MbaS in *E. coli*, 3) confirm MbaS activation of the *mbaJ* and *mbaE* promoters, 4) characterize the MbaS DNA binding sequence, 5) characterize the specific amino acids in the function of MbaS, and 6) confirm the relationship between studies conducted in *E. coli* and *B. pseudomallei*.

As demonstrated in Section III, we constructed a plasmid for the fusion of assorted promoter truncations with endogenous start codons to identify various promoter elements of *mbaS* and to characterize the functional start codon of the *mbaS* open reading frame. We observed that the ATG located upstream of the annotated start codon by 90 nucleotides was necessary for expression and that the *mbaS* endogenous promoter must be longer than 41 nucleotides from this upstream start codon to retain the iron responsive regulation. However, it is possible that it is

not the ATG that is necessary for expression, but is instead in the *mbaS* promoter. Further work is necessary to irrefutably claim this as the start codon of MbaS. First would be to utilize 5'-RACE on the RNA transcript of *mbaS* to identify that the transcription initiation lies upstream of our functional start codon. Genetically, the start codon could be confirmed by site directed mutagenesis to generate a non-methionine codon at this location, which would then be complemented by a second mutation to convert the second predicted codon to a methionine. Additionally, purification of MbaS followed by N-terminal sequencing utilizing Adman degradation would allow for sequencing the N-terminal 50 amino acids.

We constructed a two-plasmid system used as a functional readout for MbaS. This system was developed with the consideration that both plasmids must be functional in *E. coli* and *B. pseudomallei* to minimize cloning and possible differences resulting from various plasmid backbones. Although we have not yet demonstrated the functionality of the pQF50:Zeo plasmids derivatives in *B. pseudomallei*, the pMMB208:Km derivatives work well provided that there is sufficient endogenous promoter encoded with the gene of interest to allow for transcription.

We utilized this two-plasmid system to not only confirm genetically that MbaS is capable of activating the *mbaJ* and *mbaE* promoters, but also that it binds to the TAAAA(N16)CGT sequence in the promoter of *mbaJ*. This binding site is consistent with what has been demonstrated for PvdS (156), the *P. aeruginosa* homolog of MbaS, and suggested for the MbaS homolog OrbS in *B. cenocepacia* (1). Further characterization is possible with the purification of MbaS followed by

electromobility shift assays and DNase footprinting to confirm this interaction. DNase footprinting in particular will determine if MbaS will "protect" the promoter region of *mbaJ* over a larger region than that of only the -10 and -35 DNA binding sites. Additionally, purification of MbaS would allow for determining the binding strength determined by circular dichroism.

We confirmed the MbaS protein expression using an MbaS specific antibody generated for this work. In doing so, we had several unexpected results. First, the molecular weight of wild type MbaS when expressed in *E. coli* resulted in an apparent size of 28-30 kiloDaltons, significantly larger than the predicted 25.6 kiloDaltons. Second, two mutants of MbaS, the 120ENTY:AAAA and the 126DEDD:AAAA quadruple mutations, resulted in MbaS protein bands that were smaller than the rest of the mutant proteins expressed. And third, when MbaS was expressed from the plasmid in *B. pseudomallei*, two protein bands corresponding to the MbaS protein were present. These three points lead to the hypothesis that MbaS is post-translationally modified in an as yet unknown manner. This could also explain how MbaS can function in a manner similar to PvdS without the ECF control mechanisms described for PvdS.

The most likely cause of the double MbaS bands in the culture samples would be proteolysis of the protein. It has been demonstrate by Spencer, et al., 2008 (122) that PvdS undergoes proteolysis when the cultures were grown under oxygen limitation. One method this could be determined genetically would be to generate a dual tagged MbaS protein with an epitope tag on each terminus of the MbaS protein.

If the protein is cleaved then there should be at least three identifiable bands on the western blots. The first, and largest, would contain both epitope tags and could be recognized by all three antibodies (α-MbaS, α-C-terminus tag, and α-N-terminus tag). The second band, which would correspond to the slightly smaller protein seen in the western blots, would react with one of the two epitope tag antibodies and the MbaS antibody, while the third band would react with the second of the two epitope antibodies.

An additional possibility for the protein doublets seen in the western blots would be post-translational modifications such as phosphorylation. To explore this possibility, a single epitope tagged MbaS protein could be purified. Since *E. coli* predominately expressed a single band, the protein would likely need to be isolated from *B. pseudomallei* to purify the two different bands. However, an alternative to working in the BSL3 facility with *B. pseudomallei*, would be to express the protein in *B. thailandensis*, a non-pathogenic Burkholderia species. After separating the two bands via size-exclusion chromatography, mass spectrophotometry would be used to identify the type and location of the modification.

In the MbaS mutagenesis studies we demonstrated that four of our six mutants generated in the three functional domains of MbaS suffered a strong loss of activity, similar to what was report for the corresponding mutants of PvdS. However, those two mutations in Region 4.2, the -35 DNA sequence recognition domain, were able to activate both the *mbaJ* and *mbaE* promoters at levels comparable to wild type MbaS. Further comparison of this region with the

published crystal structure of RpoE from *E. coli* (79) revealed that the mutations generated in MbaS likely lie towards the N-terminal side of the actual residues mediating the -35 DNA recognition. Further mutagenesis of residues Q189, T190, F194, and M195 would likely abolish the ability of MbaS to recognize the -35 DNA sequence. Additional characterization of all of the non-functional mutants is necessary to confirm the roles played by each of these residues. Specifically, all mutant proteins would need to be purified, RNA core polymerase interaction confirmed by co-immunoprecipitation, and DNA binding confirmed by electromobility gel shift assays.

We demonstrated that the assays developed for studying the function of MbaS in *E. coli* are a faithful indication of the ability of those mutations to function in *B. pseudomallei*. One of the limiting factors in understanding the virulence mechanisms of *B. pseudomallei* is its classification as a Biosafety Level 3 (BSL3) Select Agent. This classification requires that all work be conducted in a BSL3 Laboratory with the associated safety protocols. These measures significantly slow the rate at which data can be generated and in many instances exclude the possibility of some experimental procedures. Having generated and validated a system for MbaS characterization that can be conducted in the BSL2 Laboratory, these studies can proceed at an increased pace.

It is likely that MbaS regulates the expression of genes outside of the malleobactin locus described in this work. To identify these genes, A. Alice conducted a microarray analysis comparing the expression profiles of two strains (a

wild type and an *mbaS* deletion) grown under iron limitation. In this study, the replicates were highly variable. My attempts to validate those genes with differential expression were not reproducible. This is most likely due to the high degree of morphological switching seen in the *mbaS* deletion strain (personal observations). This morphological switching may be influenced by the lack of MbaS and the subsequent dis-regulation of the potential MbaS regulon. Further work needs to be conducted to identify culture conditions that would minimize these variations and thereby generate more consistent results. Additionally, the microarray needs to be conducted with a complemented control of the *mbaS* deletion to differentiate those genes that are MbaS regulated and those whose regulation has been modified through repeated culturing in what appears to be sub-optimal conditions.

Finally, increased proteolysis of PvdS was seen under growth conditions with limited oxygen availability (122). It is of interest to determine if MbaS is differentially maintained within *B. pseudomallei* under various nutrient availability conditions, as it directly pertains to the role of MbaS during infection when the host is attempting to minimize the nutrients available to the pathogen. This could be studied by utilizing the MbaS antibody generated for this study. *B. pseudomallei* cultures would be grown in liquid medium with assorted nutrient deficiencies and the MbaS protein analyzed.

Further work is necessary to characterize additional iron acquisition systems of *B. pseudomallei*. As discussed in the Introduction, *B. pseudomallei* encodes for a

heme/hemin acquisition system that is up regulated under iron limiting growth in both published microarray studies (BPSS0242-BPSS0244) (2, 140). An attempt was made to characterize this locus. Previous studies in other bacteria have observed that a deletion of the hemin receptor would result in growth inhibition in iron limiting media that could not be recovered by supplemented with hemin (92, 97, 99, 163). After generating a deletion of BPSL0244, the annotated heme/hemin uptake receptor of *B. pseudomallei*, we were unable to see any growth inhibition in iron limiting media (data not shown).

These findings could be due to several reasons. The first reason could be the possible incorrect annotation of this locus. However, this is unlikely as the entire locus contains homology to proven bacterial hemin uptake loci. The second reason for the failure of this initial study is the possibility that *B. pseudomallei* may utilize the produced siderophores to sequester the iron molecules from the hemin complex. Due to the published findings that malleobactin can utilize iron from both transferrin and lactoferrin molecules, it is likely that malleobactin functions similarly in this case. In order to conclusively state that this is occurring, it is necessary to generated a malleobactin-producing null mutant, as could be done by a genomic deletion of *mbaJ*, followed by deletion of the putative hemin receptor.

The published role of malleobactin in the virulence of *B. pseudomallei* is not conclusive. A single study utilized a clinical isolate that had a large (130.7 kilobase) genomic deletion spanning the malleobactin locus to support the statement that malleobactin had no role in virulence (137). However, there are several issues with

how this study was conducted. First it is important to note, as repeatedly described in the Introduction, many identified virulence factors, when deleted or mutated, result in only a mild attenuation of virulence of 10 to 100 fold. This is likely due to the incredible number of complementing virulence mechanisms employed by *B. pseudomallei*. In the published study, the genomic deletion strain (708a) was used to infect BALB/c mice at a concentration of approximately 200 fold over that of the assumed parental strain (1028b) (137). In this case, the average time to death for both strains was between two and three days. These findings led the researchers to conclude that the malleobactin system must therefore play no role in virulence. However, unpublished data from the Crosa Laboratory contradicts this statement. In a virulence study conducted by A. Alice, a deletion of the *mbaA* gene, required for malleobactin production, resulted in an increased LD_{50} of approximately 25 fold. Additionally, the deletion of the *mbaS* gene resulted in an approximate attenuation of virulence of 100 fold. These results lead to several interesting conclusions. First, when working with a bacterium that employs such a wide variety of virulence mechanisms, it is critical to look at the relatively "small" changes that may be occurring in addition to the more dramatic. Secondly, and perhaps even more important, *mbaS* must be regulating additional genes outside of the malleobactin locus in order for us to see differences in virulence between the Δ*mbaA* deletion strain and the Δ*mbaS* deletion strain.

To conclude, the characterization presented in this work demonstrate 1) the annotated *mbaS* open reading frame is incorrect, 2) *mbaS* expression is regulated in

an iron concentration dependent manner, 3) the MbaS binding site of *mbaJ* is TAAAA(N16)CGT, and 4) that although the sequence of MbaS may be closer to that of PvdS, the structure-function relationship of Region 4.2 is more likely closer to RpoE of *E. coli*.

VII. Bibliography:

1. **Agnoli, K., C. A. Lowe, K. L. Farmer, S. I. Husnain, and M. S. Thomas**. 2006. The ornibactin biosynthesis and transport genes of Burkholderia cenocepacia are regulated by an extracytoplasmic function sigma factor which is a part of the Fur regulon. J Bacteriol **188**:3631-3644.
2. **Alice, A. F., C. S. Lopez, C. A. Lowe, M. A. Ledesma, and J. H. Crosa**. 2006. Genetic and transcriptional analysis of the siderophore malleobactin biosynthesis and transport genes in the human pathogen Burkholderia pseudomallei K96243. J Bacteriol **188**:1551-1566.
3. **Anderson, J. K., T. G. Smith, and T. R. Hoover**. 2010. Sense and sensibility: flagellum-mediated gene regulation. Trends Microbiol **18**:30-37.
4. **Andrews, S. C., A. K. Robinson, and F. Rodriguez-Quinones**. 2003. Bacterial iron homeostasis. FEMS Microbiol Rev **27**:215-237.
5. **Angerer, A., S. Enz, M. Ochs, and V. Braun**. 1995. Transcriptional regulation of ferric citrate transport in Escherichia coli K-12. FecI belongs to a new subfamily of sigma 70-type factors that respond to extracytoplasmic stimuli. Mol Microbiol **18**:163-174.
6. **Arjcharoen, S., C. Wikraiphat, M. Pudla, K. Limposuwan, D. E. Woods, S. Sirisinha, and P. Utaisincharoen**. 2007. Fate of a Burkholderia pseudomallei lipopolysaccharide mutant in the mouse macrophage cell line RAW 264.7: possible

role for the O-antigenic polysaccharide moiety of lipopolysaccharide in internalization and intracellular survival. Infect Immun **75**:4298-4304.

7. **Arsene, F., T. Tomoyasu, and B. Bukau**. 2000. The heat shock response of Escherichia coli. Int J Food Microbiol **55**:3-9.
8. **Balasubramanian, D., K. F. Kong, S. R. Jayawardena, S. M. Leal, R. T. Sautter, and K. Mathee**. 2011. Co-regulation of {beta}-lactam resistance, alginate production and quorum sensing in Pseudomonas aeruginosa. J Med Microbiol **60**:147-156.
9. **Barembruch, C., and R. Hengge**. 2007. Cellular levels and activity of the flagellar sigma factor FliA of Escherichia coli are controlled by FlgM-modulated proteolysis. Mol Microbiol **65**:76-89.
10. **Block, A., G. Li, Z. Q. Fu, and J. R. Alfano**. 2008. Phytopathogen type III effector weaponry and their plant targets. Curr Opin Plant Biol **11**:396-403.
11. **Bluhm, W. F., B. Beran, C. Bi, D. Dimitropoulos, A. Prlic, G. B. Quinn, P. W. Rose, C. Shah, J. Young, B. Yukich, H. M. Berman, and P. E. Bourne**. 2011. Quality assurance for the query and distribution systems of the RCSB Protein Data Bank. Database (Oxford) **2011**:bar003.
12. **Boddey, J. A., C. P. Flegg, C. J. Day, I. R. Beacham, and I. R. Peak**. 2006. Temperature-regulated microcolony formation by Burkholderia pseudomallei requires pilA and enhances association with cultured human cells. Infect Immun **74**:5374-5381.

13. **Bonemann, G., A. Pietrosiuk, and A. Mogk**. 2010. Tubules and donuts: a type VI secretion story. Mol Microbiol **76**:815-821.

14. **Braun, V., and F. Endriss**. 2007. Energy-coupled outer membrane transport proteins and regulatory proteins. Biometals **20**:219-231.

15. **Bredenbruch, F., R. Geffers, M. Nimtz, J. Buer, and S. Haussler**. 2006. The Pseudomonas aeruginosa quinolone signal (PQS) has an iron-chelating activity. Environ Microbiol **8**:1318-1329.

16. **Breitbach, K., S. Klocke, T. Tschernig, N. van Rooijen, U. Baumann, and I. Steinmetz**. 2006. Role of inducible nitric oxide synthase and NADPH oxidase in early control of Burkholderia pseudomallei infection in mice. Infect Immun **74**:6300-6309.

17. **Breitbach, K., P. Wongprompitak, and I. Steinmetz**. 2011. Distinct roles for nitric oxide in resistant C57BL/6 and susceptible BALB/c mice to control Burkholderia pseudomallei infection. BMC Immunol **12**:20.

18. **Brett, P. J., M. N. Burtnick, and D. E. Woods**. 2003. The wbiA locus is required for the 2-O-acetylation of lipopolysaccharides expressed by Burkholderia pseudomallei and Burkholderia thailandensis. FEMS Microbiol Lett **218**:323-328.

19. **Bullen, J. J., H. J. Rogers, and E. Griffiths**. 1978. Role of iron in bacterial infection. Curr Top Microbiol Immunol **80**:1-35.

20. **Burtnick, M. N., P. J. Brett, S. V. Harding, S. A. Ngugi, W. J. Ribot, N. Chantratita, A. Scorpio, T. S. Milne, R. E. Dean, D. L. Fritz, S. J. Peacock, J. L. Prior, T. P. Atkins, and D. Deshazer**. 2011. The cluster 1 type VI secretion

system is a major virulence determinant in Burkholderia pseudomallei. Infect Immun **79**:1512-1525.

21. **Burtnick, M. N., P. J. Brett, V. Nair, J. M. Warawa, D. E. Woods, and F. C. Gherardini**. 2008. Burkholderia pseudomallei type III secretion system mutants exhibit delayed vacuolar escape phenotypes in RAW 264.7 murine macrophages. Infect Immun **76**:2991-3000.
22. **Byers, B. R., and J. E. Arceneaux**. 1998. Microbial iron transport: iron acquisition by pathogenic microorganisms. Met Ions Biol Syst **35**:37-66.
23. **Prevention, C. f. D. C. a**. 2010. Melioidosis.
24. **Chan, Y. Y., H. S. Bian, T. M. Tan, M. E. Mattmann, G. D. Geske, J. Igarashi, T. Hatano, H. Suga, H. E. Blackwell, and K. L. Chua**. 2007. Control of quorum sensing by a Burkholderia pseudomallei multidrug efflux pump. J Bacteriol **189**:4320-4324.
25. **Chan, Y. Y., and K. L. Chua**. 2005. The Burkholderia pseudomallei BpeAB-OprB efflux pump: expression and impact on quorum sensing and virulence. J Bacteriol **187**:4707-4719.
26. **Chan, Y. Y., and K. L. Chua**. 2010. Growth-related changes in intracellular spermidine and its effect on efflux pump expression and quorum sensing in Burkholderia pseudomallei. Microbiology **156**:1144-1154.
27. **Chodimella, U., W. L. Hoppes, S. Whalen, A. J. Ognibene, and G. W. Rutecki**. 1997. Septicemia and suppuration in a Vietnam veteran. Hosp Pract (Minneap) **32**:219-221.

28. 2009. Biosafety in Microbiological and Biomedical Laboratories (BMBL), 5th Edition, Chosewood, C. L., and Wilson, DE. (ed.), Centers for Disease Control and Prevension, Atlanta, GA.

29. **Chuaygud, T., S. Tungpradabkul, S. Sirisinha, K. L. Chua, and P. Utaisincharoen**. 2008. A role of Burkholderia pseudomallei flagella as a virulent factor. Trans R Soc Trop Med Hyg **102 Suppl 1**:S140-4.

30. **Coy, M., and J. B. Neilands**. 1991. Structural dynamics and functional domains of the fur protein. Biochemistry **30**:8201-8210.

31. **Cozy, L. M., and D. B. Kearns**. 2010. Gene position in a long operon governs motility development in Bacillus subtilis. Mol Microbiol **76**:273-285.

32. **Cullinane, M., L. Gong, X. Li, N. Lazar-Adler, T. Tra, E. Wolvetang, M. Prescott, J. D. Boyce, R. J. Devenish, and B. Adler**. 2008. Stimulation of autophagy suppresses the intracellular survival of Burkholderia pseudomallei in mammalian cell lines. Autophagy **4**:744-753.

33. **Cunliffe, H. E., T. R. Merriman, and I. L. Lamont**. 1995. Cloning and characterization of pvdS, a gene required for pyoverdine synthesis in Pseudomonas aeruginosa: PvdS is probably an alternative sigma factor. J Bacteriol **177**:2744-2750.

34. **Currie, B. J**. 2008. Advances and remaining uncertainties in the epidemiology of Burkholderia pseudomallei and melioidosis. Trans R Soc Trop Med Hyg **102**:225-227.

35. **Currie, B. J., and S. P. Jacups**. 2003. Intensity of rainfall and severity of melioidosis, Australia. Emerg Infect Dis **9**:1538-1542.

36. **Currie, B. J., L. Ward, and A. C. Cheng**. 2010. The epidemiology and clinical spectrum of melioidosis: 540 cases from the 20 year Darwin prospective study. PLoS Negl Trop Dis **4**:e900.

37. **de Lorenzo, V., F. Giovannini, M. Herrero, and J. B. Neilands**. 1988. Metal ion regulation of gene expression. Fur repressor-operator interaction at the promoter region of the aerobactin system of pColV-K30. J Mol Biol **203**:875-884.

38. **DeShazer, D., P. J. Brett, M. N. Burtnick, and D. E. Woods**. 1999. Molecular characterization of genetic loci required for secretion of exoproducts in Burkholderia pseudomallei. J Bacteriol **181**:4661-4664.

39. **DeShazer, D., P. J. Brett, R. Carlyon, and D. E. Woods**. 1997. Mutagenesis of Burkholderia pseudomallei with Tn5-OT182: isolation of motility mutants and molecular characterization of the flagellin structural gene. J Bacteriol **179**:2116-2125.

40. **DeShazer, D., P. J. Brett, and D. E. Woods**. 1998. The type II O-antigenic polysaccharide moiety of Burkholderia pseudomallei lipopolysaccharide is required for serum resistance and virulence. Mol Microbiol **30**:1081-1100.

41. **Deziel, E., F. Lepine, S. Milot, J. He, M. N. Mindrinos, R. G. Tompkins, and L. G. Rahme**. 2004. Analysis of Pseudomonas aeruginosa 4-hydroxy-2-alkylquinolines (HAQs) reveals a role for 4-hydroxy-2-heptylquinoline in cell-to-cell communication. Proc Natl Acad Sci U S A **101**:1339-1344.

42. **Draper, A. D., M. Mayo, G. Harrington, D. Karp, D. Yinfoo, L. Ward, A. Haslem, B. J. Currie, and M. Kaestli**. 2010. Association of the melioidosis agent Burkholderia pseudomallei with water parameters in rural water supplies in Northern Australia. Appl Environ Microbiol **76**:5305-5307.

43. **Eberl, L**. 2006. Quorum sensing in the genus Burkholderia. Int J Med Microbiol **296**:103-110.

44. **Egan, A. M., and D. L. Gordon**. 1996. Burkholderia pseudomallei activates complement and is ingested but not killed by polymorphonuclear leukocytes. Infect Immun **64**:4952-4959.

45. **Escolar, L., J. Perez-Martin, and V. de Lorenzo**. 1998. Binding of the fur (ferric uptake regulator) repressor of Escherichia coli to arrays of the GATAAT sequence. J Mol Biol **283**:537-547.

46. **Essex-Lopresti, A. E., J. A. Boddey, R. Thomas, M. P. Smith, M. G. Hartley, T. Atkins, N. F. Brown, C. H. Tsang, I. R. Peak, J. Hill, I. R. Beacham, and R. W. Titball**. 2005. A type IV pilin, PilA, Contributes To Adherence of Burkholderia pseudomallei and virulence in vivo. Infect Immun **73**:1260-1264.

47. **Eymann, C., S. Schulz, K. Gronau, D. Becher, M. Hecker, and C. W. Price**. 2011. In vivo phosphorylation patterns of key stressosome proteins define a second feedback loop that limits activation of Bacillus subtilis sigmaB. Mol Microbiol **80**:798-810.

48. **Ferguson, A. D., R. Chakraborty, B. S. Smith, L. Esser, D. van der Helm, and J. Deisenhofer**. 2002. Structural basis of gating by the outer membrane transporter FecA. Science **295**:1715-1719.

49. **Furrer, J. L., D. N. Sanders, I. G. Hook-Barnard, and M. A. McIntosh**. 2002. Export of the siderophore enterobactin in Escherichia coli: involvement of a 43 kDa membrane exporter. Mol Microbiol **44**:1225-1234.

50. **Gaines, J. M., N. L. Carty, F. Tiburzi, M. Davinic, P. Visca, J. A. Colmer-Hamood, and A. N. Hamood**. 2007. Regulation of the Pseudomonas aeruginosa toxA, regA and ptxR genes by the iron-starvation sigma factor PvdS under reduced levels of oxygen. Microbiology **153**:4219-4233.

51. **Galyov, E. E., P. J. Brett, and D. DeShazer**. 2010. Molecular insights into Burkholderia pseudomallei and Burkholderia mallei pathogenesis. Annu Rev Microbiol **64**:495-517.

52. **Gamage, A. M., G. Shui, M. R. Wenk, and K. L. Chua**. 2011. N-octanoyl homoserine lactone signaling mediated by the BpsI-BpsR quorum sensing system plays a major role in biofilm formation of Burkholderia pseudomallei. Microbiology

53. **Gong, L., M. Cullinane, P. Treerat, G. Ramm, M. Prescott, B. Adler, J. D. Boyce, and R. J. Devenish**. 2011. The Burkholderia pseudomallei type III secretion system and BopA are required for evasion of LC3-associated phagocytosis. PLoS One **6**:e17852.

54. **Goshorn, R. K**. 1987. Recrudescent pulmonary melioidosis. A case report involving the so-called 'Vietnamese time bomb'. Indiana Med **80**:247-249.

55. **Gouin, E., M. D. Welch, and P. Cossart**. 2005. Actin-based motility of intracellular pathogens. Curr Opin Microbiol **8**:35-45.

56. **Gourse, R. L., W. Ross, and S. T. Rutherford**. 2006. General pathway for turning on promoters transcribed by RNA polymerases containing alternative sigma factors. J Bacteriol **188**:4589-4591.

57. **Griffith, K. L., and R. E. J. Wolf**. 2002. Measuring beta-galactosidase activity in bacteria: cell growth, permeabilization, and enzyme assays in 96-well arrays. Biochem Biophys Res Commun **290**:397-402.

58. **Guerinot, M. L**. 1994. Microbial iron transport. Annu Rev Microbiol **48**:743-772.

59. **Guerinot, M. L., and Y. Yi**. 1994. Iron: Nutritious, Noxious, and Not Readily Available. Plant Physiol **104**:815-820.

60. **Harley, V. S., D. A. Dance, G. Tovey, M. V. McCrossan, and B. S. Drasar**. 1998. An ultrastructural study of the phagocytosis of Burkholderia pseudomallei. Microbios **94**:35-45.

61. **Hassan, M. R., S. P. Pani, N. P. Peng, K. Voralu, N. Vijayalakshmi, R. Mehanderkar, N. A. Aziz, and E. Michael**. 2010. Incidence, risk factors and clinical epidemiology of melioidosis: a complex socio-ecological emerging infectious disease in the Alor Setar region of Kedah, Malaysia. BMC Infect Dis **10**:302.

62. **Helmann, J. D., and M. J. Chamberlin**. 1988. Structure and function of bacterial sigma factors. Annu Rev Biochem **57**:839-872.

63. **Hengge, R**. 2009. Proteolysis of sigmaS (RpoS) and the general stress response in Escherichia coli. Res Microbiol **160**:667-676.

64. **Higgs, P. I., P. S. Myers, and K. Postle**. 1998. Interactions in the TonB-dependent energy transduction complex: ExbB and ExbD form homomultimers. J Bacteriol **180**:6031-6038.

65. **Holden, M. T., R. W. Titball, S. J. Peacock, A. M. Cerdeno-Tarraga, T. Atkins, L. C. Crossman, T. Pitt, C. Churcher, K. Mungall, S. D. Bentley, M. Sebaihia, N. R. Thomson, N. Bason, I. R. Beacham, K. Brooks, K. A. Brown, N. F. Brown, G. L. Challis, I. Cherevach, T. Chillingworth, A. Cronin, B. Crossett, P. Davis, D. DeShazer, T. Feltwell, A. Fraser, Z. Hance, H. Hauser, S. Holroyd, K. Jagels, K. E. Keith, M. Maddison, S. Moule, C. Price, M. A. Quail, E. Rabbinowitsch, K. Rutherford, M. Sanders, M. Simmonds, S. Songsivilai, K. Stevens, S. Tumapa, M. Vesaratchavest, S. Whitehead, C. Yeats, B. G. Barrell, P. C. Oyston, and J. Parkhill**. 2004. Genomic plasticity of the causative agent of melioidosis, Burkholderia pseudomallei. Proc Natl Acad Sci U S A **101**:14240-14245.

66. **Howard, K., and T. J. Inglis**. 2005. Disinfection of Burkholderia pseudomallei in potable water. Water Res **39**:1085-1092.

67. **Hubber, A., and C. R. Roy**. 2010. Modulation of host cell function by Legionella pneumophila type IV effectors. Annu Rev Cell Dev Biol **26**:261-283.

68. **Imperi, F., F. Tiburzi, and P. Visca**. 2009. Molecular basis of pyoverdine siderophore recycling in Pseudomonas aeruginosa. Proc Natl Acad Sci U S A **106**:20440-20445.

69. **Inglis, T. J., A. Levy, A. J. Merritt, M. Hodge, R. McDonald, and D. E. Woods**. 2009. Melioidosis risk in a tropical industrial environment. Am J Trop Med Hyg **80**:78-84.

70. **Inglis, T. J., and A. Q. Sousa**. 2009. The public health implications of melioidosis. Braz J Infect Dis **13**:59-66.

71. **Inoue, A., Y. Murata, H. Takahashi, N. Tsuji, S. Fujisaki, and J. Kato**. 2008. Involvement of an essential gene, mviN, in murein synthesis in Escherichia coli. J Bacteriol **190**:7298-7301.

72. **Jani, A. J., and P. A. Cotter**. 2010. Type VI secretion: not just for pathogenesis anymore. Cell Host Microbe **8**:2-6.

73. **Jubelin, G., C. V. Chavez, F. Taieb, M. J. Banfield, A. Samba-Louaka, R. Nobe, J. P. Nougayrede, R. Zumbihl, A. Givaudan, J. M. Escoubas, and E. Oswald**. 2009. Cycle inhibiting factors (CIFs) are a growing family of functional cyclomodulins present in invertebrate and mammal bacterial pathogens. PLoS One **4**:e4855.

74. **Kazmierczak, M. J., M. Wiedmann, and K. J. Boor**. 2005. Alternative sigma factors and their roles in bacterial virulence. Microbiol Mol Biol Rev **69**:527-543.

75. **Kespichayawattana, W., S. Rattanachetkul, T. Wanun, P. Utaisincharoen, and S. Sirisinha**. 2000. Burkholderia pseudomallei induces cell fusion and actin-

associated membrane protrusion: a possible mechanism for cell-to-cell spreading. Infect Immun **68**:5377-5384.

76. **Kiratisin, P., and S. Sanmee**. 2008. Roles and interactions of Burkholderia pseudomallei BpsIR quorum-sensing system determinants. J Bacteriol **190**:7291-7297.

77. **Korbsrisate, S., N. Suwanasai, A. Leelaporn, T. Ezaki, Y. Kawamura, and S. Sarasombath**. 1999. Cloning and characterization of a nonhemolytic phospholipase C gene from Burkholderia pseudomallei. J Clin Microbiol **37**:3742-3745.

78. **Kuehl, C. J., and J. H. Crosa**. 2009. Molecular and genetic characterization of the TonB2-cluster TtpC protein in pathogenic vibrios. Biometals **22**:109-115.

79. **Lane, W. J., and S. A. Darst**. 2006. The structural basis for promoter -35 element recognition by the group IV sigma factors. PLoS Biol **4**:e269.

80. **Larsen, J. C., and N. H. Johnson**. 2009. Pathogenesis of Burkholderia pseudomallei and Burkholderia mallei. Mil Med **174**:647-651.

81. **Lazar Adler, N. R., B. Govan, M. Cullinane, M. Harper, B. Adler, and J. D. Boyce**. 2009. The molecular and cellular basis of pathogenesis in melioidosis: how does Burkholderia pseudomallei cause disease? FEMS Microbiol Rev **33**:1079-1099.

82. **Lesic, B., F. Lepine, E. Deziel, J. Zhang, Q. Zhang, K. Padfield, M. H. Castonguay, S. Milot, S. Stachel, A. A. Tzika, R. G. Tompkins, and L. G. Rahme**. 2007. Inhibitors of pathogen intercellular signals as selective anti-infective compounds. PLoS Pathog **3**:1229-1239.

83. **Limmathurotsakul, D., and S. J. Peacock**. 2011. Melioidosis: a clinical overview. Br Med Bull

84. **Ling, J. M., R. A. Moore, M. G. Surette, and D. E. Woods**. 2006. The mviN homolog in Burkholderia pseudomallei is essential for viability and virulence. Can J Microbiol **52**:831-842.

85. **Lumjiaktase, P., S. P. Diggle, S. Loprasert, S. Tungpradabkul, M. Daykin, M. Camara, P. Williams, and M. Kunakorn**. 2006. Quorum sensing regulates dpsA and the oxidative stress response in Burkholderia pseudomallei. Microbiology **152**:3651-3659.

86. **Maglott, D., J. Ostell, K. D. Pruitt, and T. Tatusova**. 2011. Entrez Gene: gene-centered information at NCBI. Nucleic Acids Res **39**:D52-7.

87. **Merrick, M. J**. 1993. In a class of its own--the RNA polymerase sigma factor sigma 54 (sigma N). Mol Microbiol **10**:903-909.

88. **Miethke, M., and M. A. Marahiel**. 2007. Siderophore-based iron acquisition and pathogen control. Microbiol Mol Biol Rev **71**:413-451.

89. **Mima, T., and H. P. Schweizer**. 2010. The BpeAB-OprB efflux pump of Burkholderia pseudomallei 1026b does not play a role in quorum sensing, virulence factor production, or extrusion of aminoglycosides but is a broad-spectrum drug efflux system. Antimicrob Agents Chemother **54**:3113-3120.

90. **Mohamed, R., S. Nathan, N. Embi, N. Razak, and G. Ismail**. 1989. Inhibition of macromolecular synthesis in cultured macrophages by Pseudomonas pseudomallei exotoxin. Microbiol Immunol **33**:811-820.

91. **Muangsombut, V., S. Suparak, P. Pumirat, S. Damnin, P. Vattanaviboon, V. Thongboonkerd, and S. Korbsrisate**. 2008. Inactivation of Burkholderia pseudomallei bsaQ results in decreased invasion efficiency and delayed escape of bacteria from endocytic vesicles. Arch Microbiol **190**:623-631.

92. **Najimi, M., M. L. Lemos, and C. R. Osorio**. 2008. Identification of heme uptake genes in the fish pathogen Aeromonas salmonicida subsp. salmonicida. Arch Microbiol **190**:439-449.

93. **Nathan, S. A., R. Qvist, and S. D. Puthucheary**. 2005. Kinetic studies of bioactive products nitric oxide and 8-iso-PGF(2alpha) in Burkholderia pseudomallei infected human macrophages, and their role in the intracellular survival of these organisms. FEMS Immunol Med Microbiol **43**:177-183.

94. **Nelson, M., J. L. Prior, M. S. Lever, H. E. Jones, T. P. Atkins, and R. W. Titball**. 2004. Evaluation of lipopolysaccharide and capsular polysaccharide as subunit vaccines against experimental melioidosis. J Med Microbiol **53**:1177-1182.

95. **Ngauy, V., Y. Lemeshev, L. Sadkowski, and G. Crawford**. 2005. Cutaneous melioidosis in a man who was taken as a prisoner of war by the Japanese during World War II. J Clin Microbiol **43**:970-972.

96. **Noor, R., M. Murata, H. Nagamitsu, G. Klein, S. Raina, and M. Yamada**. 2009. Dissection of sigma(E)-dependent cell lysis in Escherichia coli: roles of RpoE regulators RseA, RseB and periplasmic folding catalyst PpiD. Genes Cells **14**:885-899.

97. **Olczak, T., A. Sroka, J. Potempa, and M. Olczak**. 2008. Porphyromonas gingivalis HmuY and HmuR: further characterization of a novel mechanism of heme utilization. Arch Microbiol **189**:197-210.

98. **Paget, M. S., and J. D. Helmann**. 2003. The sigma70 family of sigma factors. Genome Biol **4**:203.

99. **Parrow, N. L., J. Abbott, A. R. Lockwood, J. M. Battisti, and M. F. Minnick**. 2009. Function, regulation, and transcriptional organization of the hemin utilization locus of Bartonella quintana. Infect Immun **77**:307-316.

100. **Pilatz, S., K. Breitbach, N. Hein, B. Fehlhaber, J. Schulze, B. Brenneke, L. Eberl, and I. Steinmetz**. 2006. Identification of Burkholderia pseudomallei genes required for the intracellular life cycle and in vivo virulence. Infect Immun **74**:3576-3586.

101. **Postle, K**. 1993. TonB protein and energy transduction between membranes. J Bioenerg Biomembr **25**:591-601.

102. **Potvin, E., F. Sanschagrin, and R. C. Levesque**. 2008. Sigma factors in Pseudomonas aeruginosa. FEMS Microbiol Rev **32**:38-55.

103. **Rahman, M., M. R. Hasan, and K. Shimizu**. 2008. Growth phase-dependent changes in the expression of global regulatory genes and associated metabolic pathways in Escherichia coli. Biotechnol Lett **30**:853-860.

104. **Ratledge, C., and L. G. Dover**. 2000. Iron metabolism in pathogenic bacteria. Annu Rev Microbiol **54**:881-941.

105. **Ray, K., B. Marteyn, P. J. Sansonetti, and C. M. Tang**. 2009. Life on the inside: the intracellular lifestyle of cytosolic bacteria. Nat Rev Microbiol **7**:333-340.

106. **Reckseidler-Zenteno, S. L., R. DeVinney, and D. E. Woods**. 2005. The capsular polysaccharide of Burkholderia pseudomallei contributes to survival in serum by reducing complement factor C3b deposition. Infect Immun **73**:1106-1115.

107. **Reckseidler-Zenteno, S. L., D. F. Viteri, R. Moore, E. Wong, A. Tuanyok, and D. E. Woods**. 2010. Characterization of the type III capsular polysaccharide produced by Burkholderia pseudomallei. J Med Microbiol **59**:1403-1414.

108. **Redly, G. A., and K. Poole**. 2003. Pyoverdine-mediated regulation of FpvA synthesis in Pseudomonas aeruginosa: involvement of a probable extracytoplasmic-function sigma factor, FpvI. J Bacteriol **185**:1261-1265.

109. **Redly, G. A., and K. Poole**. 2005. FpvIR control of fpvA ferric pyoverdine receptor gene expression in Pseudomonas aeruginosa: demonstration of an interaction between FpvI and FpvR and identification of mutations in each compromising this interaction. J Bacteriol **187**:5648-5657.

110. **Reitzer, L**. 2003. Nitrogen assimilation and global regulation in Escherichia coli. Annu Rev Microbiol **57**:155-176.

111. **Rost, B., and J. Liu**. 2003. The PredictProtein server. Nucleic Acids Res **31**:3300-3304.

112. **Sarkar-Tyson, M., J. E. Thwaite, S. V. Harding, S. J. Smither, P. C. Oyston, T. P. Atkins, and R. W. Titball**. 2007. Polysaccharides and virulence of Burkholderia pseudomallei. J Med Microbiol **56**:1005-1010.

113. **Schaible, U. E., and S. H. Kaufmann**. 2004. Iron and microbial infection. Nat Rev Microbiol **2**:946-953.

114. **Schalk, I. J**. 2008. Metal trafficking via siderophores in Gram-negative bacteria: specificities and characteristics of the pyoverdine pathway. J Inorg Biochem **102**:1159-1169.

115. **Shalom, G., J. G. Shaw, and M. S. Thomas**. 2007. In vivo expression technology identifies a type VI secretion system locus in Burkholderia pseudomallei that is induced upon invasion of macrophages. Microbiology **153**:2689-2699.

116. **Shirley, M., and I. L. Lamont**. 2009. Role of TonB1 in pyoverdine-mediated signaling in Pseudomonas aeruginosa. J Bacteriol **191**:5634-5640.

117. **Sitthidet, C., S. Korbsrisate, A. N. Layton, T. R. Field, M. P. Stevens, and J. M. Stevens**. 2011. Identification of Motifs of Burkholderia pseudomallei BimA Required for Intracellular Motility, Actin Binding, and Actin Polymerization. J Bacteriol **193**:1901-1910.

118. **Sokol, P. A., R. J. Malott, K. Riedel, and L. Eberl**. 2007. Communication systems in the genus Burkholderia: global regulators and targets for novel antipathogenic drugs. Future Microbiol **2**:555-563.

119. **Solovyev, V. V., and I. A. Shahmuradov**. 2003. PromH: Promoters identification using orthologous genomic sequences. Nucleic Acids Res **31**:3540-3545.

120. **Song, Y., C. Xie, Y. M. Ong, Y. H. Gan, and K. L. Chua**. 2005. The BpsIR quorum-sensing system of Burkholderia pseudomallei. J Bacteriol **187**:785-790.

121. **Sorenson, M. K., S. S. Ray, and S. A. Darst**. 2004. Crystal structure of the flagellar sigma/anti-sigma complex sigma(28)/FlgM reveals an intact sigma factor in an inactive conformation. Mol Cell **14**:127-138.

122. **Spencer, M. R., P. A. Beare, and I. L. Lamont**. 2008. Role of cell surface signaling in proteolysis of an alternative sigma factor in Pseudomonas aeruginosa. J Bacteriol **190**:4865-4869.

123. **Steinmetz, I., M. Rohde, and B. Brenneke**. 1995. Purification and characterization of an exopolysaccharide of Burkholderia (Pseudomonas) pseudomallei. Infect Immun **63**:3959-3965.

124. **Stevens, J. M., E. E. Galyov, and M. P. Stevens**. 2006. Actin-dependent movement of bacterial pathogens. Nat Rev Microbiol **4**:91-101.

125. **Stevens, J. M., R. L. Ulrich, L. A. Taylor, M. W. Wood, D. Deshazer, M. P. Stevens, and E. E. Galyov**. 2005. Actin-binding proteins from Burkholderia mallei and Burkholderia thailandensis can functionally compensate for the actin-based motility defect of a Burkholderia pseudomallei bimA mutant. J Bacteriol **187**:7857-7862.

126. **Stevens, M. P., A. Friebel, L. A. Taylor, M. W. Wood, P. J. Brown, W. D. Hardt, and E. E. Galyov**. 2003. A Burkholderia pseudomallei type III secreted protein, BopE, facilitates bacterial invasion of epithelial cells and exhibits guanine nucleotide exchange factor activity. J Bacteriol **185**:4992-4996.

127. **Stevens, M. P., and E. E. Galyov**. 2004. Exploitation of host cells by Burkholderia pseudomallei. Int J Med Microbiol **293**:549-555.

128. **Stevens, M. P., A. Haque, T. Atkins, J. Hill, M. W. Wood, A. Easton, M. Nelson, C. Underwood-Fowler, R. W. Titball, G. J. Bancroft, and E. E. Galyov**. 2004. Attenuated virulence and protective efficacy of a Burkholderia pseudomallei bsa type III secretion mutant in murine models of melioidosis. Microbiology **150**:2669-2676.

129. **Stevens, M. P., J. M. Stevens, R. L. Jeng, L. A. Taylor, M. W. Wood, P. Hawes, P. Monaghan, M. D. Welch, and E. E. Galyov**. 2005. Identification of a bacterial factor required for actin-based motility of Burkholderia pseudomallei. Mol Microbiol **56**:40-53.

130. **Stevens, M. P., M. W. Wood, L. A. Taylor, P. Monaghan, P. Hawes, P. W. Jones, T. S. Wallis, and E. E. Galyov**. 2002. An Inv/Mxi-Spa-like type III protein secretion system in Burkholderia pseudomallei modulates intracellular behaviour of the pathogen. Mol Microbiol **46**:649-659.

131. **Stojiljkovic, I., and K. Hantke**. 1995. Functional domains of the Escherichia coli ferric uptake regulator protein (Fur). Mol Gen Genet **247**:199-205.

132. **Stork, M., B. R. Otto, and J. H. Crosa**. 2007. A novel protein, TtpC, is a required component of the TonB2 complex for specific iron transport in the pathogens Vibrio anguillarum and Vibrio cholerae. J Bacteriol **189**:1803-1815.

133. **Sun, G. W., Y. Chen, Y. Liu, G. Y. Tan, C. Ong, P. Tan, and Y. H. Gan**. 2010. Identification of a regulatory cascade controlling Type III Secretion System 3 gene expression in Burkholderia pseudomallei. Mol Microbiol **76**:677-689.

134. **Thompson, J. D., T. J. Gibson, and D. G. Higgins**. 2002. Multiple sequence alignment using ClustalW and ClustalX. Curr Protoc Bioinformatics **Chapter 2**:Unit 2.3.

135. **Thummakul, T., H. Wilde, and T. Tantawichien**. 1999. Melioidosis, an environmental and occupational hazard in Thailand. Mil Med **164**:658-662.

136. **Tiwari, A., G. Balazsi, M. L. Gennaro, and O. A. Igoshin**. 2010. The interplay of multiple feedback loops with post-translational kinetics results in bistability of mycobacterial stress response. Phys Biol **7**:036005.

137. **Trunck, L. A., K. L. Propst, V. Wuthiekanun, A. Tuanyok, S. M. Beckstrom-Sternberg, J. S. Beckstrom-Sternberg, S. J. Peacock, P. Keim, S. W. Dow, and H. P. Schweizer**. 2009. Molecular basis of rare aminoglycoside susceptibility and pathogenesis of Burkholderia pseudomallei clinical isolates from Thailand. PLoS Negl Trop Dis **3**:e519.

138. **Tsang, K. W., and T. M. J. File**. 2008. Respiratory infections unique to Asia. Respirology **13**:937-949.

139. **Tuanyok, A., H. S. Kim, W. C. Nierman, Y. Yu, J. Dunbar, R. A. Moore, P. Baker, M. Tom, J. M. Ling, and D. E. Woods**. 2005. Genome-wide expression analysis of iron regulation in Burkholderia pseudomallei and Burkholderia mallei using DNA microarrays. FEMS Microbiol Lett **252**:327-335.

140. **Tuanyok, A., M. Tom, J. Dunbar, and D. E. Woods**. 2006. Genome-wide expression analysis of Burkholderia pseudomallei infection in a hamster model of acute melioidosis. Infect Immun **74**:5465-5476.

141. **Ulrich, R. L., D. Deshazer, E. E. Brueggemann, H. B. Hines, P. C. Oyston, and J. A. Jeddeloh**. 2004. Role of quorum sensing in the pathogenicity of Burkholderia pseudomallei. J Med Microbiol **53**:1053-1064.

142. **Upadhyay, A., H. L. Wu, C. Williams, T. Field, E. E. Galyov, J. M. van den Elsen, and S. Bagby**. 2008. The guanine-nucleotide-exchange factor BopE from Burkholderia pseudomallei adopts a compact version of the Salmonella SopE/SopE2 fold and undergoes a closed-to-open conformational change upon interaction with Cdc42. Biochem J **411**:485-493.

143. **Utaisincharoen, P., S. Arjcharoen, K. Limposuwan, S. Tungpradabkul, and S. Sirisinha**. 2006. Burkholderia pseudomallei RpoS regulates multinucleated giant cell formation and inducible nitric oxide synthase expression in mouse macrophage cell line (RAW 264.7). Microb Pathog **40**:184-189.

144. **Utaisincharoen, P., N. Tangthawornchaikul, W. Kespichayawattana, P. Chaisuriya, and S. Sirisinha**. 2001. Burkholderia pseudomallei interferes with inducible nitric oxide synthase (iNOS) production: a possible mechanism of evading macrophage killing. Microbiol Immunol **45**:307-313.

145. **Vasil, M. L**. 2007. How we learnt about iron acquisition in Pseudomonas aeruginosa: a series of very fortunate events. Biometals **20**:587-601.

146. **Vial, L., F. Lepine, S. Milot, M. C. Groleau, V. Dekimpe, D. E. Woods, and E. Deziel**. 2008. Burkholderia pseudomallei, B. thailandensis, and B. ambifaria produce 4-hydroxy-2-alkylquinoline analogues with a methyl group at the 3 position that is required for quorum-sensing regulation. J Bacteriol **190**:5339-5352.

147. **Visca, P., L. Leoni, M. J. Wilson, and I. L. Lamont**. 2002. Iron transport and regulation, cell signalling and genomics: lessons from Escherichia coli and Pseudomonas. Mol Microbiol **45**:1177-1190.

148. **Ward, T. R., A. Lutz, S. P. Parel, J. Ensling, P. Gutlich, P. Buglyo, and C. Orvig**. 1999. An Iron-Based Molecular Redox Switch as a Model for Iron Release from Enterobactin via the Salicylate Binding Mode. Inorg Chem **38**:5007-5017.

149. **Warrens, A. N., M. D. Jones, and R. I. Lechler**. 1997. Splicing by overlap extension by PCR using asymmetric amplification: an improved technique for the generation of hybrid proteins of immunological interest. Gene **186**:29-35.

150. **White, N. J**. 2003. Melioidosis. Lancet **361**:1715-1722.

151. **A., W**. 1913. An account of a glanders-like disease occurring in Rangoon. J. Hygiene **13**:1-34.

152. **Wiersinga, W. J., and T. van der Poll**. 2009. Immunity to Burkholderia pseudomallei. Curr Opin Infect Dis **22**:102-108.

153. **Wiersinga, W. J., and T. van der Poll**. 2009. Burkholderia pseudomallei tropism and the melioidosis road map. J Infect Dis **199**:1720-1722.

154. **Wiersinga, W. J., T. van der Poll, N. J. White, N. P. Day, and S. J. Peacock**. 2006. Melioidosis: insights into the pathogenicity of Burkholderia pseudomallei. Nat Rev Microbiol **4**:272-282.

155. **Wikraiphat, C., J. Charoensap, P. Utaisincharoen, S. Wongratanacheewin, S. Taweechaisupapong, D. E. Woods, J. G. Bolscher, and S. Sirisinha**. 2009. Comparative in vivo and in vitro analyses of putative virulence factors of

Burkholderia pseudomallei using lipopolysaccharide, capsule and flagellin mutants. FEMS Immunol Med Microbiol **56**:253-259.

156. **Wilson, M. J., and I. L. Lamont**. 2006. Mutational analysis of an extracytoplasmic-function sigma factor to investigate its interactions with RNA polymerase and DNA. J Bacteriol **188**:1935-1942.

157. **Wilson, M. J., B. J. McMorran, and I. L. Lamont**. 2001. Analysis of promoters recognized by PvdS, an extracytoplasmic-function sigma factor protein from Pseudomonas aeruginosa. J Bacteriol **183**:2151-2155.

158. **Wong, K. T., S. D. Puthucheary, and J. Vadivelu**. 1995. The histopathology of human melioidosis. Histopathology **26**:51-55.

159. **Yang, H., C. D. Kooi, and P. A. Sokol**. 1993. Ability of Pseudomonas pseudomallei malleobactin to acquire transferrin-bound, lactoferrin-bound, and cell-derived iron. Infect Immun **61**:656-662.

160. **Yang, H. M., W. Chaowagul, and P. A. Sokol**. 1991. Siderophore production by Pseudomonas pseudomallei. Infect Immun **59**:776-780.

161. **Yao, Q., J. Cui, Y. Zhu, G. Wang, L. Hu, C. Long, R. Cao, X. Liu, N. Huang, S. Chen, L. Liu, and F. Shao**. 2009. A bacterial type III effector family uses the papain-like hydrolytic activity to arrest the host cell cycle. Proc Natl Acad Sci U S A **106**:3716-3721.

162. **Zaborina, O., F. Lepine, G. Xiao, V. Valuckaite, Y. Chen, T. Li, M. Ciancio, A. Zaborin, E. O. Petrof, J. R. Turner, L. G. Rahme, E. Chang, and J. C. Alverdy**.

2007. Dynorphin activates quorum sensing quinolone signaling in Pseudomonas aeruginosa. PLoS Pathog **3**:e35.

163. **Zimbler, D. L., W. F. Penwell, J. A. Gaddy, S. M. Menke, A. P. Tomaras, P. L. Connerly, and L. A. Actis**. 2009. Iron acquisition functions expressed by the human pathogen Acinetobacter baumannii. Biometals **22**:23-32.